ELECTROSTATIC SPACE FOCUSING OF MOLECULAR BEAMS: SOME METHODS AND APPLICATIONS.

by

Robert Charles Sweeting

A thesis
submitted to the University of Keele
for the Degree of Doctor of Philosophy

Department of Physics,
University of Keele,
Staffordshire.

June, 1972.

ACKNOWLEDGEMENTS

The author would like to gratefully thank:

Professor D.J.E. Ingram for the provision of experimental facilities in the Physics Department.

Dr. D.C. Lainé for his many helpful discussions and enthusiastic supervision.

Mr. G.D.S. Smart for his valuable advice and the construction of some of the experimental apparatus.

Dr. P. Smith, of the Mathematics Department, for mathematical assistance.

Mr. P.R. Lefrère and other colleagues in the Physics Department for many useful discussions.

Mr. F. Rowerth and the Physics Department technical and workshop staffs for their advice and continued assistance.

Mr. H. Wardell and the staff of the University Workshop for their help.

The staff of the library for copying and other facilities.

The Science Research Council for providing personal financial support.

Mrs. A. Gunston for diligently typing the text of this thesis.

Mr. M. Cheney for carefully preparing the photographs for this thesis.

My wife, Elizabeth, for her sustained assistance and constructive criticism during the preparation of this thesis.

ABSTRACT

Electrostatic space focusing of molecular beams has been introduced by means of a brief review of some methods which have been employed in the development of microwave spectroscopy of molecules.

Some electrostatic focuser configurations suitable for space focusing molecules that decrease in energy in an applied electric field have been experimentally investigated. These designs include the coaxial, single-wire and a new configuration, the crossed-wire focuser. Characteristic results which have been obtained indicate the crossed-wire focuser to be the most efficient for focusing molecules in the lower inversion states of the rotational energy levels of ammonia.

For the first time, the operation of electrostatic focusers has been achieved in a beam maser without recourse to the continual use of external EHT supplies. This development involved the employment of electret focusers. In particular, solid ammonia electrets have been formed and the time dependence of their external electric field has been monitored in a beam maser. The method employed here of monitoring the external electret electric field by probing with a neutral molecular beam, has not previously been utilised.

A space focused ammonia molecular beam has been used to observe electric resonance "beating of beats". This effect, which is analogous to a similar effect observed in nuclear magnetic

resonance, followed the rapid passage of an exciting signal through the resolved components of the naturally split main line of the $J = 1, K = 1$ inversion transition.

CONTENTS

CHAPTER II (continued)

CHAPTER I

MICROWAVE SPECTROSCOPY OF MOLECULES

1.1 Introduction

During the period 1945-50 microwave molecular spectroscopy received much attention, particularly in the area of bulk gas techniques. Molecular beams, which were electrostatically space focused to be in a predominantly emissive state, were utilised in the early 1950's when the first MASER was developed. This device has, since then, proved to be very useful in quantum electronics research and in particular as a spectroscopic tool. A major difficulty of enhanced absorption beam spectroscopy has been the dearth of practical devices capable of space focusing molecules that decrease in energy in an applied electric field.

Although molecular spectroscopy techniques also include the electric resonance deflection method (Hughes, 1947), the review given here concentrates on methods whereby the resonant interaction of molecules and radiation field is observed directly via the radiation field itself.

1.2 Bulk gas spectroscopy

In essence, bulk gas spectroscopy involves the passage of microwave radiation through a cell containing the gas to be analysed. The transmitted or reflected power is then measured

as a function of the input microwave frequency. The sensitivity of early absorption spectrometers was limited basically by three factors:

(a) random amplitude fluctuations of microwave oscillator output power,

(b) changes in microwave power which varied systematically with microwave oscillator frequency,

and (c) loss in signal power when the microwave signal was converted by a detector into a low frequency which was suitable for display on an oscilloscope or a recorder.

Increased sensitivity was achieved by Hughes and Wilson (1947) who introduced Stark modulation techniques. When an electric field is applied to molecules that interact with such fields, the molecular absorption frequencies are shifted because of the Stark effect. If the electric field is applied when the microwave frequency coincides with the peak of an absorption line, the absorption signal amplitude then decreases by a maximum amount. Thus high frequency modulation can be obtained by periodically applying an electric field to the gas. Consequently a narrow band phase sensitive detection technique can be employed, which reduces the noise bandwidth. In addition to the reduction in crystal noise at the high modulation frequency, this method is almost insensitive to microwave power variations, excepting

those due to spectral lines. The magnetic analogue of this type of spectrometer is the Zeeman spectrometer in which paramagnetic molecules and free radicals can be studied. The high frequency magnetic field is generally applied by a solenoid that surrounds the waveguide. Unless the modulation frequency is low, the waveguide is slotted to reduce induced eddy currents. A glass tube surrounds the waveguide and is used to support the solenoid and contain the gas.

Bridge spectrometers, that operate with a microwave balancing arm in the network, have been successfully operated for many years. Geschwind et al (1952) originated the technique at Columbia University. Although it has good sensitivity, the bridge spectrometer is less suitable for searching for spectra than modulation spectrometers. Nonetheless, linewidths not much greater than the Doppler width can be obtained. Later, Townes (1954) equipped a bridge spectrometer with Stark modulation facilities which increased the sensitivity tenfold over that obtained by Geschwind.

The principal sources of spectral line broadening which have to be reduced in bulk gas spectrometers are (a) pressure broadening, (b) molecular collisions with the cell walls, (c) modulation broadening, (d) microwave power saturation, (e) microwave source frequency fluctuations and (f) Doppler broadening. Newell and Dicke (1951) realised that of the various contributions to microwave linewidths the natural linewidth

is negligible, while the collision and saturation broadening could be greatly reduced. Doppler broadening remained as the dominant factor.

To reduce Doppler broadening, Newell and Dicke developed the "Stark wave" technique which employed a gas cell that was used in reflection. The cell contained equispaced, parallel, plane wire grids. The grids were spaced by $\lambda/4$, where λ was the free space wavelength of the microwaves. Electrical connections were made to the grids to produce a modulating field which was periodic in space and time and was superposed upon a static electric field. In this way so-called "Stark waves" were produced in the gas cell. This method permitted only those molecules with a specified Doppler shift to contribute to the reflected microwaves. When applied to the $J = 3$, $K = 3$ inversion transition of ammonia, the method achieved a reduction of the spectral linewidth, between half power points, to approximately a quarter of the normal Doppler linewidth, at room temperature. For ammonia at room temperature, the normal value of the Doppler linewidth, between half power points, is approximately 70 kHz.

A further bulk gas spectroscopy technique was reported by Romer and Dicke (1955). The essential feature of the spectrometer was a "pill-box" shaped cavity. It consisted of two flat plates, almost 15λ in diameter, separated by $\lambda/2$, where λ was the free space wavelength of the microwaves. In the experiment

performed, the gas was excited by a sequence of microwave pulses, such that the phase of the microwave oscillation was preserved between pulses. After each pulse the gas radiated a coherent wave of decaying amplitude whose phase was determined by the phase of the exciting microwaves. Using this spectrometer the $J = 3$, $K = 3$ inversion transition of ammonia was observed. Bulk gas was used at low pressure and room temperature. A reduction of spectral linewidth comparable to that achieved by the "Stark wave" technique employed by Newell and Dicke was obtained.

Norton (1957) has also discussed the application of the pulsed resonance excitation technique to bulk gas spectroscopy. Hill et al (1967) have applied the method to OCS gas contained in an S-band gas cell.

Bulk gas spectroscopy has continued to be applied to the analysis of complex mixtures of gases. Commercial spectrometers such as the Hewlett-Packard HP8460A are now available. This instrument employs a backward wave oscillator, which is phase locked to a harmonic of a reference oscillator, as a microwave source that covers the range 8.0 to 40.0 GHz. Signal detection sensitivity is improved by Stark modulation of the gas cell.

1.3 Molecular beam spectroscopy

The spectral linewidth in the case of a molecular beam is primarily determined by the time of flight of the molecules

in the microwave field. When only one electric field maximum of the microwave field lies in the molecular flight path, then the linewidth will be (Gordon et al, 1955),

$$\Delta\nu \doteq \frac{1}{\tau} \qquad (1.1)$$

where τ is the time of flight of the molecules in the microwave field.

For a univelocity beam travelling at 500 m s^{-1} through 0.1 m of microwave field, then,

$$\Delta\nu \doteq 5 \text{ kHz} \qquad (1.2)$$

In the case of a real molecular beam, where there is a distribution of velocities, it might appear necessary to consider Doppler broadening in the beam. Basow and Prokhorov (1954) indicated that the displacement of frequency is determined by the ratio between the molecular velocity and the phase velocity of the microwaves in the direction of beam propogation. Thus it is possible to eliminate the Doppler broadening in a molecular beam by exciting in the cavity the type of mode whose phase velocity in the direction of beam propogation is infinite. However, divergent molecules possess velocity components perpendicular to the fundamental wave and introduce a Doppler broadening factor. This can be minimised if the spectrometer has a well collimated beam.

The sensitivity of a molecular beam spectrometer is determined by the noise level of the crystal detector which monitors the absorption or emission of microwave power by the molecules. At low incident power levels, the noise of the crystal varies little with the change of incident microwave power. Thus the sensitivity of the spectrometer increases with the absolute power absorbed by the molecules. If no saturation effect takes place, the magnitude of the absorbed power is proportional to the power of the microwave radiation through which the molecular beam passes.

In the case of a molecular beam spectrometer the density of the microwave radiation is less than that used with bulk gas spectrometers. This is because the narrower spectral line obtained with the molecular beam method may be easily saturation broadened. The use of superheterodyne detection (SHD), in connection with a molecular beam spectrometer, improves the sensitivity, as indicated in the following power considerations :

If the power is P and the minimum detectable change in power is ΔP against a background noise, when a SHD receiver is used, then (Townes and Geshwind 1948),

$$\Delta P = 2\sqrt{P_N P} \qquad (1.3)$$

where P_N, the SHD receiver noise power is given by,

$$P_N = F_N kT\Delta F \tag{1.4}$$

where ΔF is the effective bandpass of the receiver and F_N is the noise factor of the receiver, and where k and T are respectively Boltzmann's constant and absolute temperature. Since the signal to noise ratio for an absorption spectrometer is a function of the number of molecules available for taking part in the absorption process, as large a number of active molecules as possible are required to interact with the microwave radiation.

The relative molecular populations of the energy levels of molecules are governed by the Boltzmann distribution. For a pair of energy states, between which transitions can take place, the lower one has the greater population when the system is in thermal equilibrium. If the molecular populations are n_2 and n_1 for the upper and lower energy states respectively of a suitable microwave transition, then the ratio of the number of molecules in the two energy states in thermal equilibrium is given, omitting statistical weights, by,

$$\frac{n_1}{n_2} = \exp\left[\frac{h\nu}{kT}\right] \tag{1.5}$$

$$\doteq 1 + \frac{h\nu}{kT} \tag{1.6}$$

where T = 290 K and ν = microwave frequency and $h\nu \ll kT$.

Thus the number of active molecules (n) is given by,

$$n = n_1 - n_2 \tag{1.7}$$

$$\doteq n_2 \frac{h\nu}{kT} \tag{1.8}$$

and, therefore, the signal to noise ratio is proportional to $h\nu/kT$ times the population in the upper energy states. This result indicates that increased signal to noise ratios are attainable at higher transition frequencies.

Johnson and Strandberg (1952) obtained a reduction in linewidth of the J = 3, K = 3 transition of the ammonia spectrum when a molecular beam was used. A halfwidth, between half power points, of 20 kHz was obtained. A plane polarised wave was transmitted transversely through the beam by an aerial and was reflected back through the beam into the same aerial after interacting with the beam. The input and output signals of the aerial were separated in a microwave magic-tee. Low frequency (660 Hz) Stark modulation was applied to the molecular beam to aid detection but this modulation did not significantly degrade the linewidth. The value of linewidth was greater than expected because of lack of receiver sensitivity.

Strandberg and Dreicer (1954) reported further experiments on the ammonia J = 3, K = 3 inversion transition. Results were

given that compared the absorption spectral linewidths, between half power points. In the case of a molecular beam spectrometer a reduction of the Doppler linewidth by a factor of 6 was obtained.

Molecular beam absorption studies have continued and have been extended to investigations at millimetre wavelengths. For example, Rusk and Gordy (1962) reported millimetre wave absorption spectra from molecular beams of alkali bromides and iodides. The apparatus used differed only in the waveguide cell from that used by King and Gordy (1953) who measured millimetre wave absorption in OCS and other molecular beams. The new cell consisted of a section of S-band waveguide with a slot in the narrow side to allow molecules from an oven, after collimation, to pass across the cell, in a perpendicular direction to the propagation of microwave radiation.

Clouser and Gordy (1964) modified the spectrometer of Rusk and Gordy by the addition of high pass microwave filters which reduced detector-crystal noise and passed higher microwave harmonics. PTFE microwave lenses were added to the input and output of the gas cell and these increased the efficiency of microwave transmission through the cell. With this spectrometer, Clouser and Gordy investigated pure rotational spectra of the alkali chlorides in the 0.96 mm to 3 mm wavelength region of the microwave spectrum.

In 1966 Huiszoon and Dymanus briefly described their high resolution millimetre wavelength beam spectrometer. Two copper plates 400 mm long, 100 mm wide and separated by 10 mm formed the cell. Input and output coupling to the cell was via two microwave horns with microwave lenses interposed to increase the transmission of microwave power. Use of this molecular beam spectrometer on the rotational spectrum of hydrogen sulphide allowed a spectral linewidth measurement, between half power points, of 9 kHz on the $1_{01} - 1_{10}$ transition to be made. This linewidth measurement represented a reduction of 50 over conventional bulk gas techniques. Details of the spectrometer were published by Huiszoon (1971).

1.4 State separated molecular beams

Since molecules in a molecular beam do not interact, there is no compensation for any disturbance of the Boltzmann distribution of the energy levels in which the molecules exist. This allows the possibility of increasing the number of active molecules by sorting the beam with respect to energy levels. The terms focuser and state-separator are used extensively in the literature on focusing systems for molecular beams to describe the same type of device. Such a device captures and focuses molecules in certain quantum states : hence the term focuser. The same device usually defocuses other quantum states and is

therefore also known as a state-separator. Particular reference will be made here to electrostatic space focusing systems.

Nethercot (1951) proposed, on behalf of Townes, a molecular oscillator. This device was to employ a focused molecular beam of upper inversion state molecules, in conjunction with a resonant cavity. Gordon et al (1954) reported the operation of the first molecular beam maser which used the $J = 3$, $K = 3$ inversion transition of ammonia. The beam was electrostatically space focused. A spectral linewidth, between half power points, of 7 kHz was achieved using this emission spectrometer. Of the total spectral linewidth, 2 to 4 kHz was attributed to spurious frequency fluctuations of the exciting microwave source.

Concurrently with the work of Gordon et al, Basov and Prokhorov (1954) of the Lebedev Research Group published their discussion of the application of molecular beams to spectroscopy. They gave analyses for sorted molecular beam devices of both the emissive and absorptive types. Advancements in molecular beam masers up to 1970 have been reviewed by Lainé (1970) together with descriptions of the various focusing systems which have been employed. Typical focuser designs are discussed in Chapter II and serve as an introduction to the more difficult problem of focusing absorptive molecular beams.

A focusing system for lower energy state ammonia molecules was built by Helmer et al (1960). They collected and focused

lower state molecules, produced by maser oscillation, into an ion detector. A coaxial design was employed. Auerbach et al (1966) reviewed the various schemes available in principle to focus neutral particles which decrease in energy in an applied electric field. In particular, the alternate-gradient principle was proposed for this application. The first successful operation of an alternate-gradient focuser on a molecular beam was reported by Kakati and Lainé (1967) for ammonia. Investigations of this type of device were reported in full later when the theory and experimental details were given (Kakati and Lainé, 1971). It was noted that the measurement of spectral linewidths, using an absorptive molecular beam, avoids the problem of regenerative spectral line narrowing that is common in molecular beam masers (Zuev and Cheremiskin, 1962).

1.5 Spectral line broadening

In section 1.2 it was noted that in bulk gas spectroscopy at low pressures, Doppler line broadening is dominant. The response from each molecule, if it were stationary, would be a resonance linewidth, between half power points, of $\Delta\nu$, consisting of lifetime and collision broadening mechanisms. The resonance would be centred at the resonance frequency ν_o. However, the result of the kinetic motion of the gas is to further broaden the spectral line because of the individual response of the molecules, whose centre frequencies are

spread over a range determined by the extent of Doppler broadening. Therefore, to generalise, if molecules were motionless, an applied signal at any frequency ν , more than a few resonance linewidths away from the centre frequency ν_o , would produce little response. In a real system however, where the molecules are in random motion, Doppler broadening would be present. Some molecules would have their centre frequencies shifted towards the applied signal and a response would be achieved.

Collisions experienced by molecules colliding with each other, or the walls of their container, may be "elastic" or "inelastic" and different relaxation mechanisms can result. Following an elastic collision, the internal motion of a molecule has the same amount of energy as before the collision, but the phase of this motion is randomly altered. Elastic collisions thus provide, what is termed in the literature, a "dephasing" (T_2) process without contributing an "energy decay" (T_1) process.

The internal energy of a molecule which undergoes an inelastic collision may be transformed into kinetic energy of the same molecule or another molecule. Energy may be given to the walls of the container. Such inelastic collisions not only have dephasing effects (T_2) but also contribute to the overall energy damping of the system (T_1). Elastic and inelastic collision processes can occur simultaneously, at different collision rates, in the same molecular ensemble.

CHAPTER II

ELECTROSTATIC SPACE FOCUSING OF MOLECULAR BEAMS

2.1 Introduction

Techniques for space focusing molecules in an emissive quantum state have been comprehensively investigated in connection with the development of molecular beam masers. However, devices capable of focusing molecules in an absorptive state appear to have been neglected. The mechanics of the various techniques employed in electrostatically focusing molecular beams, whose energy changes in an applied electric field, may be formalised in a general way. This formalism, due to Auerbach et al (1966), is summarised here and related to existing schemes that have been used previously to focus molecular beams. Other factors, that affect focusing, such as spatial reorientation and the population distribution of molecules have also been considered. Particular reference has been made to molecular beams of ammonia.

The characteristics of focusers proposed by Auerbach et al (1966) for particles which decrease in energy in an applied electric field have been investigated experimentally. The crossed-wire focuser, a completely new electrode configuration, has been designed and developed. Results indicate that it has substantially improved characteristics over existing focusers used to focus

molecules with a negative slope Stark interaction.

The term "state-separator" is often used to describe a device which,

(a) sorts a molecular beam with respect to quantum state,

(b) defocuses the unwanted states,

and (c) converges the required molecules and directs them in a given direction.

However, as noted in section 1.4, the same device is also conveniently described as a "focuser". The latter term will be predominantly used in this chapter. It should be noted, however, that the term "focuser" does not apply in the strictly optical sense. Molecules starting at the entrance of the device, with the same position, but different velocities and directions, do not necessarily converge to the same point after passing through the focuser (Vonbun 1958).

This limitation does not altogether preclude analysing the behaviour of such a device by a composition of analogous optical lens elements. Such an analysis has been performed on the alternate-gradient focuser by Kakati and Lainé (1971).

2.2 Mechanics of focusing

The function of a molecular beam focuser is to create a non-equilibrium population distribution with respect to the energy states of molecules in the beam. That is, from equation (1.5), a molecular beam focuser produces the condition where,

$$\frac{n_1}{n_2} \neq \exp\left[\frac{h\nu}{kT}\right] \qquad (2.1)$$

Depending on whether the required focused beam has to be emissive, or absorptive, the desired molecules must be reconverged, while superfluous molecules are ejected from the beam so that no unnecessary scattering occurs.

For a force field to maintain a molecule in static equilibrium two conditions should be fulfilled :

(a) The applied force $\overline{F}$ must vanish at the same point so that there is a position at which the molecules experience no acceleration.

(b) The static equilibrium position should be such that near to it the force field should restore the particle to its original position.

In a force field where $\nabla\overline{F}$ is diagonal in a cartesian co-ordinate system,

$$\frac{\partial F_x}{\partial x}, \quad \frac{\partial F_y}{\partial y}, \quad \frac{\partial F_z}{\partial z} \qquad (2.2)$$

are then the non-vanishing derivatives of $\overline{F}$. For the forces to be restorative each partial derivative must be negative. Then it

is necessary that the divergence of $\bar{F}$ be negative, where $\nabla.\bar{F}$ is given by,

$$\nabla.\bar{F} = \frac{\partial F_x}{\partial x} + \frac{\partial F_y}{\partial y} + \frac{\partial F_z}{\partial z} \qquad (2.3)$$

In practice a molecular beam is injected into an array of electrodes. Molecules occupying a central trajectory through the electrode array define the "axial trajectory". The differential motion of neighbouring molecules is obtained by making the assumption that they experience the same force field as the axial molecules plus a first order correction force $\bar{F}_c$ where,

$$\bar{F}_c = + \bar{r}.\nabla\bar{F} \qquad (2.4)$$

and $\nabla\bar{F}$ is evaluated on the axial trajectory and $\bar{r}$ is the displacement vector referred to the axial trajectory.

It is possible that $\nabla.\bar{F}$ is negative, in which case near-axial molecules would oscillate about the axial trajectory. Here the axial crossing points would define the "focal points" of the system. An analogy may be made between the principal values of the force constants of a three dimensional harmonic oscillator and the negative values of the principal derivatives, along the axis of the system,

$$\frac{\partial F_x}{\partial x}, \frac{\partial F_y}{\partial y}, \frac{\partial F_z}{\partial z}$$

These analogous "force constants" may vary along the molecular trajectory and therefore introduce a time-varying parameter which is not included in the first order or "static" focusing criterion already established. The only previous requirement is that $\nabla.\bar{F}$ be negative.

Velocity independent potentials are assumed for molecules and therefore the divergence of the force field is obtained by considering only a scalar potential energy. It is common for molecular states to have their potential energy varying as the second or first power of the applied electric field. Here, a second order interaction will be considered.

$$W = -\frac{1}{2}\alpha_m|\bar{E}|^2 \qquad (2.5)$$

represents a second order interaction with electric field, where W is the potential energy, α_m is a molecular polarisation constant that depends on the quantum state of the molecule and $|\bar{E}|$ is the magnitude of the applied electric field. Assuming that $\bar{E}$ acts in a source-free region,

$$\nabla.\bar{E} = 0 \qquad (2.6)$$

and that E is the negative gradient of some scalar function ϕ, then,

$$\bar{E} = -\nabla\phi \qquad (2.7)$$

The force on the particle is given by the negative gradient of the potential energy,

$$\bar{F} = -\nabla W \qquad (2.8)$$

According to Auerbach et al (1966) who combined these equations and wrote the vectors in terms of their components, i,j,k,

$$\nabla.\bar{F} = \alpha_m \sum_{i,j=1}^{3} \left[\frac{\partial^2 \phi}{\partial x_i \partial x_j} \right]^2 \qquad (2.9)$$

Then re-writing in terms of a co-ordinate system formed from the principal axes of the quadratic power series expansion of ϕ,

$$\nabla.\bar{F} = \alpha_m \sum_{p=1}^{3} \left[\frac{\partial^2 \phi}{\partial x_p^2} \right]^2 \qquad (2.10)$$

where p subscripts refer to principal axes.

The sign of α_m indicates whether the molecular state gains or loses energy in an applied electric field. Molecules in a given quantum state, with a given sign of α_m, will be focused or defocused depending on the electric field configuration.

The force acting on molecules in a focuser may be generalised in the following form, (Kakati 1968),

$$F = \mp \chi r^n \qquad (2.11)$$

where upper and lower signs respectively refer to upper $(-\alpha_m)$ and lower $(+\alpha_m)$ molecular energy states. Here n and χ are constants and, in particular, n is determined by the electrode

configuration. Certain cases may be considered :

(a) $n > 1$: Here the focuser has a minimum field on the axis, increasing in magnitude with radial distance from the axis. This is the case apertaining to multipole focusers which are used in beam masers : n increases with the number of poles.

(b) $0 < n < 1$: This case obtains when a cylindrical cavity is excited by a radio frequency signal to produce the required mode with a spatial gradient that will discriminate between quantum states. A discussion of this device has been given by Higa (1957). It is necessary that the resonant frequency of the required molecules is much higher than the cavity resonant frequency.

(c) $n < 0$: In this case the focuser has a maximum field near the axis decreasing with radial distance outwards. This device is capable of sorting and focusing molecules that decrease in energy in an applied field, for example, lower inversion state ammonia molecules.

2.3 The ammonia molecule

In the focusing systems to be described, ammonia gas has been employed as the working substance. The reasons for its selection are discussed here.

The ammonia molecule, NH_3, is of the symmetrical top type and its configuration is shown in figure 2.1. The electronic spectrum of the molecule, caused by the motion of electrons, allows transitions which fall in the optical frequency range.

Figure 2.1

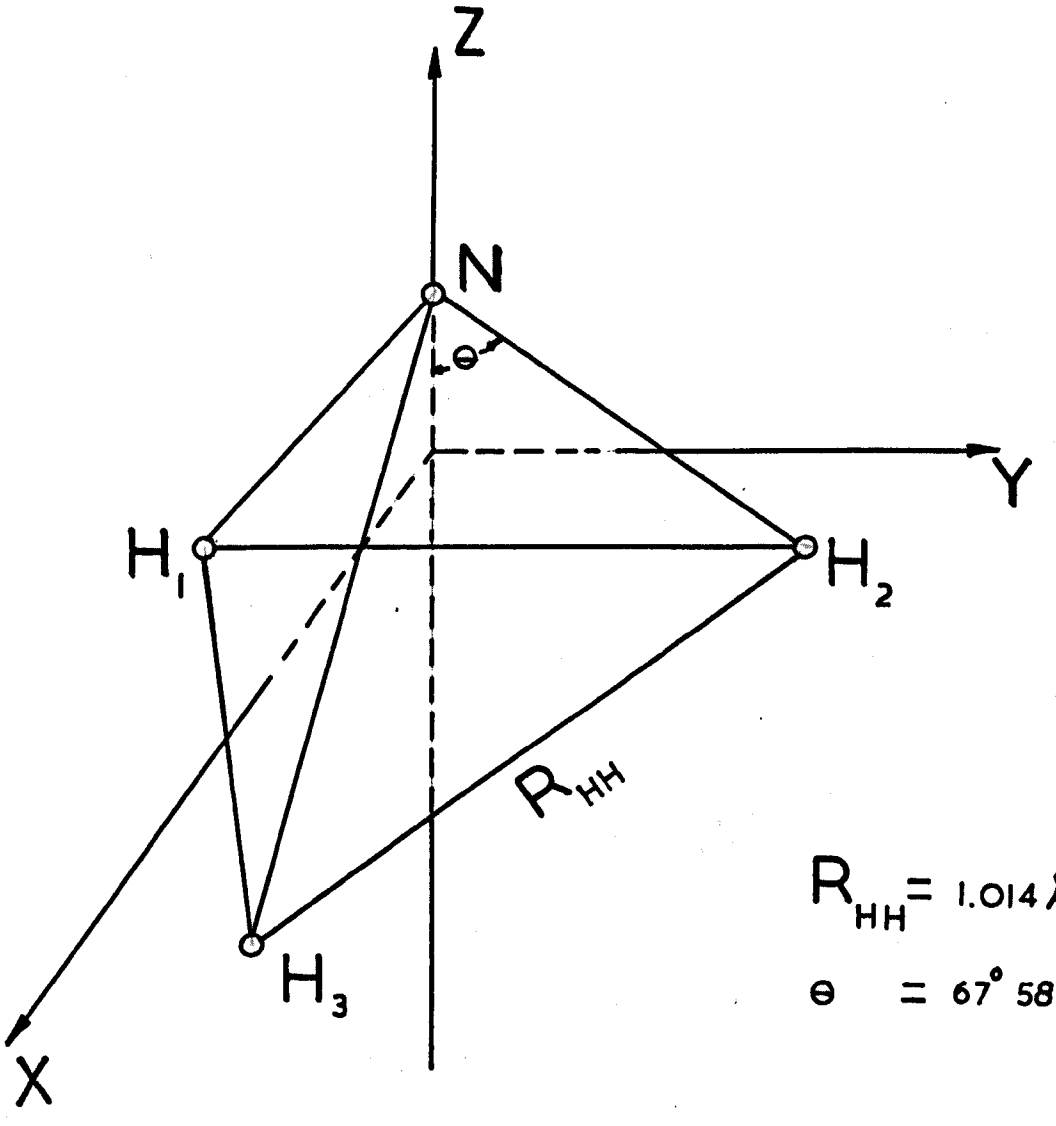

Geometrical structure of an ammonia molecule.

At room temperature the populations of the electronic energy levels are insignificantly small, since,

$$h\nu_{res} \gg kT \tag{2.12}$$

where ν_{res} is the resonant transition frequency between electronic energy levels and h,k and T have their usual meaning.

The vibrational spectrum of ammonia molecules lies in the infra-red range of the electromagnetic spectrum. As a result, at room temperature, vibrational energy levels are essentially unexcited.

The rotational energy levels of ammonia (since ammonia is of the symmetrical top type) may be described by the following equation (Oraevskii, 1964),

$$E_{JK} = hBJ(J+1) + h(A-B)K^2 \tag{2.13}$$

where J is the rotational quantum number of the molecule and K is a second rotational quantum number which is equal to the projection of J along the axis of symmetry of the molecule. A and B are rotational constants and depend on the moments of inertia of the molecule I_A and I_B, where,

$$A = \frac{h}{8\pi^2 I_A} \qquad B = \frac{h}{8\pi^2 I_B} \tag{2.14}$$

I_A is the moment of inertia of the molecule about the symmetry axis and I_B is the moment of inertia of the molecule about the axis that is perpendicular to the symmetry axis and passes through the centre of mass of the molecule. For ammonia molecules $A = 189$ GHz and $B = 298$ GHz.

Transitions between rotational energy levels are governed by the selection rule,

$$\Delta J = 0, \pm 1$$
$$\Delta K = 0 \qquad (2.15)$$

The transition frequencies between rotational energy levels are determined by the selection rule (2.15) and are given by,

$$\nu_{JK} = \frac{1}{h}(E_{J+1,K} - E_{J,K})$$
$$= 2B(J+1) \qquad (2.16)$$

Therefore, from equation (2.16), the rotational transition frequencies lie in the submillimetre wavelength range.

The ammonia spectrum has fine structure caused by inversion splitting of the energy levels. The splitting originates from the fact that the nitrogen nucleus may be found on either side of the plane of the hydrogen nuclei. On each side of the plane the nitrogen nucleus may have a stable, equilibrium position. The stable positions of the molecule are divided by a potential

barrier with finite height.

The nitrogen nucleus can oscillate about the equilibrium positions and the oscillation frequencies are identical since the potential energy function of the molecule is symmetrical with respect to the plane of the hydrogen nuclei, as shown in figure 2.2. The quantum mechanical tunnel effect allows the nitrogen nucleus to tunnel through the potential barrier dividing the equilibrium positions. Thus the oscillations of the nitrogen nucleus on either side of the hydrogen nuclei plane are not independent of each other. Therefore, in this case, the energy levels of an ammonia molecule are split into two sublevels. The splitting is termed inversion splitting. The magnitude of the splitting is determined by the oscillatory and rotational states of the molecule. The dependence upon the rotational quantum numbers J and K, of the inversion splitting, is given by (Oraevskii, (1964)),

$$h\nu_{inv} = h\Big[\nu_o \exp\big[aJ(J+1) + bK^2 + cJ^2(J+1)^2 + dJ(J+1)K^2 + eK^4\big] + \Delta\nu\Big] \qquad (2.17)$$

where,

ν_o = 23.785 GHz

a = -6.36996×10^{-3}

b = 8.88986×10^{-3}

c = 8.6922×10^{-7}

$-d = 1.7845 \times 10^{-6}$

e = 5.3075×10^{-7}

Figure 2.2

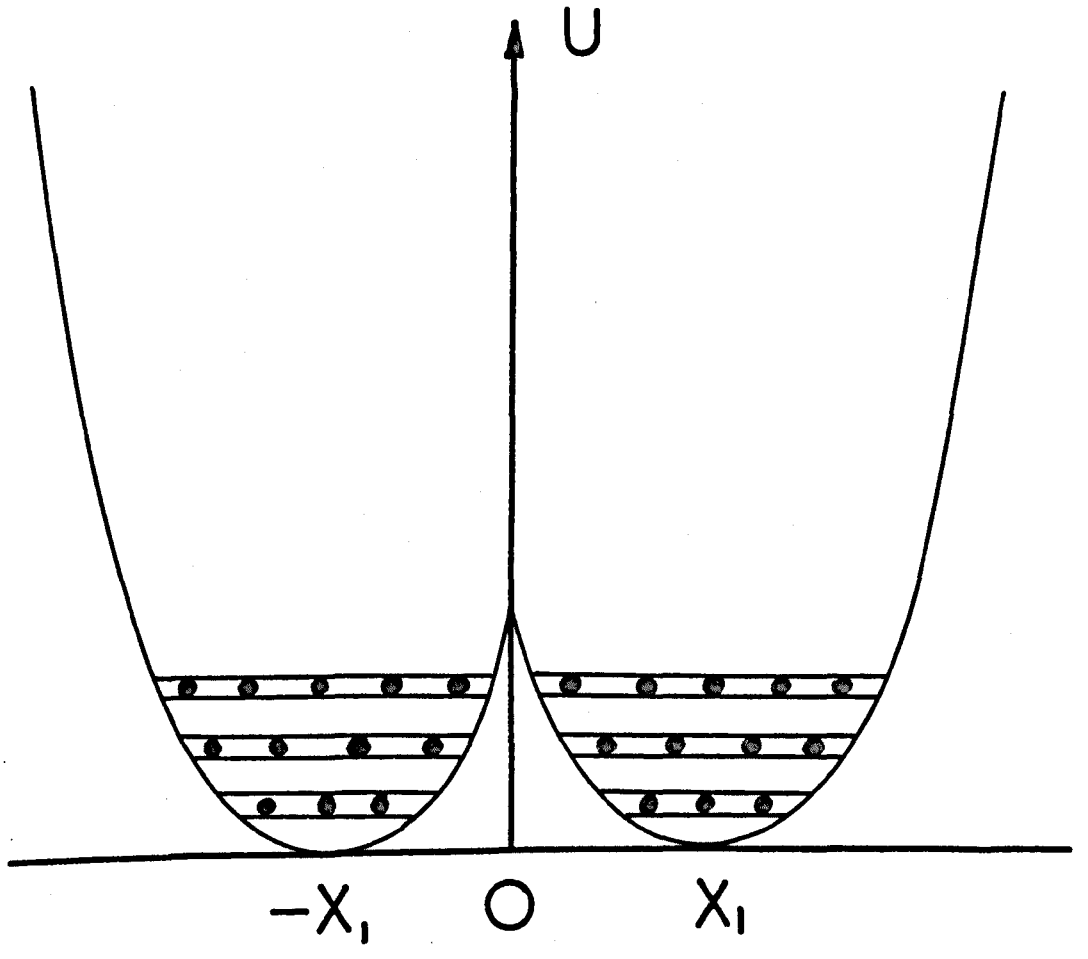

The form of the potential energy of an ammonia molecule as a function of distance between the nitrogen nucleus and the plane defined by hydrogen atoms.

(after Oraevskii, 1964)

$$\Delta\nu = \begin{cases} 0 & \text{for } K \neq 3 \\ 3.5\times10^{-4} J(J+1)[J(J+1)-2][J(J+1)-6] & \text{for } K = 3 \end{cases}$$

and

The selection rules given in (2.15) are insufficient to describe the inversion spectrum of ammonia. Therefore, new selection rules are required. All energy transitions in ammonia molecules are accompanied by a change of the inversion state, since the symmetry of the quantum mechanical wave function is different for upper and lower sublevels. Denoting the upper sublevel by (U) and the lower sublevel by (L) then the selection rules for the rotational-inversion spectrum are given by,

$$\Delta J = 0, \pm 1 \; ; \; \Delta K = 0 \; ; \; U \rightleftarrows L \qquad (2.18)$$

when, according to Oraevskii (1964),

$$\Delta J = \Delta K = 0 \; ; \; U \rightleftarrows L \qquad (2.19)$$

the purely inversion spectrum of ammonia is obtained.
From equation (2.17), the inversion spectrum should lie at $\lambda \sim 1.25$ cm.

The spectral lines of ammonia, in this part of the spectrum are relatively intense since,

(a) the dipole moment is quite large (1.47 debye),

and (b) the rotational constants of ammonia are sufficiently large to allow suitable energy separations between rotational energy levels.

The matrix element of the dipole moment for the

inversion transition is given by (Townes and Schawlow, 1955),

$$\mu_{U\to L} = \mu_o \frac{KM_J}{J(J+1)} \qquad (2.20)$$

where μ_o is the permanent dipole moment that a molecule would have in the absence of inversion and M_J is the quantum number governing the component of the total angular momentum of the molecule along the axis of the applied electric field. The matrix element is maximised when J = K. Since the intensity of spectral lines is proportional to $|\mu_{U\to L}|^2$ it may be noted that lines where J = K will be more intense than those where $J \neq K$.

The energy spectrum of ammonia also contains hyperfine structure, caused by intra-molecular interactions. The interactions may be sub-divided as follows :

(a) Quadrupole interactions: These originate from the interaction of the quadrupole electric moments of nitrogen nuclei with the intra-molecular electric field. In the presence of quadrupole hyperfine structure it is necessary to add the following selection rule to those given in (2.18),

$$\Delta F_1 = 0, \pm 1 \qquad (2.21)$$

where, if I_N is the spin of the nitrogen nucleus,

$$F_1 = I_N + J \qquad (2.22)$$

(b) Magnetic interactions: These arise from the interaction of magnetic moments of nuclei in molecules with each other and with the magnetic field induced by rotation of the molecule. An additional selection rule is required in the form of,

$$\Delta F = 0, \pm 1 \tag{2.23}$$

$$F = F_1 + I_H \tag{2.23a}$$

where I_H is the total spin of the hydrogen nuclei, such that

$$\begin{aligned} I_H &= 3/2 \text{ when K is a multiple of 3} \\ I_H &= 1/2 \text{ when K is not a multiple of 3} \end{aligned} \tag{2.24}$$

Details of the analysis summarised above have been given by Oraevskii (1964), and a composite vector diagram for moments in an ammonia molecule is shown in figure 2.3.

2.4 Ammonia molecules in electric fields

Forces are exerted on ammonia molecules in inhomogeneous electric fields because of their induced dipole moments. In zero electric fields, as a result of their inversion, ammonia molecules have no average dipole moment. With increasing electric field, the inversion is slowly quenched and an average dipole moment appears. Neglecting hyperfine effects, the energies of the inversion states may be written as (Gordon 1955),

$$W(E) = W = W_o \pm \left[\left[\frac{h\nu_o}{2} \right]^2 + \left[\frac{\mu_o M_J K E}{J(J+1)} \right]^2 \right]^{1/2} \tag{2.25}$$

Figure 2.3

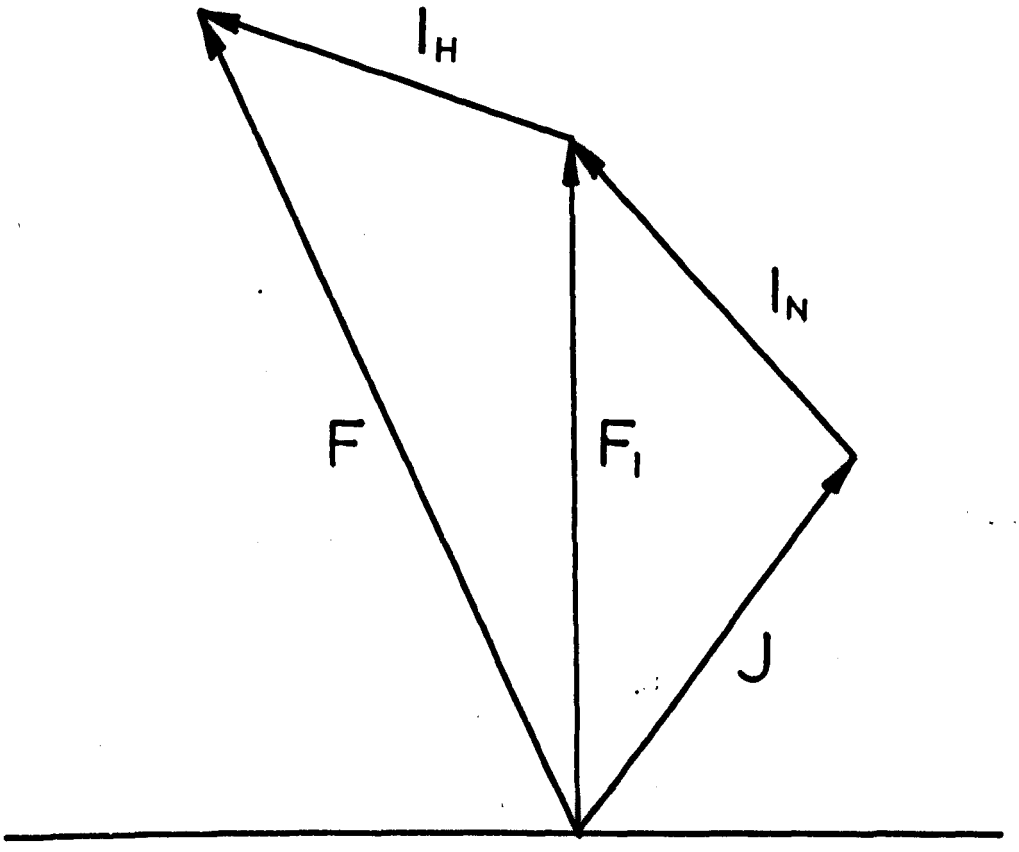

Vector diagram illustrating the composition of moments in a molecule of ammonia.

where ,

W_o = average energy of the upper and lower levels.

ν_o = inversion frequency in zero electric field.

E = the magnitude of the static electric field.

Equation (2.25) can be written in the form,

$$W = W_o \pm \left[A^2 + \mu^2 E^2\right]^{1/2} \qquad (2.26)$$

where, $$A = \left[\frac{h\nu_o}{2}\right]$$

and, $$\mu = \frac{\mu_o M_J K}{J(J+1)}$$

which can be taken as the "effective" dipole moment. The action of an electric field upon an ammonia molecule is shown in figure 2.4. It should be noted that $M_J = 0$ states are not affected by electric fields but that states where $M_J \neq 0$ will have different energies. The upper inversion energy states, with the exception of the $M_J = 0$ level, increase in energy with increasing electric field, whereas lower inversion states decrease in energy with increasing electric field.

From equation (2.8), the force on the molecule is given by,

$$F = -\nabla W = \pm \frac{\mu^2 E \nabla E}{\left[\left[\frac{h\nu}{2}\right]^2 + \mu^2 E^2\right]^{1/2}} \qquad (2.27)$$

Molecules in the upper inversion state will experience a force in the direction of minimum electric fields, while molecules in the

Figure 2.4

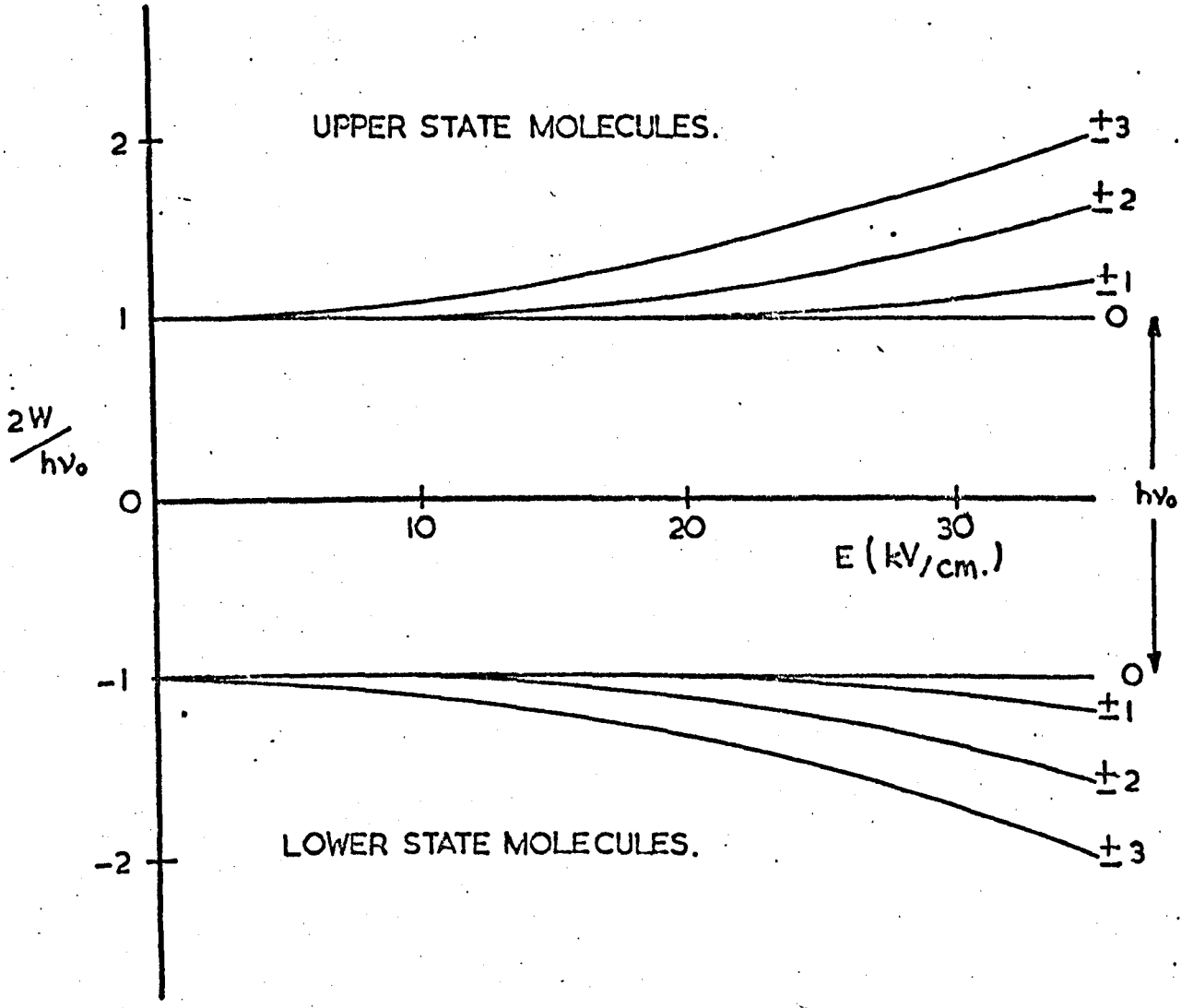

Stark effect for J=3,K=3 inversion transition of NH_3.

lower inversion state will experience an equal force but in the opposite direction.

A necessary condition for focusing is that the radial kinetic energy of the molecules is less than the maximum Stark energy ($\Delta W_{E\ max}$). The Stark energy ΔW_E for upper inversion states is given by,

$$\Delta W_E = \left[A^2 + \mu^2 E^2\right]^{1/2} - A \qquad (2.28)$$

In general, the Stark energy, as a function of transverse distance (x) across the focuser, forms a potential well, as shown in figure 2.6.

Focusing of molecules occurs when,

$$\frac{1}{2} m v_t^2 < \Delta W_{E_{max}} = \frac{1}{2} m v_c^2 \qquad (2.29)$$

where,

m = the mass of a molecule

v_t = the transverse velocity of molecules

v_c = the critical transverse velocity for focusing to occur .

2.5 Strong electric fields

In ammonia and other molecules, a complicating effect is the change in molecular constants at high electric field values. The Stark energy of ammonia undergoes a transition

from second to first order for electric field strengths > 30 kV cm^{-1}. Fields in excess of 30 kV cm^{-1} are easily attained in many of the focusers to be described later in this chapter.

Molecules with small rotational constants will not be focused efficiently in high electric fields, as a result of a reversal of slope of their Stark energy function. Peter and Strandberg (1957) calculated, for various electric field strengths, the Stark energy of sodium chloride (rotational constant $B = 6.54$ GHz). It was shown that for each quantum state there was a critical electric field value at which the force on the molecule vanished. A lattice structure of charged rods was proposed by Peter et al (1960) for focusing sodium chloride molecules, but it proved to be inefficient in practice.

2.6 Adiabatic focusing approximation

Shimoda (1961) has established a focusing criterion in the form of an adiabatic focusing approximation. This criterion is necessary, since the electric field experienced by the molecule, as it passes through the focuser, is a function of time. It is defined such that the molecule does not make any transition between unperturbed energy levels W_1 and W_2 during the time of flight through the focuser.

This restraint can be expressed by,

$$\frac{h}{(W_2 - W_1)^2}\left[\frac{\partial H'}{\partial t_{12}}\right] \ll 1 \qquad (2.30)$$

where, $\left[\frac{\partial H'}{\partial t}_{12}\right]$ is the matrix element of the time derivative of the interaction Hamiltonian between the two unperturbed energy levels W_1 and W_2. For a six pole focuser, (2.30) reduces to (Shimoda,1961),

$$\frac{\omega_\theta}{\omega_o} \cdot \frac{\Delta W}{\hbar \omega_o} \ll 1 \qquad (2.31)$$

where ω_θ is the angular frequency of the perturbing electric field as seen from in the frame of reference of a moving molecule and ω_o is the molecular transition frequency between unperturbed levels.

Putting in numerical values,

$$\frac{\omega_\theta}{\omega_o} \cdot \frac{\Delta W}{\hbar \omega_o} \longrightarrow 10^{-7} \qquad (2.32)$$

at microwave frequencies ($\sim$20 GHz). Whereas, at radio frequencies of several MHz,

$$\frac{\omega_\theta}{\omega_o} \cdot \frac{\Delta W}{\hbar \omega_o} \longrightarrow 1 \text{ to } 10 \qquad (2.33)$$

These results indicate that the adiabatic focusing approximation is not good at low frequencies.

Gordon (1955) observed that the spacing of the magnetic hyperfine lines in the ammonia microwave spectrum was sufficiently close for Fourier components of the focuser electric field to induce transitions between energy levels of moving

molecules. Consequently, the populations of the F_1 levels may be disturbed from thermal equilibrium.

2.7 Population distribution

When ammonia gas is maintained in thermal equilibrium, the fraction of molecules in any particular inversion state is given by (Townes and Schawlow,1955),

$$f = f_v \times f_r \tag{2.34}$$

where f_v is the fraction of molecules in the particular vibrational state of interest and f_r is the fraction of these molecules in a particular rotational state. For lower rotational states, f_r is approximately given by (Townes and Schawlow,1955),

$$f_r = \frac{(2J+1)g_r}{4I^2+4I+1}\left|\frac{B^2Ch^3}{\pi(kT)^3}\right|^{\frac{1}{2}} \tag{2.35}$$

where I is the spin of the hydrogen nuclei and B and C are rotational constants of the molecules. Here g_r is the degeneracy associated with spin and inversion.

Approximately 6% of the total number of molecules exist in the J = 3,K = 3 ground vibrational state at room temperature, making it the most populated level. Denoting the populations of the upper and lower energy levels respectively as N_2 and N_1, then the ratio of populations for the J = 3, K = 3 inversion state of ammonia may be deduced from the Boltzmann distribution to be,

$$\frac{N_2}{N_1} = \frac{250}{251} \qquad (2.36)$$

2.8 Molecular orientations in an electric field

The way in which the molecules in the beam are spatially orientated is an important factor. It is the spatial orientation of the molecules that determines the degree of interaction between them and the microwave electric field in the resonator. Moreover, the relative orientations of the electric sorting field and the microwave electric field in the resonator, affect the performance of the spectrometer, according to calculations of Mednikov and Parygin (1963).

Mednikov and Parygin, in their calculations, assumed that a cylindrical cavity operating in the E_{010} mode (longitudinal electric field) was employed. They indicated that a maser fitted with this type of cavity and operated using focusers with longitudinal fields would be more efficient at utilising molecules than one using focusers with transverse fields.

However, experimentally, Krupnov and Skvortsov (1963) did not obtain results that agreed with those theoretically provided by Mednikov and Parygin. Two masers, identical but for their focusers were used. One was fitted with a ring type focuser, the other with a quadrupole type. (Details of these types of focuser will be given in subsequent sections). For the same electric field strengths, both of the masers had approximately the same efficiency.

This discrepancy between theory and practice is explained by the "end effect" electric fields of the focuser systems. Detailed studies of the spatial reorientation effect of molecules, have been made by Krupnov and Skvortsov (1965). These indicate that the stray electric fields between the end of focusers and their resonators are inherently longitudinal. This is independent of the field configuration used inside the focuser. It might be anticipated that the excitation of a resonator would be stronger if the microwave electric field configuration were longitudinal with respect to the molecular beam axis. This is because the electric dipole moments would be polarised for optimum interaction with the resonator electric field.

In subsequent sections, particular types of upper and lower energy state molecular focusers will be discussed, with an emphasis on ammonia as the working substance. The multipole type focuser, which forms the basis for the electret investigations detailed in Chapter III will be considered specifically. The alternate-gradient (A.G.) technique of focusing will also be summarised as an introduction to methods of lower state focusing schemes which have been examined. However, it should be noted that the A.G. focuser has a differential focusing effect and can be used to select a beam of either upper or lower state molecules (Kakati and Lainé, 1971).

2.9 Upper state focusers

2.9.1. Multipole focusers

In section 2.4 the behaviour of ammonia molecules in electric fields was discussed with particular reference to inhomogeneous fields. The main conclusions may be briefly summarised as follows. Molecules in upper inversion energy levels experience a force in the direction of minimum electric field, whereas molecules in the lower inversion levels experience a force towards the maximum electric field.

Multipole focusers consist of an even number of parallel rods, equally spaced to form a cylinder whose length is large compared with the mean diameter of the assembly. Adjacent rods carry opposite polarity electric charge. The electrodes produce, when charged, zero electric field along the axis, increasing to high fields at the diameter of the system. The purpose of the inhomogeneous field is to interact with the molecular beam that enters in thermal equilibrium and produce two physically separated concentric beams. The focused molecules consist of the upper state type, whereas the molecules which are deflected and diffused are predominantly in the lower state. A number of theoretical analyses of this type of focuser have been performed (Shimoda 1957, Vonbun 1958).

According to Shimoda (1957) the electrostatic potential

in a 2n-pole focuser can approximately be expressed by,

$$\phi = \frac{V}{2R^n} \mathrm{Re}(x + iy)^n \qquad (2.37)$$

where R is the grazing distance between electrodes and the axis and V is the potential difference between adjacent electrodes. The electrostatic field at a distance r from the axis is,

$$E_r = \frac{n r^{n-1}}{2R^n} \cdot V \qquad (2.38)$$

When r = R the maximum electric field is obtained,

$$E_{r_{max}} = \frac{n}{2R} \cdot V \qquad (2.39)$$

For ammonia molecules the potential energy is approximately proportional to E^2. Figure 2.5 illustrates the distribution of E^2 in a 2n-pole focuser. Making the assumption that $\mu E_r < \frac{h\nu}{2}$ and expanding equation (2.25) the energy of the ammonia molecule is given by,

$$W = W_o \pm \left[\frac{h\nu}{2} + \frac{\mu^2 E_r^2}{h\nu} \right] \qquad (2.40)$$

$$= W_o \pm \frac{h\nu}{2} \pm P(r)$$

where,

$$P(r) = \frac{\mu^2 E_r^2}{h\nu}$$

and ν is the inversion frequency in zero electric field. The radial focusing force on a molecule is given by,

Figure 2.5

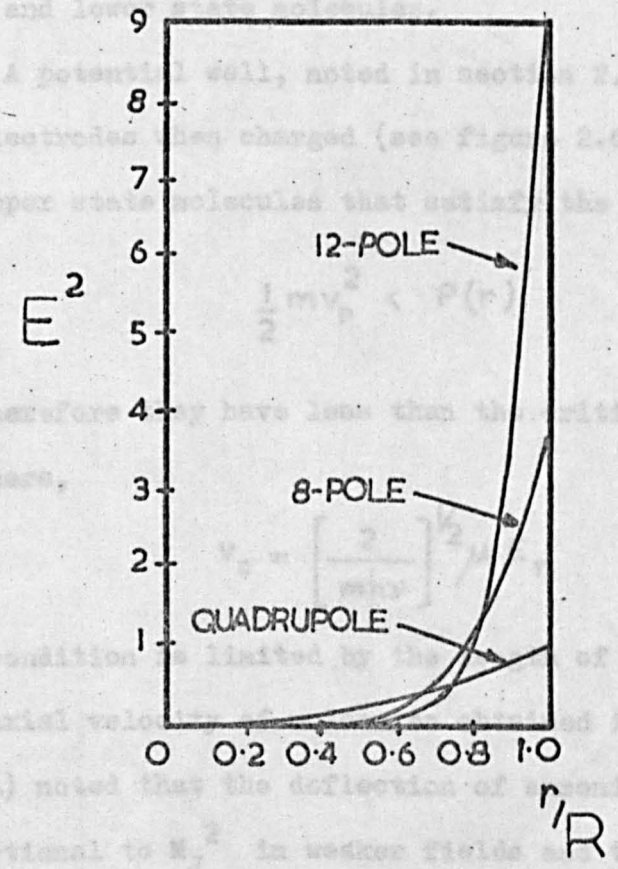

Distribution of E^2 in a 2n-pole focuser.

(after Shimoda 1957)

$$f_r = -\frac{\partial W}{\partial r} = \mp \frac{\partial P(r)}{\partial r}$$

$$= \mp \frac{2\mu^2}{h\nu} E_r \frac{\partial E_r}{\partial r} \qquad (2.41)$$

where the negative and positive signs refer respectively to upper and lower state molecules.

A potential well, noted in section 2.3, is formed by the electrodes when charged (see figure 2.6) and this confines the upper state molecules that satisfy the focusing criterion,

$$\frac{1}{2} m v_r^2 < P(r) \qquad (2.42)$$

and therefore they have less than the critical radial velocity v_c, where,

$$v_c = \left[\frac{2}{mh\nu}\right]^{1/2} \mu E_r \qquad (2.43)$$

This condition is limited by the length of the focuser and the high axial velocity of molecules obtained in practice. Becker (1963a) noted that the deflection of ammonia molecules is proportional to M_J^2 in weaker fields and to M_J in strong fields. In the first case, four pole and in the second six pole fields are the most favourable. With other even multiples of electrodes, neither of the two prerequisites is properly fulfilled.

In practice, an ideal distribution is not obtained because

Figure 2.6

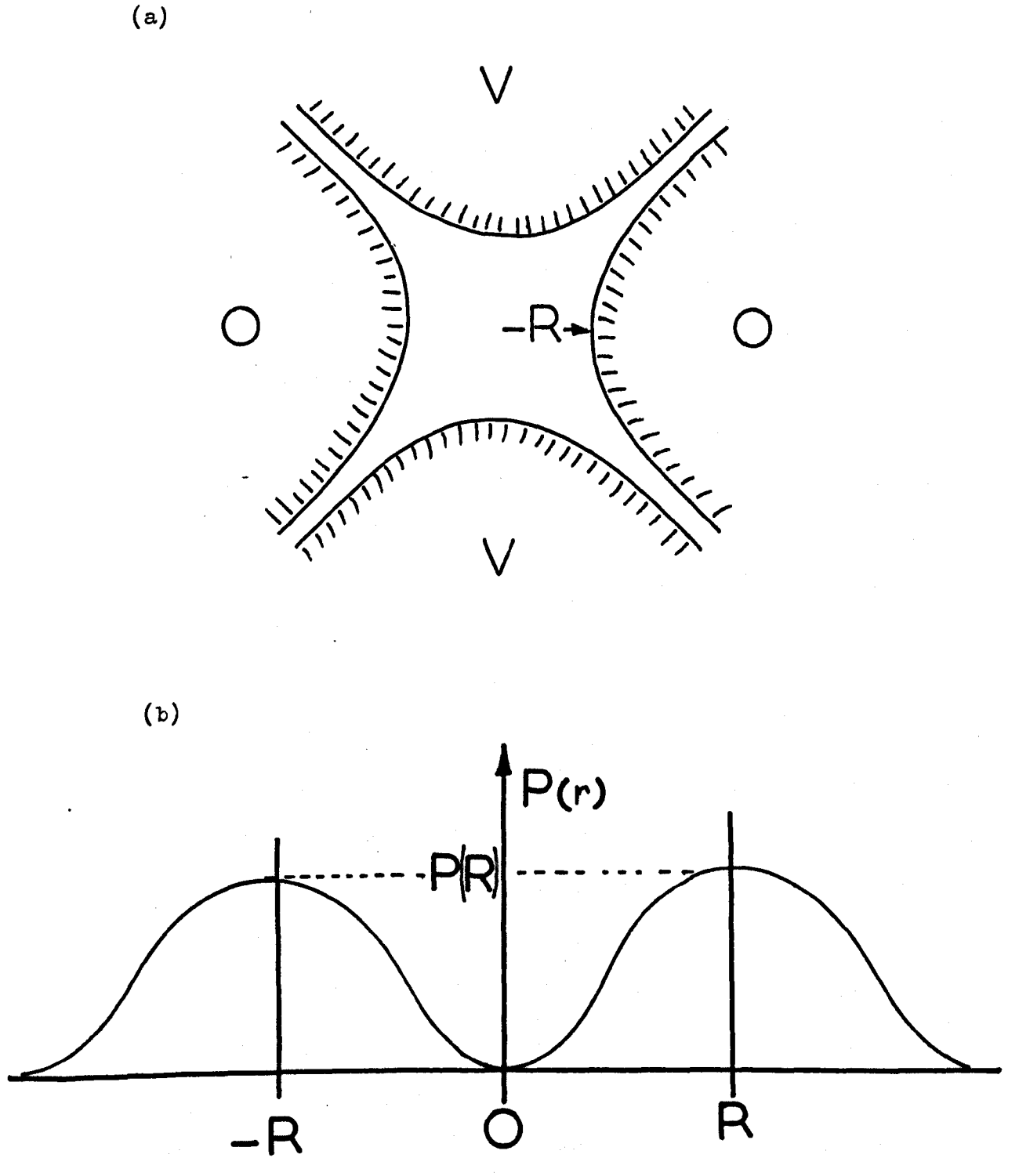

(a) Idealised quadrupole focuser cross section.

(b) Transverse potential well in a quadrupole focuser.

the electrodes are usually round in cross-section, whereas to conform to theory they should be hyperbolic. Nonetheless, with reasonable electrode diameters (~ 1.5 mm) equations (2.38) to (2.40) are satisfied to a good approximation.

Computer analysis by Vonbun (1958) indicates that in addition to state separation and focusing, multipole focusers give a degree of velocity selection. Under optimum conditions, the effect of the velocity distribution in the beam and the focuser selection are such that all molecules that arrive at the entrance of the resonator fall within a narrow velocity range. This property is useful when constructing a maser frequency standard.

2.9.2. Longitudinal fields in focusers

The sorting field in multipole focusers is essentially transverse to the molecular beam axis. Another category of upper state focuser which includes the ring and helix configurations, has the electric field longitudinal with respect to the beam axis.

The ring focuser was proposed by Krupnov (1959). The inhomogeneous electric field in this device is produced by a series of identical ring electrodes, which have a common axis and equal separation. The rings are alternately charged positively and negatively and the field increases from the axis to the periphery. Krupnov indicated that the optimum ratio of

ring radius R_o to ring separation Z_o, ε_{opt} , should be,

$$\varepsilon_{opt} = \frac{R_o}{Z_o} \sim 1 \qquad (2.44)$$

Scheglov (1961) performed a detailed analysis of the ring separator and deduced the number of active molecules which are obtained.

Also, according to Scheglov (1961) the electric field in the ring system is given by,

$$E = \frac{V_o}{I_o\left[\frac{2\pi R}{L}\right]} \cdot \frac{\sin\frac{\pi}{2}\left[1 - \frac{2\delta}{L}\right]}{\frac{\pi}{2}\left[1 - \frac{2\delta}{L}\right]} \frac{2\pi}{L} Y \qquad (2.45)$$

where, $$Y^2 = I_o^2\left[\frac{2\pi r}{L}\right]\cos^2\left[\frac{2\pi Z}{L}\right] + \left[I_o'\right]^2\left[\frac{2\pi r}{L}\right]\sin^2\left[\frac{2\pi Z}{L}\right]$$

and, $$I_o(x) = 1 + \frac{x^2}{4} - \frac{x^4}{2^4(2!)^2}$$

$$\doteq 1 + \frac{x^2}{4} \qquad \text{when } x \text{ is small}$$

$I_o(x)$ is a modified Bessel function of the first kind of

zero order, L is the period of the ring system, R is the radius and δ is the ring thickness. With δ = 0 and r = 0 (paraxial case), Kakati (1968), has noted that,

$$E = \frac{4V_o}{L}\left[1 + \left[\frac{\pi R}{L}\right]^2\right]^{-1} \cdot \cos\left[\frac{2\pi Z}{L}\right] \qquad (2.46)$$

Thus the field on the axis varies periodically between a maximum and zero and so an advantage of this system is its efficiency at focusing axial molecules. However, the transparency of the electrode system to diffused lower state molecules of ammonia is less than that of multipole systems, because lower state molecules are most likely to be scattered by the focuser electrodes, thereby reducing the sorting efficiency.

Becker (1963a) has shown that the aperture ratio is independent of focuser diameter where: aperture ratio = B/f and $B = 2R_o$, f = focal length of an equivalent lens system. The need to use large ring diameters, therefore, does not arise. More compact focusers can be made that have better efficiency than comparable multipole designs. The ring focuser design has the facility of easy variation of cross-sectional area. This in turn varies the form of the

electric field that sorts the molecular beam.

2.9.3. Parabolic focusers : a variant

Helmer et al (1960) investigated the focusing of ammonia molecular beams for a maser, both theoretically and experimentally. The shape of the focuser is determined primarily by an upper limit on the rate of change of the cross-sectional area of the beam. Thus a constraint is made on the variation of beam diameter. The criterion for this is,

$$\frac{dT}{2\pi dt} \ll 1 \qquad (2.47)$$

which restrains the period T of the molecular trajectory to change sufficiently slowly. In this way, the period in space of the molecular trajectories changes sufficiently slowly along the path of the beam, so that maximum beam transmission is obtained.

When the condition $\frac{dT}{dt}$ = constant is applied in the case of multipole design the result is,

$$R^2 = At + B \qquad (2.48)$$

where R is the inscribed radius. This is the equation of a parabolic focuser.

The focuser criterion (2.47) may be satisfied by a linear taper. When $R_b = R_o$,

$$\frac{dT}{2\pi dt} = 1 \qquad (2.49)$$

Then, when $R_b < R_o$ $\quad \frac{dT}{2\pi dt} < 1$

where R_b is the beam radius and R_o is the radius of the focuser output aperture.

Experimentally, Helmer et al showed that the molecular flow from a "point source" effuser, used in conjunction with a parabolic focuser, could be reduced by a factor of 8, for the same power output from the maser obtained when using a conventional multipole focuser.

2.9.4. Other variants

Focusers have been made to supply "flat" sorted beams for open resonators using ladder electrode configurations (Becker (1963b), Lainé and Smart (1971)). It is possible to improve the stability of maser oscillators and the resolution of beam spectrometers by employing a focused beam of slow molecules. A successful method has been the curved state-separator of the ring type, made by Strakhovskii and Tatarenkov (1964). A review of methods for obtaining slow molecules has been given by Basov and Oraevskii (1960).

The natural alternative to a focused beam of upper

state molecules for spectroscopy is one predominantly consisting of molecules in the lower energy state. The more difficult problem of obtaining absorptive focused molecular beams will be discussed in subsequent sections, with direct reference being made to experimental investigations which have been performed. A new technique will be described together with an assessment of its efficiency.

2.10 Lower state focusers

As noted in section 1.4, absorptive molecular beams are of interest from the spectroscopic viewpoint, where a large number of active molecules offers increased sensitivity, without the possibility of regenerative narrowing of spectral lines (Zuev and Cheremiskin, 1962).

Structures capable of focusing lower energy state molecules are also of interest in the development of neutral particle accelerators.

Up to the present time, only two methods of focusing absorptive molecular beams have operated successfully and been reported in the literature.

(a) A coaxial type focuser was employed by Helmer et al (1960) when a predominantly lower state molecular beam, produced by maser oscillation, was focused onto an ionisation detector.

(b) The alternate-gradient principle was applied to the

focusing of an ammonia beam by Kakati and Lainé (1967,1971). Under certain operating parameters, an absorptive focused beam was obtained.

2.10.1. The alternate-gradient focuser

The principle of alternate-gradient (AG) focusing originated in nuclear physics with application to particle accelerators. It was discussed by Courant et al (1952) but the principle was embodied in an independent patent proposal by Christofolis (1950). Auerbach et al (1966) produced a theoretical review of methods of focusing particles which decrease in energy in an applied electric field. The application of the electric AG technique was cited in particular. Kakati and Lainé (1971) have investigated this technique with particular reference to ammonia molecular beams.

Mechanically, the AG focuser consisted of a series of dipole electrodes with the beam axis as the centre of the dipoles. Adjacent dipoles were orthogonal (see figure 2.7). It was shown that molecules in both upper and lower inversion states could be focused, but those in the upper state were more highly converged.

On the basis of a simple univelocity theory, the net differential spatial focusing was predicted for a

Figure 2.7

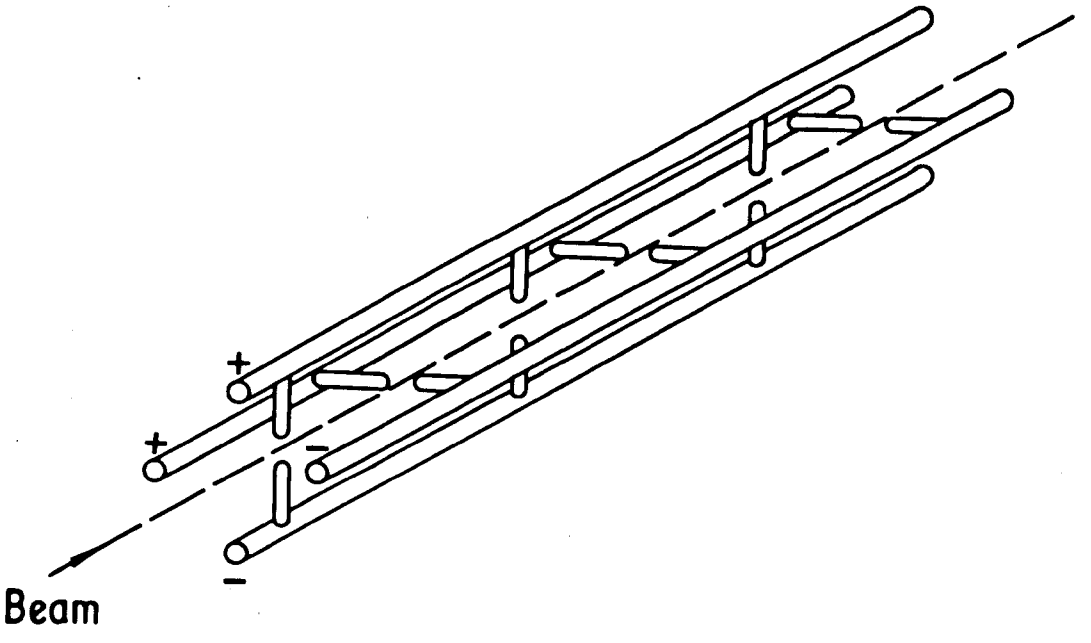

Diagram of an alternate gradient focuser.

(after Kakati and Lainé,1971)

point charge model, in which the upper state molecules were more highly converged than the lower state molecules. A similar but smaller differential focusing effect was predicted using a line charge model. It was expected that a practical design of alternate-gradient focuser would behave in an intermediate manner indicated by the point and line charge theoretical models.

With the need for devices capable of sorting molecules which decrease in energy in an applied electric field, various electrode configurations have been experimentally investigated. New electrode designs have been considered and in particular the development of the "crossed-wire" focuser is also described and discussed.

To evaluate the performance of the various designs of focusers, a conventional molecular beam spectrometer was employed. Details of the spectrometer are described in Appendix I.

2.10.2 The coaxial focuser

The coaxial focusers employed by Helmer et al (1960) had the property of defocusing any higher energy state molecules that entered it. An optimum ratio of inner electrode diameter to outer electrode diameter of 1 : 3 or 4, for efficient focusing action, was reported.

Helmer et al used their coaxial focuser after the resonant cavity and monitored the beam with an ionisation detector. In the experiments to be described a coaxial focuser was used before the resonant cavity and the beam was observed spectroscopically.

(i) Design of the coaxial focuser

The coaxial focuser is illustrated in figure 2.8. The active centre electrode was a 100 mm long metal taper, 3.1 mm diameter near the effuser and 1.5 mm at the exit. The cross-section of the centre electrode allowed a clear trajectory for molecules leaving the effuser to pass to the end of the electrode and then to enter the resonant cavity.

The effuser consisted of six holes (1 mm in diameter and 10 mm long) in a diameter to length ratio that may be considered optimum after investigations on the directivity of ammonia molecular beams by Naumov (1963). The channels were set on a 10 mm pitch circle diameter. The centre electrode did not abut directly against the plane of the end of the effuser. This was because it was found in preliminary experiments that electrical breakdown occurred across the face of the effuser. This was probably due to a localised increase in gas pressure, before the beam was formed, in the vicinity of the effuser exit. The problem was solved by extending the centre electrode on an insulating spigot made out of PTFE.

Figure 2.8

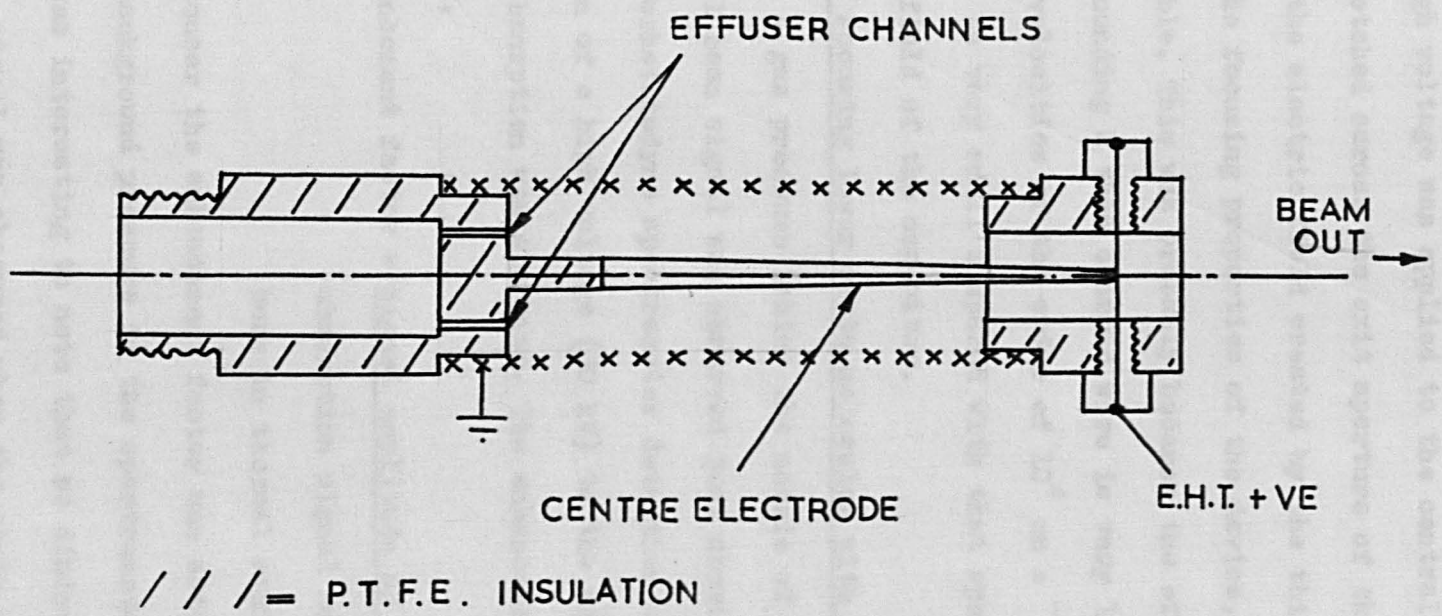

The coaxial focuser.

A high voltage was applied to the central electrode via a wire stretched across the exit aperture of the focuser. The effect of the electric field created by the thin transverse wire, on the focusing properties of the device, was found to be negligible. This was probably because the effective electric field surrounding a thin charged wire is very localised and with molecular velocities of the order of 10^4 cm s^{-1} the interaction time would be very small compared with that spent in the strong, extensive field of the capacitor.

(ii) Focusing lower state molecules with the coaxial focuser

With a gas pressure behind the nozzle of 0.95 torr the thermal beam signal was observed just above the noise level of the superheterodyne spectrometer detection system. Upon application of a high voltage (30 kV) to the separator a signal of enhanced absorption was observed. The enhancement factor is defined by,

$$\text{enhancement factor} = \frac{\text{signal amplitude of enhanced absorption}}{\text{absorption signal amplitude of a molecular beam in thermal equilibrium.}}$$

In this focuser the enhancement factor was estimated to be ~ 2, when the background pressure in the spectrometer was $\sim 1 \times 10^{-5}$ torr.

It was interesting to note that no diminution of the enhanced absorption signal was observed when the earth connection to the outer

electrode was removed. In this situation, the actual earthing boundary for the central electrode was determined by the cylindrical metal dewar that surrounded the focuser. The dewar served to reduce the pressure in the system by freezing-out, (a) impurities, (b) higher energy state molecules ejected from the focuser and (c) molecules not captured by the focuser. The radial symmetry of the electric sorting field surrounding the central electrode was preserved and thus provided efficient molecular sorting. This fact has been previously noted, theoretically, by Auerbach et al (1966), when they indicated in their conclusions that the single-wire electric field is essentially the same, in its focusing behaviour, as the cylindrical capacitor electric field.

2.10.3 The single-wire focuser

A single-wire focuser has several design features to recommend it. In particular, these are ease of construction, use with an on-axis effuser and transparency to ejected molecules.

(i) Design of the single-wire focuser

The single-wire focuser, illustrated in figure 2.9, consisted of a 100 mm length of wire (approximately 0.6 mm in diameter) suspended on the molecular axis by two thin transverse wires which in turn were supported on two parallel brass rods 30 mm apart. It was established, experimentally, that the supporting system alone did not affect the focusing of the

Figure 2.9

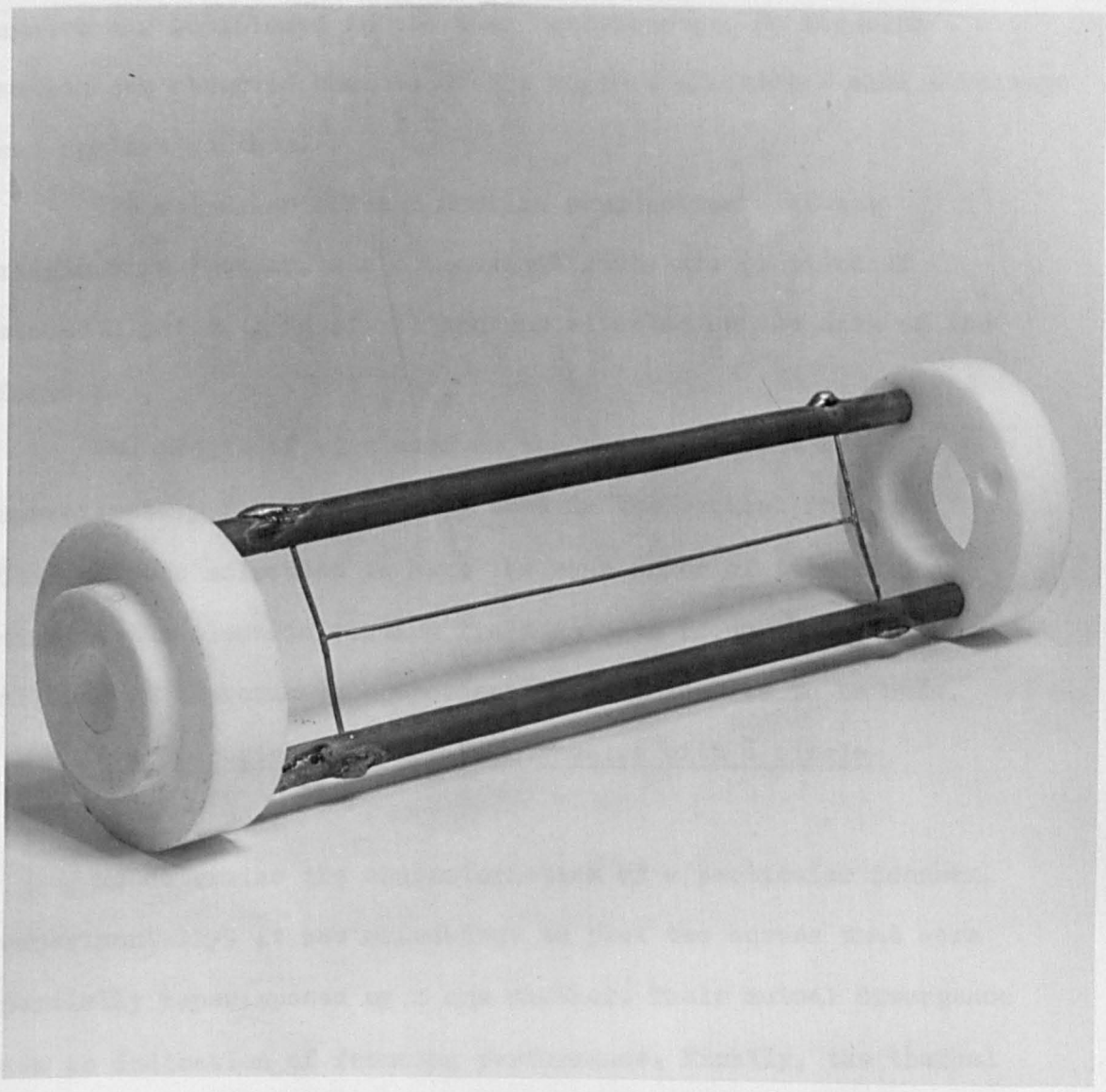

The single-wire focuser.

molecular beam significantly as follows. The 100 mm long active element was removed from its supports and the supporting system was positioned in the beam spectrometer. No focusing action was observed because of the support electrodes when a voltage was applied to them.

The molecular effuser used in conjunction with the single-wire focuser, was a honeycomb structure (a piece of etched klystron grid stock) and was situated on the axis of the focuser.

The length of wire used as the active element was approximately the same as that used in the coaxial focuser. This allowed molecules to have the same order of interaction time in the electric sorting field in both focusers and thus allowed an approximate comparison of efficiencies to be made.

(ii) Focusing lower state molecules with a single-wire focuser

To determine the characteristics of a particular focuser, experimentally, it was convenient to plot two curves that were partially superimposed upon one another. Their mutual divergence was an indication of focusing performance. Firstly, the thermal beam absorption signal amplitude was plotted as a function of the nozzle pressure. Secondly, with the maximum voltage available (30 kV) upon the focuser, the enhanced absorption signal amplitude was plotted as a function of nozzle pressure. The

resulting curves may be seen in figure 2.10 together with a curve indicating the variation of background pressure with nozzle pressure.

The divergence of the thermal beam and enhanced absorption curves, results from space focusing of lower state molecules preferentially with respect to higher state molecules .

When the nozzle pressure was set at the optimum value obtained from the characteristic shown in figure 2.10 the variation of signal amplitude with separator voltage was plotted. This characteristic, shown in figure 2.11, indicates the separator voltage at which effective sorting of molecules commences. It may be noted, from the curve shown in figure 2.11, that the number of active molecules in the enhanced beam can be increased, if required, by increasing the separator voltage beyond 30 kV.

2.10.4 The Maltese - cross focuser

Auerbach et al (1966) proposed that the Maltese - cross geometry should be suitable for focusing electrically neutral particles which decrease in energy in an applied electric field. The structure is shown in figure 2.12. They commented that, at first sight, the design of the electrodes would create the required sorting field but added that the Maltese - cross geometry would focus lower energy state molecules in the radial plane (indicated by R) but would defocus in the Θ plane (Θ and

Figure 2.10

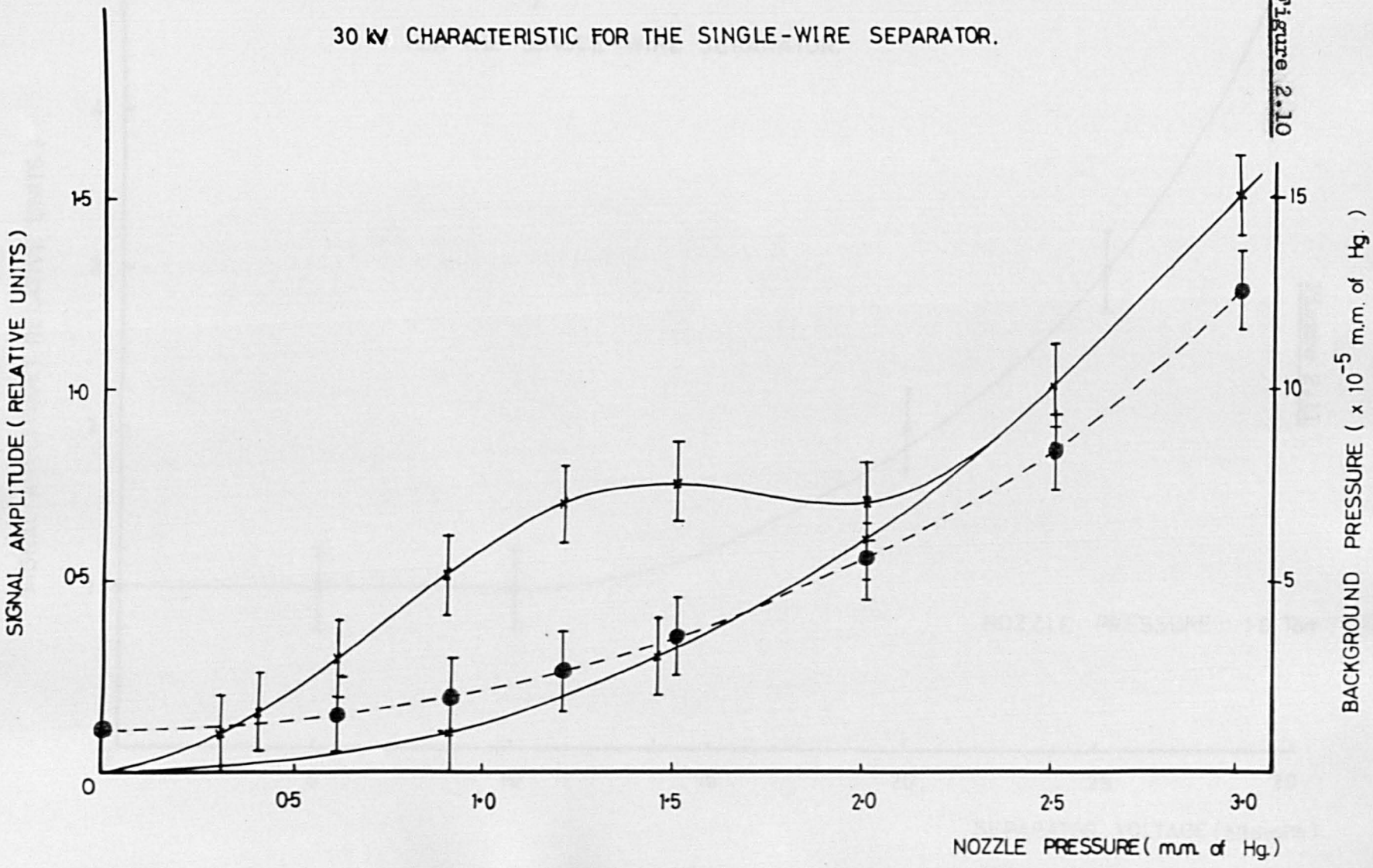
30 kV CHARACTERISTIC FOR THE SINGLE-WIRE SEPARATOR.
SIGNAL AMPLITUDE (RELATIVE UNITS)
BACKGROUND PRESSURE (x 10⁻⁵ m.m. of Hg.)
NOZZLE PRESSURE (m.m. of Hg.)
0
0·5
1·0
1·5
2·0
2·5
3·0
5
10
15

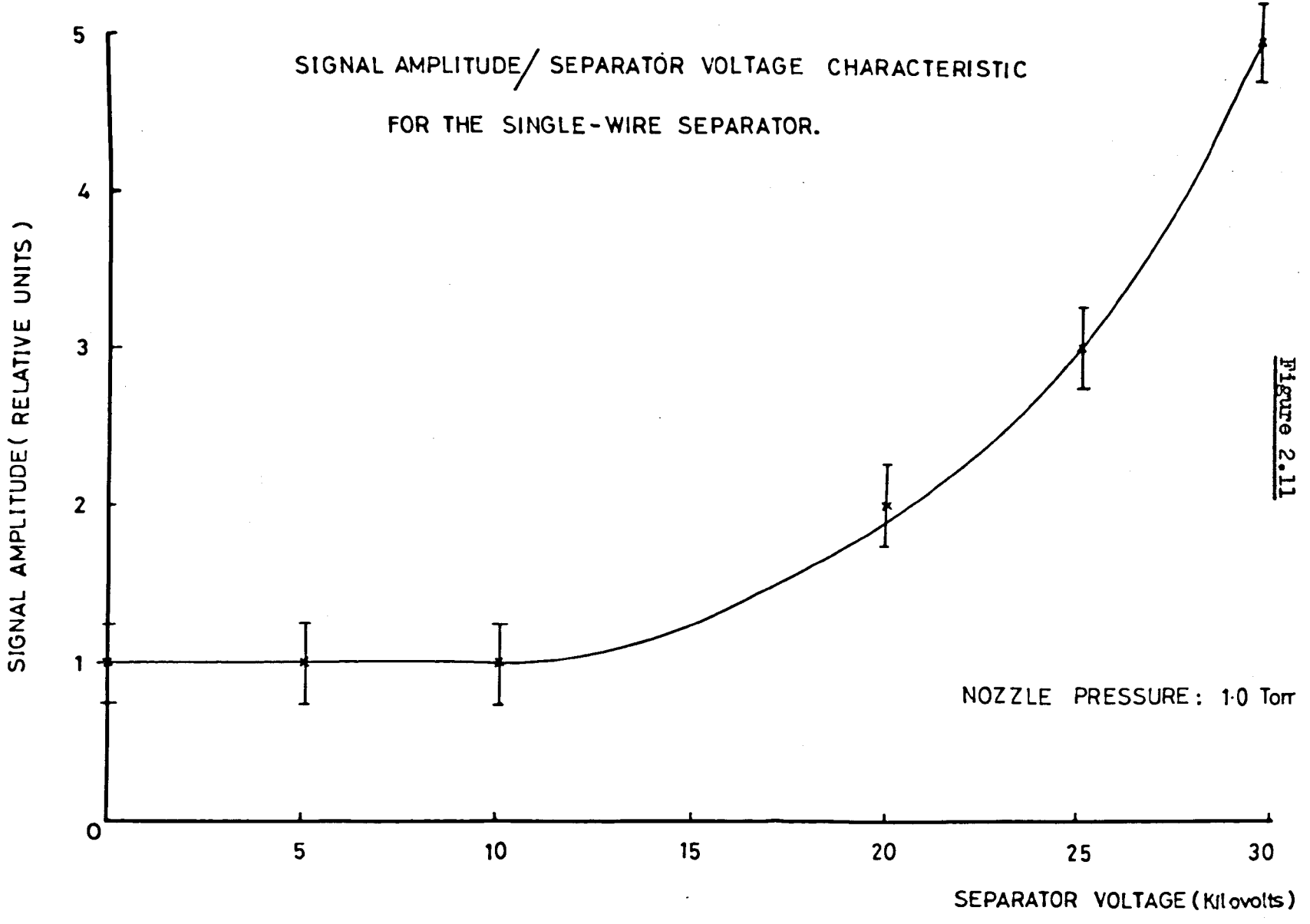
SIGNAL AMPLITUDE/ SEPARATOR VOLTAGE CHARACTERISTIC
FOR THE SINGLE-WIRE SEPARATOR.
SIGNAL AMPLITUDE (RELATIVE UNITS)
0
1
2
3
4
5
5
10
15
20
25
30
SEPARATOR VOLTAGE (Kilovolts)
NOZZLE PRESSURE: 1·0 Torr

Figure 2.11

Figure 2.12

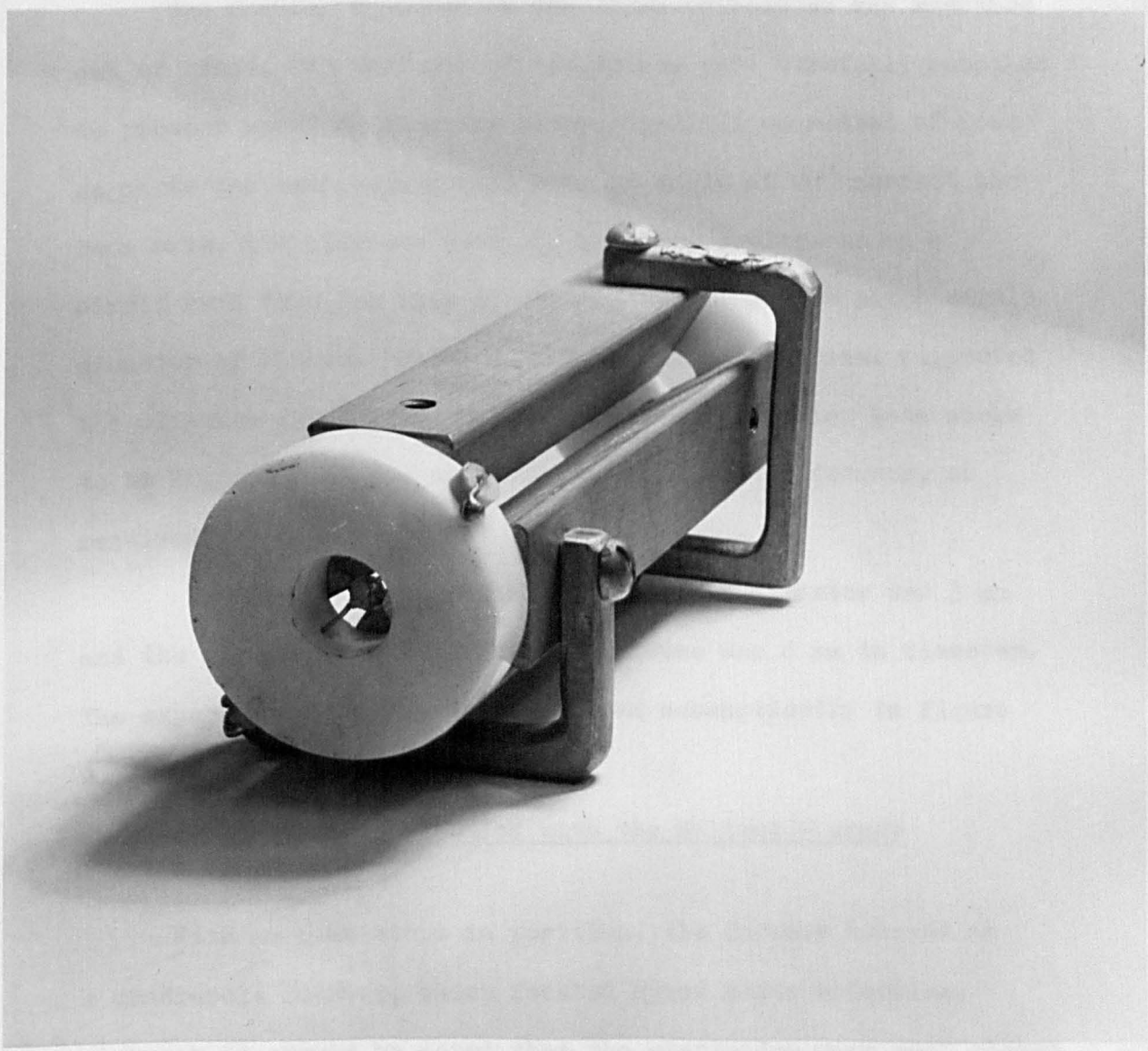

The Maltese-cross focuser.

R are shown in figure 2.13).

(i) Design of the Maltese - cross focuser

The focuser designed on the above principles was machined out of brass. The surfaces of the device were carefully smoothed to prevent sparking from any sharp edges. It consisted of four segments and each segment had a wedge angle of 60° nearest the beam axis. The elements were 100 mm long, equispaced on a circle such that the apex of each element lay on a pitch circle diameter of 2.4 mm. Rings of PTFE insulation material supported the elements in position and were machined to allow beam stops to be supported at the entrance and exit of the focuser, as required.

The honeycomb molecular beam effuser diameter was 3 mm and the resonant cavity entrance aperture was 4 mm in diameter. The experimental arrangement is shown schematically in figure 2.14.

(ii) Focusing molecules with the Maltese - cross focuser

With no beam stops in position, the focuser behaved as a quadrupole focuser, which focused upper state molecules, although it should be noted that the electrodes were much closer to the molecular beam axis than in a conventional quadrupole focuser. Positions I and II as indicated in figure 2.14 were available to place beam stops in the focuser. The beam stops were employed in an effort to obtain an absorptive signal,

Figure 2.13

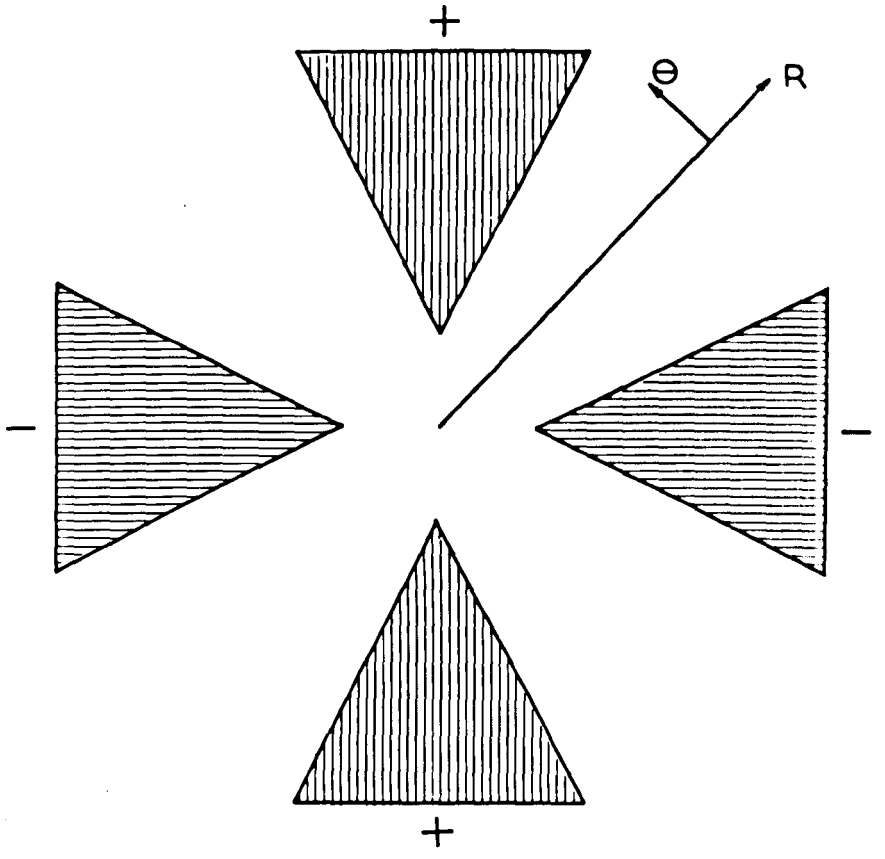

MALTESE-CROSS SEPARATOR IN CROSS-SECTION.

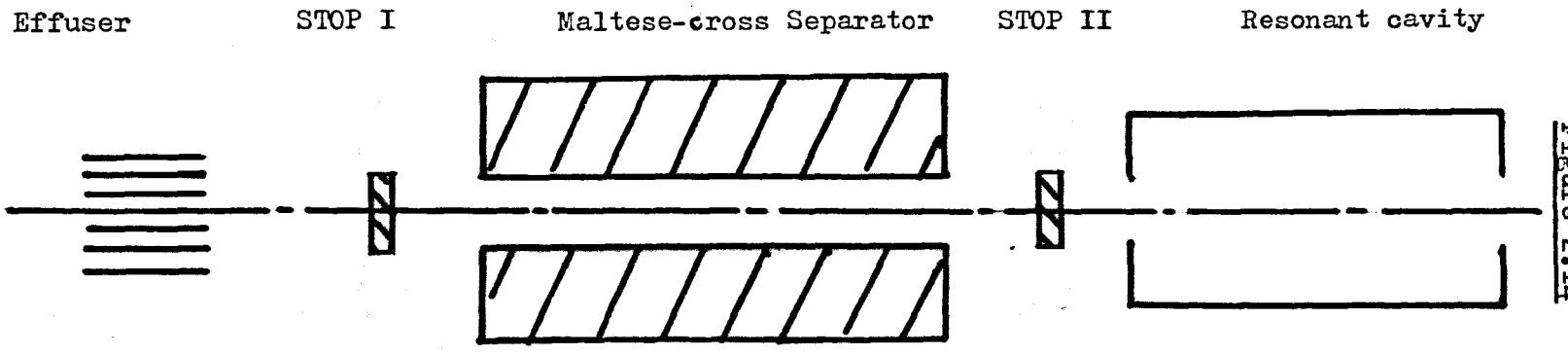

Figure 2.14

Scheme of the apparatus used in the investigations of the Maltese-cross Separator.

(Not to scale.)

rather than a stimulated emission signal.

The object of inserting the beam stops was two fold:

(a) Stop position I was intended to prevent molecules which left the effuser from entering the on-axis electric field between the elements of the focuser. Molecules entering this portion of the electric field would, most probably, have been state selected to give an emissive molecular beam.

(b) Stop position II was intended to prevent the ammonia molecules (probably higher energy state) that left the device on-axis, from entering the resonant cavity. This should have ensured that only lower energy state molecules, focused in the segment electric field between adjacent electrodes, were able to enter the resonant cavity.

These beam stops should have also prevented molecules in the $M_J = 0$ state from entering the cavity.

Stops equivalent to 0.5 and 1.25 times the effuser area were fabricated. They were used, one at a time, in each of modes (I) and (II) described above. However, in all cases except one, (when the 1.25 area stop was in position I and no signal was observed, since no molecular beam was probably formed) a stimulated emission signal was observed.

(iii) Discussion

The behaviour of the Maltese - cross focuser may be intuitively deduced from the fact that two electric field

configurations were available with which the ammonia molecules could interact as they passed through the focuser. A plot of the equipotentials for the Maltese - cross focuser may be seen in figure 2.15. The form of the electric field in the structure is governed by the condition that electric field lines are orthogonal to equipotential lines. An intense quadrupole type electric field exists in the volume described by the edges of the electrodes, whereas there is a much weaker diverging electric field between the elements of the focuser.

The dominant quadrupole electric field probably space sorted upper energy state molecules and ejected lower energy state molecules, giving them a considerable radial velocity component. The weaker, lower energy state focusing electric field between the segments of the focuser was probably unable to apply a sufficiently large restoring force to molecules which decrease in energy in an applied electric field. Therefore, the latter molecules would be lost from the system.

2.10.5. The crossed-wire focuser

(i) Introduction

Helmer et al (1960) noted the catastrophic increase in electric field strengths as the central electrode of a coaxial focuser was approached. This characteristic prevents the coaxial design from being a "true" focuser, in that molecules are unable to attain a periodic motion about the axis of the

Figure 2.15

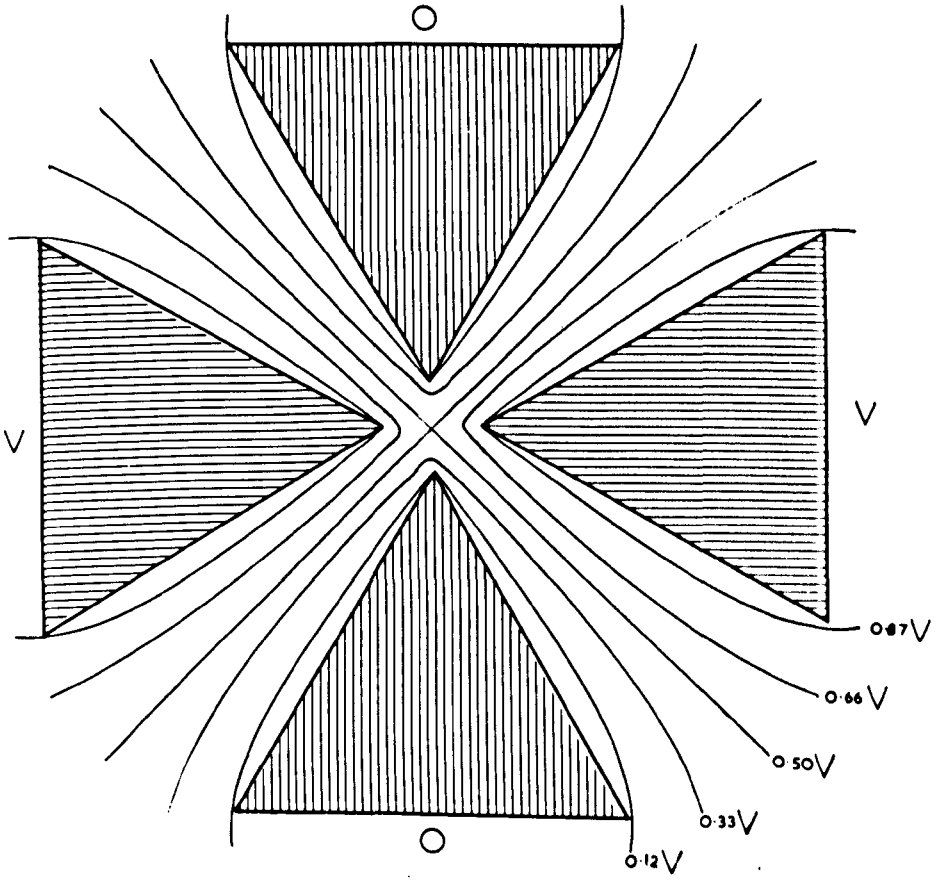

MALTESE-CROSS: ELECTRIC FIELD EQUIPOTENTIALS.

device. Removal of portions of the central electrode would allow a periodic motion for molecules but the practical problems involved in supporting the electrode elements appear to outweigh the advantages.

A radically new design of focuser for molecules which decrease in energy in an applied electric field has been developed using ammonia as the working substance. It has been termed the "crossed-wire" focuser (Lainé and Sweeting, 1971).

In essence, the crossed-wire focuser consists of an array of mutually perpendicular wires, adjacent wires carrying opposite polarity electric charges. This design is inherently simple and has a number of features to commend it:

(a) Intense inhomogeneous fields surround the thin wires.

(b) A strong electric field $\sim$ 200 kV cm^{-1} exists along the axis where it is most effective.

(c) A built in "beam-stop" prevents molecules with quantum number $M_J = 0$ from entering the resonant cavity. These molecules are essentially undeflected in an electric field and would tend to reduce the enhancement factor.

(d) The system has a good overall transparency to the molecular beam. Experiments have shown, however, that the wire diameter is a critical factor.

(e) Molecules are allowed to perform a periodic motion through the central axis of the separator structure.

(f) The electric sorting field is essentially longitudinal.

(ii) Preliminary design investigations

Preliminary investigations of the crossed-wire structure were required before an operational model was constructed. A number of criteria had to be satisfied. The inhomogeneous electric sorting field had to have as large a spatial extent as possible. This would allow most of the cross-sectional area of the molecular beam to interact effectively with the electric field. A limiting factor for this requirement was that the structure of the focuser should remain sufficiently transparent to keep the scattering of the beam to a minimum.

A further constraint on the focuser design was that molecules leaving from any point on the exit of the effuser, with trajectories parallel to the focuser axis, should pass through an electric field capable of sorting them efficiently. The constraint, taken in practice, was that an electric field equal to half that existing on the axis of the device should exist periodically along the focuser at a transverse distance away from the axis equal to the separation of adjacent electrodes.

The ratio of wire diameter to wire separation required to create the electric field configuration described above

was determined from a model of the focuser placed in an electrolytic tank. The electrolytic tank method that was adopted employed an alternating current technique. A "scaled-up" model of the crossed-wire focuser was constructed out of 1.5 mm diameter metal rods. The separation between adjacent rods was variable. The whole structure was immersed in a weak solution of sodium chloride in water. The electric field created by an alternating current signal was probed and null points were determined using an oscilloscope. A suitable electric field configuration was obtained when the ratio of wire diameter to wire separation was~25 : 1

(iii) Construction of the prototype

The initial version of the crossed-wire focuser will be described in some detail, since subsequent models had only minor modifications.

The crossed-wire electrodes were supported between four equispaced brass rods 4.5 mm in diameter. The support rods were fitted into two PTFE insulating rings. The focuser is illustrated in figure 2.16. The wire electrodes were 0.13 mm in diameter, while adjacent electrodes were separated, on the focuser axis, by 2.51 mm. There were 34 electrodes (17 pairs of focusing elements) giving an active focuser length of 83 mm. Voltages in excess of 30 kV could be applied to the focuser without electrical breakdown, producing electric fields well

Figure 2.16

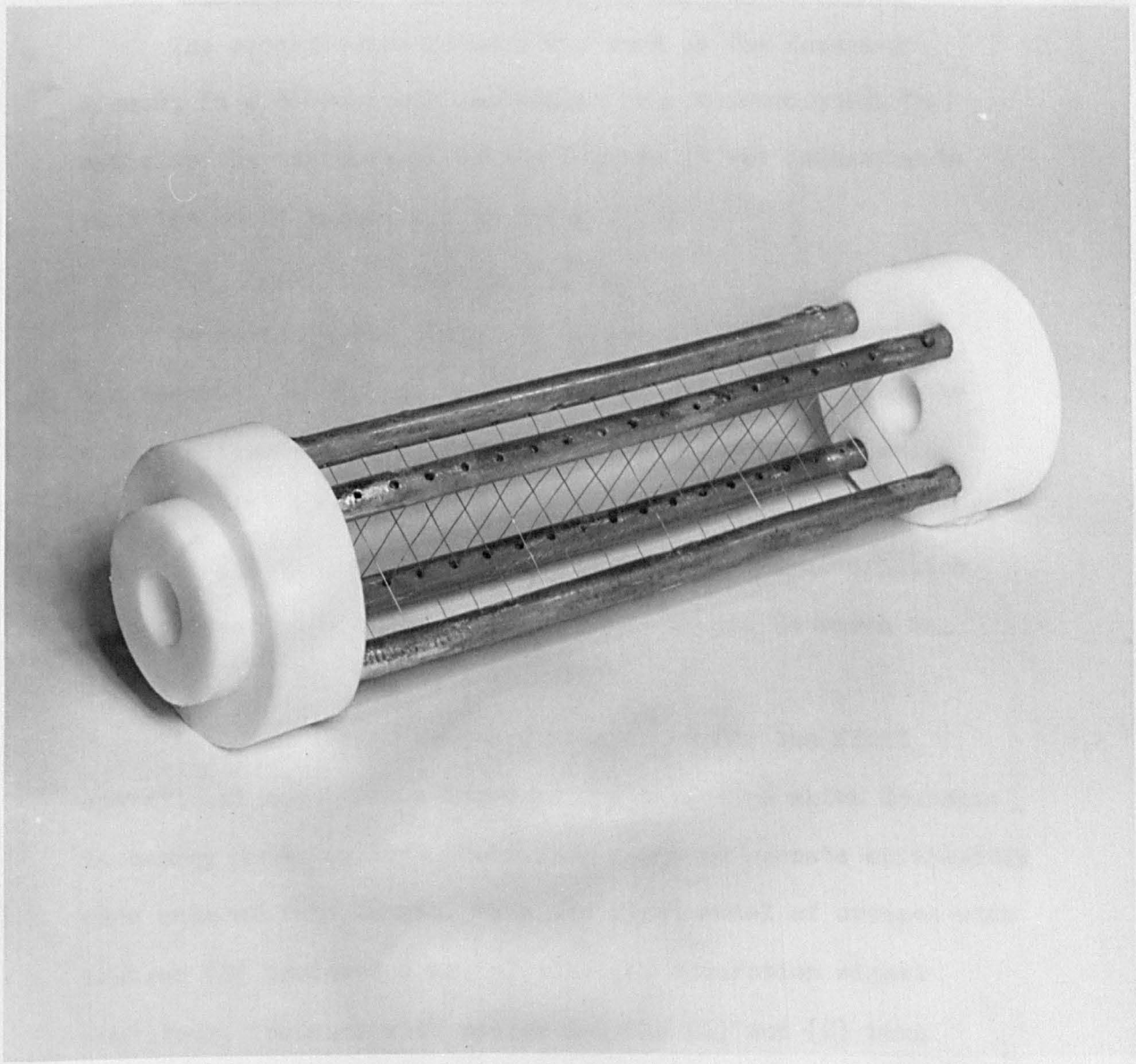

The crossed-wire focuser.

in excess of 200 kV cm^{-1}.

(iv) Parameters affecting focuser characteristics

The crossed-wire focuser was used as the focusing element in a conventional molecular beam spectrometer. To optimise the performance of the focuser it was necessary to vary the basic parameters in turn.

(a) Variation of active length

To optimise the number of active molecules entering the resonant cavity, focusers with different active lengths were constructed. These had active lengths of (A) 40 mm, (B) 80 mm (C) 120 mm.
Enhanced and thermal beam absorption signal characteristics were plotted as a function of nozzle pressure as shown in figures 2.17, 18, 19.

An 80 mm active length was selected for the first operational model since focusers for molecules which increase in energy in an applied field were found to operate efficiently when made of this length. When the first model of crossed-wire focuser (B) produced a useful enhanced absorption signal amplitude, focusers with active lengths (A) and (C) were constructed, with the other focuser parameters unchanged.

To make comparison of the crossed-wire focusers viable, it was essential that the background pressure for the longest focuser, type (C) should be particularly low. This would

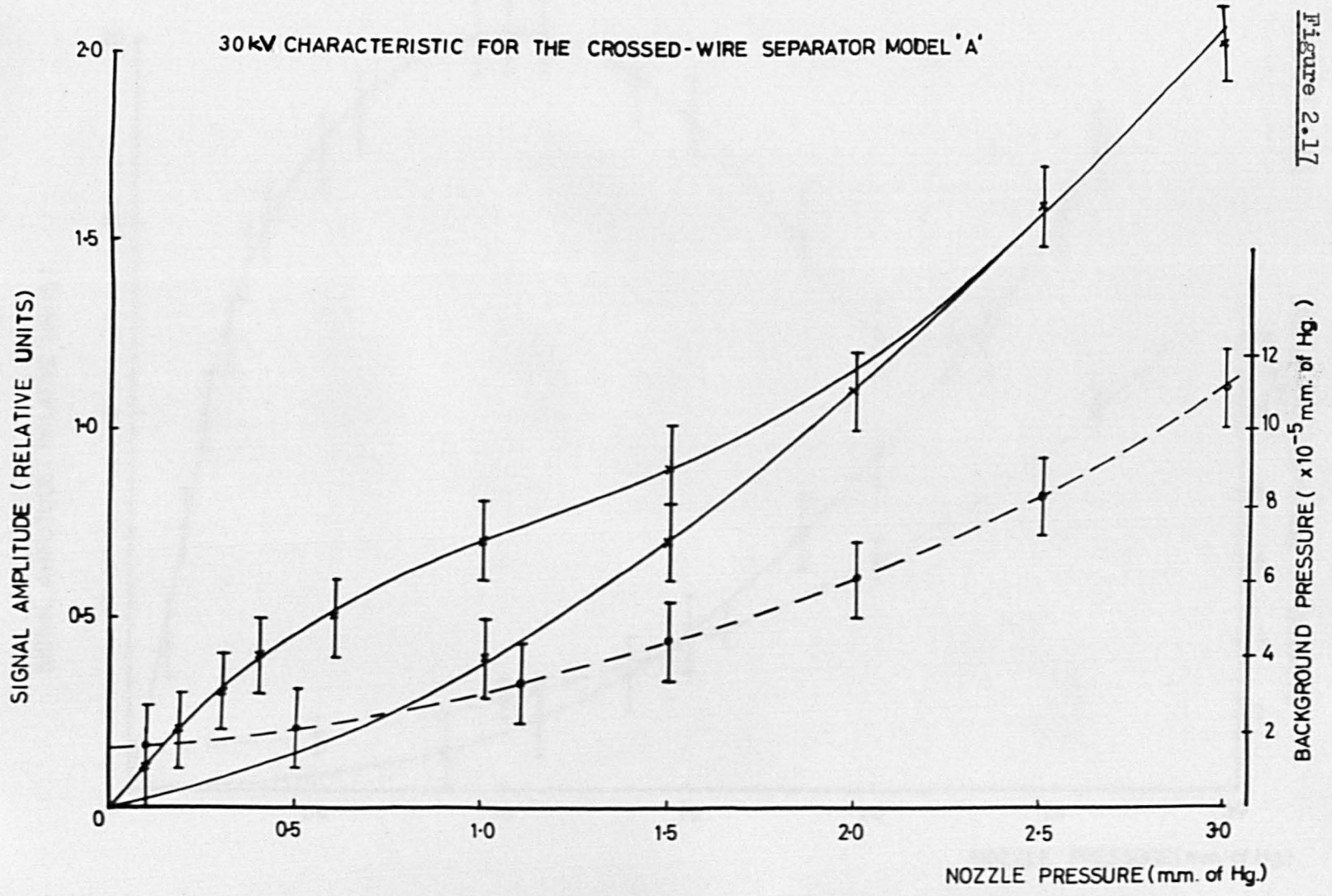
30 kV CHARACTERISTIC FOR THE CROSSED-WIRE SEPARATOR MODEL 'A'
SIGNAL AMPLITUDE (RELATIVE UNITS)
2·0
1·5
1·0
0·5
0
0·5
1·0
1·5
2·0
2·5
3·0
NOZZLE PRESSURE (mm. of Hg.)
BACKGROUND PRESSURE (x10⁻⁵ mm. of Hg.)
12
10
8
6
4
2

Figure 2.11

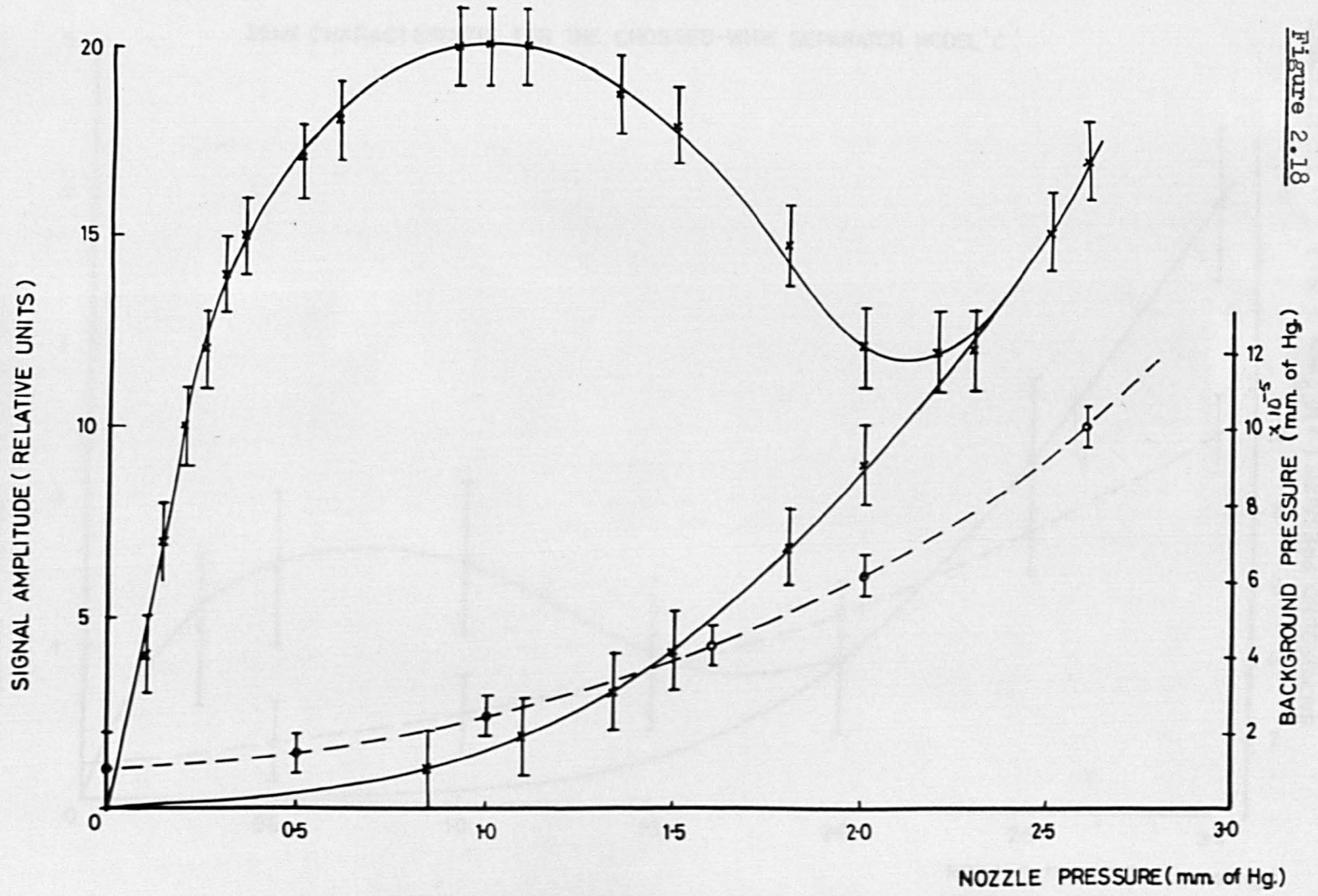
30kV CHARACTERISTIC FOR THE CROSSED-WIRE SEPARATOR MODEL 'B'
SIGNAL AMPLITUDE (RELATIVE UNITS)
BACKGROUND PRESSURE (mm. of Hg.) x 10⁻⁵
NOZZLE PRESSURE (mm. of Hg.)
0
5
10
15
20
0·5
1·0
1·5
2·0
2·5
3·0
2
4
6
8
10
12

Figure 2.18

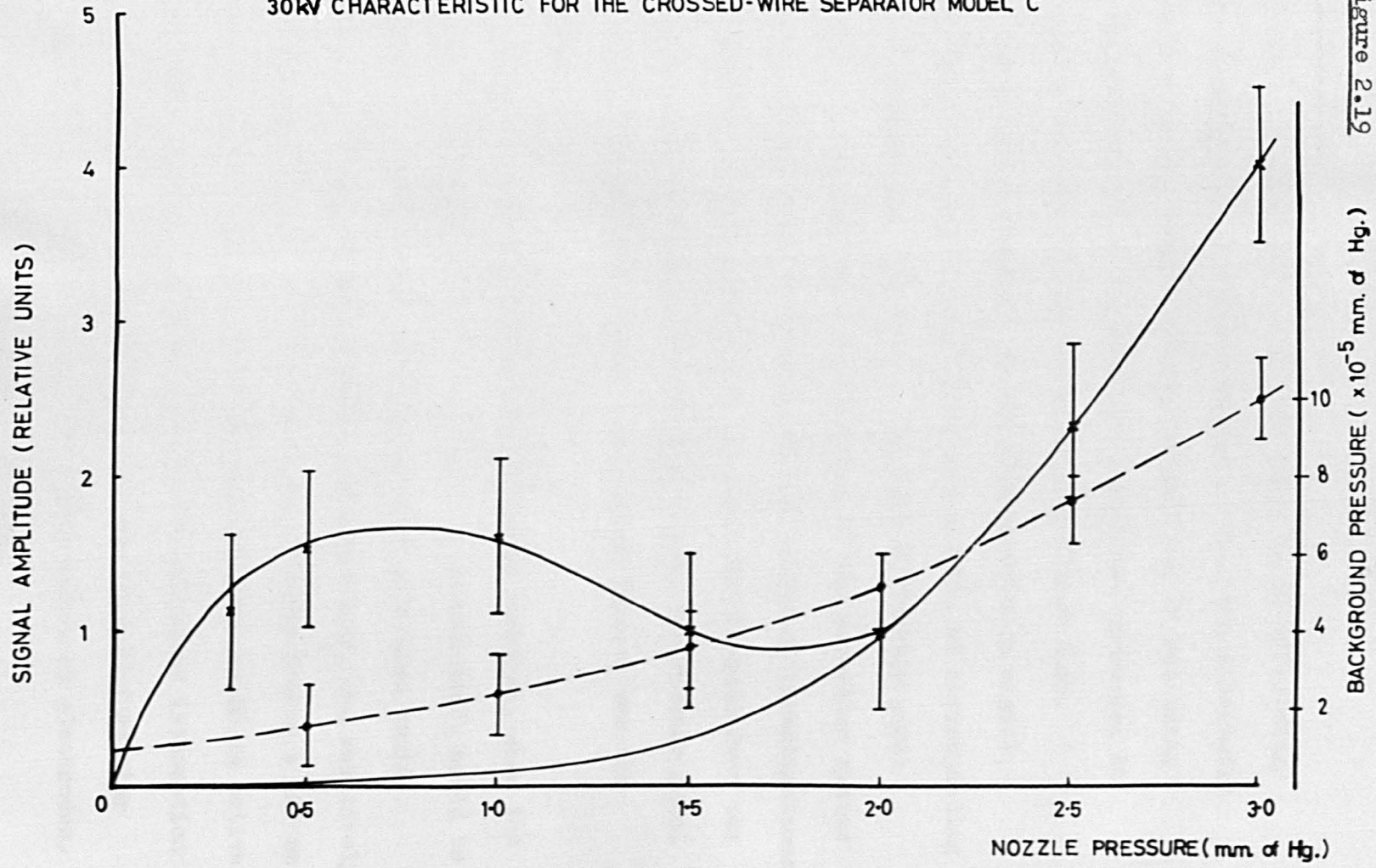
30kV CHARACTERISTIC FOR THE CROSSED-WIRE SEPARATOR MODEL 'C'
SIGNAL AMPLITUDE (RELATIVE UNITS)
BACKGROUND PRESSURE (x10⁻⁵ mm. of Hg.)
NOZZLE PRESSURE (mm. of Hg.)
0
0·5
1·0
1·5
2·0
2·5
3·0
1
2
3
4
5
2
4
6
8
10

Figure 2.19

allow molecules with long mean free paths to be efficiently sorted. However, the increased length of focuser, inherently involved molecules with a greater probability of colliding with electrodes. The relatively low background pressure, in the case of focuser (C) may be noted from figure 2.19.

The greatest increase of enhanced absorption signal, with respect to thermal beam absorption signal, at corresponding nozzle pressure, was observed in the case of focuser model (B). If it is assumed that the response of the detection system remained approximately constant over the series of investigations, then the greatest enhancement factor would be obtained from the most efficient sorting system. On this basis, the focuser model (B), which produced the largest enhancement factor, was the most efficient.

The relatively poor enhancement factor obtained, when the crossed-wire focuser with active length 40 mm was used, could be attributed to the shorter interaction time molecules would have in the electric sorting field. Alternatively, the relatively low enhancement factor obtained with the focuser having a 120 mm active length, in comparison to the focuser with an 80 mm active length, was probably not due to a limited molecular interaction time in the sorting electric field but was caused by greater scattering of the beam with the increased number of electrodes.

(b) Effect of the support electrodes

In the description of the crossed-wire focuser,

it was noted that the wire electrodes were supported between four 4.5 mm diameter brass rods. The rods were set on a 55 mm diameter pitch circle by rings of PTFE. This support system apparently formed an enlarged quadrupole type focuser for molecules that increase in energy in an applied electric field. Experiments were performed to establish whether or not the support rods possessed significant focusing properties.

The wire electrodes were removed from the support rods and the system was connected to an EHT supply, so that adjacent rods carried opposite polarity electric charge. No signal was detected from the molecular beam spectrometer when this "quadrupole focuser" was employed, apart from an increasing thermal beam absorption signal as the nozzle pressure was increased.

(c) Variation of wire diameter

Varying the diameter of the wire electrodes would simultaneously affect two physical properties of the focusing system. Firstly, the ratio of wire separation to wire diameter would alter with a consequent change in the charge distribution on the electrodes. Secondly the scattering cross-sectional area of the focuser would change. An investigation of the effect of varying the electrode diameter was performed experimentally.

Replacing approximately half the total number of electrodes in the crossed-wire focuser model (B) with wire 0.26 mm in

diameter, was sufficient to lose any indication of enhanced absorption signal. The minimum detectable thermal beam absorption signal occurred at a relatively high (~ 3 torr) nozzle pressure. This pressure was much higher than in previous experiments. Therefore, the absorption signal observed in this case was predominantly due to flooding the spectrometer with ammonia molecules. This result indicated that a molecular beam was not being formed and suggested that electrodes of reduced diameter should be employed. Therefore, the same separator, model (B), was fitted with wire electrodes 0.06 mm in diameter. A strong thermal beam absorption signal was observed at low nozzle pressures (0.4 torr), indicating that the array of electrodes was substantially transparent to ammonia molecules. However, when the focuser was electrically charged, the enhanced absorption beam signal was very weak in comparison to that obtained with model (B), when fitted with electrodes 0.13 mm in diameter. A further disadvantage was that, when the nozzle pressure was increased, any enhanced absorption signal was lost in the thermal beam background absorption signal at lower nozzle pressure than with focusers fitted with 0.13 mm diameter electrodes. This result was probably due to a reduction of the spatial extent of the effective electric field, consequent upon a decrease in diameter of the wire electrodes.

The electric field would not be as intense on the focuser axis

as in model (B), when fitted with electrodes 0.13 mm in diameter, and it would become progressively weaker with increasing radial distance from the focuser axis.

2.11 Discussion

The time a molecule spends in a focuser is an important factor affecting the probability of its being focused. Therefore, the different types of focusers constructed were all approximately of the same active length, so that comparisons could be made between their respective focusing efficiencies.

The coaxial focuser, which was used with a source producing an essentially hollow beam, appeared to be the least efficient. In practice it was only possible to obtain an enhancement factor ~ 2. The low signal to noise ratio produced by the focused beam in the spectrometer cavity precluded detailed measurements. Poor beam formation and molecules experiencing only weak electric sorting fields, would partially explain the poor performance of the coaxial focuser. Moreover, at high beam flux, the inability of defocused molecules to leave the system freely through the gaps in the outer electrode, would cause appreciable scattering of the beam.

The single-wire focuser, which relied upon nearby earthed surfaces to provide the outer electrode, proved to be more efficient. An enhancement factor ~ 5 was obtained. This device was used with an on-axis beam source, which would

project molecules into an effective sorting field near the central electrode. Molecules, once defocused, were free to leave the immediate vicinity of the beam. This feature reduced the possibility of scattering the beam. However, the major limitation of the coaxial and single-wire focusers investigated, was that molecules were unable to obtain periodic trajectories, in either device. Some molecules would inevitably collide with the central electrode, where they would experience a catastrophic increase in electric field.

The Maltese-cross focuser proved to be all-too-efficient for focusing molecules that increase in energy in an applied electric field. It was anticipated that the axial quadrupole field type region would preferentially sort and focus this type of molecule and therefore beam stops were employed. In the space between the electrodes the electric field strength decreases away from the beam axis in the radial plane R as shown in figure 2.15. However, the electric field strength in the θ plane increases as the electrodes are approached. Thus, for molecules that decrease in energy in an applied electric field, focusing occurs in the radial plane, R, but defocusing occurs in the θ plane. Use of beams stops up to an area equivalent to the full central area of the focuser, only produced a diminution of the initial emission signal that had been obtained when no beams stops were present. It is concluded, therefore, that the

Maltese-cross focuser is unsuitable, in its present form, for sorting and focusing molecules which decrease in energy in an applied electric field. This is consequent upon a lack of divergence of the electric field in the segmental region between adjacent electrodes.

Of all the focuser designs that were experimentally investigated the crossed-wire focuser was the most efficient at focusing molecules whose energy decreases in an applied electric field. Enhancement factors conservatively estimated $\sim$20 were obtained.

The crossed-wire focuser overcame a basic problem of the coaxial and single-wire designs by allowing the possibility of periodic trajectories for molecules. Moreover, the problem of the Maltese-cross focuser where electric fields coexisted for focusing molecules whose energy either increased or decreased in applied electric fields, did not apply in the case of the crossed-wire design.

The coaxial, single wire, Maltese-cross and crossed-wire focusers have been discussed by Lainé and Sweeting (1971).

CHAPTER III

ELECTRET FOCUSERS

3.1 Introduction

In this chapter, a discussion on the operation of molecular beam masers with electret focusers is developed. This includes the use of solid ammonia as an electret material. Shimoda (1958) investigated the characteristics of an ammonia beam maser and noted an anomalous effect. The effect followed electrical breakdown in the space between the end of the focuser and beam collimating diaphragm, and took the form of unexpected signal amplitudes for particular voltages applied to the focuser. At the time no mechanism was proposed for the effect. Gordon et al (1955) and Thaddeus et al (1961), when operating ammonia beam masers for long periods, reported degrading in the beam focusing systems. It is important to note that cryogenic pumping with liquid nitrogen was employed in the operation of these beam masers.

The literature on the subject of electrets is extensive. Perlman (1968) has compared and contrasted current theories on the electret state in dielectrics while Fridkin and Zheludev (1960) have given a detailed discussion on thermoelectrets in particular. A general conclusion to presently held theories is that only qualitative predictions can be made for the behaviour of electrets polarised at one temperature and which decay at another temperature. Theoretical considerations, in this chapter, are confined to

comments on the behaviour of the electret surface charge. In the context of beam masers, it is the surface charge upon the electret focuser which basically determines the molecular beam focusing field.

3.2 Electrets

Heaviside (1885) described a dielectric that was permanently polarised as an electret, but more recently the definition has been modified to include semi-permanent polarisation. Eguchi (1925) made the first electrets by polarising a carnauba wax mixture at an elevated temperature, while a strong applied electric field remained, as cooling took place. Different types of electret are now known and are designated by the physical method by which they are polarised. The original electret of Eguchi is now called the "thermoelectret". The electret obtained solely by the application of the electric field is called the "electroelectret". The electret produced by luminance is termed the "photoelectret", the one produced by gamma radiation, the "radioelectret" and the one produced in a magnetic field, the "magnetoelectret".

The electret is in many respects the electric analogue of a permanent magnet. If an electret is cut between its poles, two complete electrets are formed, which is indicative of a volume polarisation. For permanency, an electret may be kept with its charged surfaces short-circuited.

The mechanism of short-circuiting electrets has been summarised by Roos (1969). If the depolarisation of the electret is due to the motion of free charges under the influence of the internal field of the electret, then the application of a short-circuit will effectively reduce this electric field. The field is reduced because the shorted electrodes form a large capacitance parallel to the electret itself. In this way the rate of depolarisation is greatly diminished.

Gemant (1935) introduced the present day terminology for the electric charges of particular electrets. A charge on the electret of the same polarity as the adjacent electrode is called a "homocharge" and a charge of opposite sign to the polarity of the "forming" electrode, a "heterocharge". According to Gutman (1948), the heterocharge in certain dielectrics always appears initially. It declines with time and a permanent homocharge builds up. In other dielectrics there is no sign of decay of the primary heterocharge. Previously, Mikola (1925) divided electrets into two classes, (a) those of comparatively high conductivity yielding only heterocharges, and (b) those of much lower conductivity capable of yielding homocharges.

Up to the present time basically three methods have been available for studying the behaviour of electrets, (a) the dissectable capacitor, (b) the depolarisation method and (c) the vibrating - capacitor technique.

The dissectable capacitor method involves measuring the charge induced on one plate of a capacitor which is subsequently dismantled. When a wax electret is melted, it depolarises and a discharge current is produced. This property is used in the depolarisation method of investigating electrets. As Roos (1969) indicated, charge transfer by sparking can occur in the dissectable capacitor method and in the depolarisation method, the current flowing through the electret is not registered. Roos has developed a compensation technique with a vibrating capacitor method to improve the accuracy of measurements.

Monitoring the signal amplitude of a maser operated with electret focusers, indirectly affords another method of observing electret behaviour. Results, given in this chapter, indicate that any loss in strength of the external electric field of the electret, due to the focusing of the molecular beam, is negligible compared with that lost by normal electret decay processes.

3.3 Theoretical considerations

The surface charge, producing the inhomogeneous electric field required to focus molecules in a molecular beam maser, has been obtained using electrets. Surface charge phenomena, observed by Eguchi (1925), may be related to persistent polarisation in the dielectric. The physical nature of persistent polarisation is still not clear. Gubkin and Matsonashvili (1962) have suggested that in waxes the displacement of electrons in the electric field

and their subsequent capture at local levels, is significant in the establishment of the persistent polarisation.

3.3.1 The surface charge

Two types of charge are considered to be generated when an electret is formed. Electrons and ions formed on breakdown adhere to the dielectric surface and form, according to Gross (1949), the electret homocharge (ρ_1). The electret is also assumed to have a semi-permanent polarisation, P, which produces the heterocharge (ρ_2). Following Gubkin (1957), heterocharge is present in the volume of the electret with a charge density,

$$\rho_2(x) = - \operatorname{div} P(x) \qquad (3.1)$$

where x refers to distance through the electret. On the surface of the electret,

$$\rho_2 = \pm P_n \qquad (3.2)$$

where P_n is the normal component of the polarisation. The polarisation P decays according to,

$$P = P_o \exp(-\alpha t) \qquad (3.3)$$

where P_o is the initial electret polarisation and α is a relaxation rate for depolarisation that is dependent upon field and temperature.

In general, the resultant effective surface charge density, σ , is composed of the difference between homocharge (ρ_1) and heterocharge (ρ_2).

$$\sigma = e_2 - e_1 \qquad (3.4)$$

The resultant effective surface charge density, σ , is the only factor contributing to the field strength and charge leakage. The reversal of sign of the total surface charge was explained by Gross (1944) as being due to the different rates of decay of heterocharge and homocharge.

Gubkin and Matsonashvili (1962) have investigated the physical nature of the electret effect in carnauba wax. The process of electret polarisation is shown schematically in figure 3.1. When an external electric field is applied, the volume of the dielectric becomes polarised. Assuming that there is no gap between the electret and lower electrode, then the electric field, E_e , between the electret and upper electrode, is a function of the applied voltage, V, and the electret surface charge σ , (Gubkin 1957),

$$E_e = \frac{\frac{\epsilon V}{L} + 4\pi\sigma}{\frac{\epsilon \ell}{L} + 1} \qquad (3.5)$$

where ℓ is the separation of the upper electrode and electret, L is the electret thickness and ϵ is the permittivity of the electret material.

Normally, polarisation in air limits $E_e \sim 33 kV\ cm^{-1}$ because of electrical breakdown. Under vacuum conditions this limit may be raised. It was noted by Gubkin and Matsonashvilli

Figure 3.1

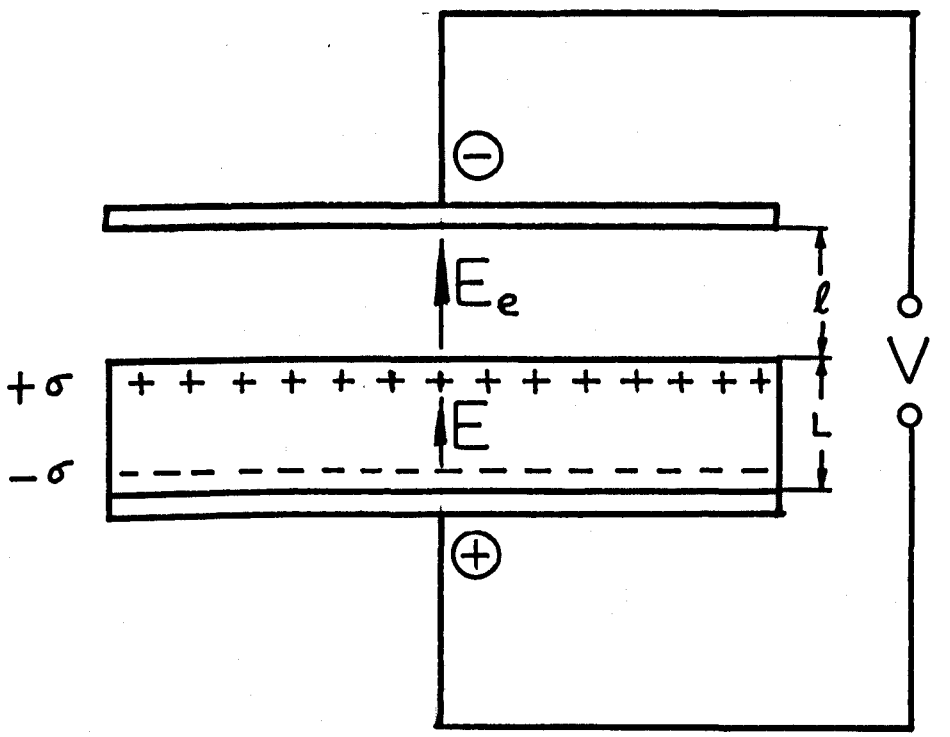

Schematic of the electret polarisation process.

(After Gubkin and Matsonashvili,1962)

(1962) that the polarity and magnitude of the initial electret surface charge σ_o depends on the applied voltage V. This feature of electret formation has also been noted by Yamanka (1954).

3.4 Surface charge monitoring

In order to use the maser as a monitoring device for the surface charge upon an electret, it is useful to estimate the response of the maser emission signal as a function of the electric field produced in the multipole focuser. The analysis used is based upon equations for :

(a) the number of molecules produced by a multipole focuser, and (b) the minimum signal detectable in a maser spectrometer. Equations (a) and (b) have been formulated by Shimoda (1960).

A plausible approximation for the distribution of molecular velocities and directions was taken, initially by Shimoda (1960), to be the Maxwell-Boltzmann distribution. Thus, the number of molecules in a unit volume having velocity components v_x, v_y and v_z (>0) is :

$$N(v_x, v_y, v_z)\,dv_x dv_y dv_z = \frac{2N}{\alpha^3 \pi^{3/2}} \exp\left[\frac{-v^2}{\alpha^2}\right] dv_x dv_y dv_z \qquad (3.6)$$

where N is the number of molecules in a unit volume and,

$$v^2 = v_x^2 + v_y^2 + v_z^2 \qquad (3.7)$$

The most probable velocity, α , is given by :

$$\frac{1}{2} m \alpha^2 = kT \tag{3.8}$$

Since a multipole focuser exerts forces with cylindrical symmetry, a cylindrical co-ordinate system is used for the velocity distribution.

$$v_r = (v_x^2 + v_y^2)^{\frac{1}{2}} \tag{3.9}$$

Therefore,

$$N(v_r, v_z)\, dv_r dv_z =$$

$$\frac{4N v_r}{\alpha^3 \pi^{1/2}} \exp\left[-\frac{v^2}{\alpha^2}\right] dv_r dv_z \tag{3.10}$$

From equation (2.25) the Stark energy of the ammonia inversion doublet is given by:

$$\pm W_E = \left[\left[\frac{h\nu_o}{2}\right]^2 - \left[\frac{\mu M_J K E}{J(J+1)}\right]^2\right]^{1/2} - \frac{h\nu_o}{2} \tag{3.11}$$

The total beam flux from the source is given by:

$$n_o = \int_o^\infty \int_o^\infty A_o N v_z \, dv_r dv_z$$

$$= A_o \frac{N\alpha}{\pi^{1/2}} \tag{3.12}$$

where A_o is the cross-sectional area of the beam at source. The flux of focused molecules in a particular state E_i, with a statistical fraction $f_i = \frac{N_i}{N}$ is given by:

$$n_i = f_i \int_0^{\infty} \int_0^{v_c} AN(v_r, v_z) v_z \, dv_r \, dv_z \qquad (3.13)$$

The critical radial velocity for molecules to be retained in the focuser is v_c and is given by,

$$W_E \equiv \frac{1}{2} m v_c^2 \qquad (3.14)$$

A is the cross-sectional area of the beam at the entrance to the microwave field region. From a simple harmonic motion calculation of the molecular motions in the focuser, the following criterion is established:

$$v_z < \frac{2L'}{\pi R} \cdot v_c \qquad (3.15)$$

where L', R are, respectively, the length and grazing internal radius of the focuser. Molecules that do not satisfy this focusing criterion are not effectively focused. Although the analysis applies to quadrupole focusers (2n = 4 electrodes, alternately charged positively and negatively) corrections for focusers where $2n \neq 4$ will be minimal.

The number of active molecules flowing into the cavity microwave field in unit time is given by :

$$n_i = f_i \int_0^{v_c} \int_0^{\left[\frac{2L'}{\pi R}\right] \cdot v_c} A N(v_r, v_z)\, dv_r dv_z \qquad (3.16)$$

$$= f_i n_o \frac{W_E}{kT} \left\{ 1 - \exp\left[- \left[\frac{2L'}{\pi R}\right]^2 \cdot \frac{W_E}{kT} \right] \right\}$$

after substituting equation (3.12). When $A = A_o$ and,

$$\left[\frac{2L'}{\pi R}\right]\left[\frac{W_E}{kT}\right] \ll 1$$

the beam flux is given by,

$$n_i \doteq f_i n_o \left[\frac{2L'}{\pi R}\right]^2 \cdot \left[\frac{W_E}{kT}\right]^2 \qquad (3.17)$$

Having determined the number of active molecules supplied by the focuser, this will be equated to the number of molecules necessary to obtain the minimum signal from a maser spectrometer ($n_{i\,min}$). The result will give an estimate of the maser spectrometer sensitivity to changes of electric field in the focuser.

Assuming a constant velocity of molecules, v, the transition probability of molecules passing through a uniform microwave field of length L is given, according to Shimoda (1960), by :

$$|a_1|^2 = \frac{S^2}{(\omega - \omega_o)^2 + S^2} \cdot \sin^2\left[(\omega - \omega_o)^2 + S^2\right]^{1/2} \frac{L}{2v} \quad (3.18)$$

where $\frac{\omega_o}{2\pi}$ is the resonant transition frequency and $S = \frac{E\mu_{12}}{\hbar}$, μ_{12} is the average dipole matrix element connecting the two energy levels.

At the resonant frequency $\omega = \omega_o$, the power emitted by the molecular beam (ΔP_m) is given by :

$$(\Delta P)_m = n_i h \nu_o \sin^2\left[\frac{LS}{2v}\right] \quad (3.19)$$

The emission of power by molecules in the cavity can be represented by:

$$\Delta\left[\frac{1}{Q_L}\right] = \frac{1}{Q_m} = \frac{\Delta P_m}{\omega_o W} \quad (3.20)$$

where W is the energy stored in the cavity, Q_L is the loaded Q and Q_m is the molecular Q factor. At the optimum level of signal power,

$$Q_L = \frac{Q_o}{2} \quad (3.21)$$

where Q_o is the unloaded cavity Q. For a reflection cavity ($Q_1 = Q_o$) the minimum detectable signal is given by,

$$\left|\frac{1}{Q_m}\right|_{min} = \frac{4}{Q_o} \cdot \left[\frac{FkT\Delta\nu}{P_i}\right]^{1/2} \quad (3.22)$$

The term $FkT\Delta\nu$ is the noise power of the microwave superheterodyne detection system where F is the overall noise figure of the

detector and $\Delta\nu$ is the effective bandwidth; $P_i = \frac{\omega_o W}{Q_o}$.

The signal is therefore detectable when :

$$\frac{1}{Q_m} = \frac{\Delta P_m}{\omega_o W} \geqslant \frac{4}{Q_o} \cdot \left[\frac{FkT\Delta\nu}{P_i}\right]^{1/2} \qquad (3.23)$$

Cavity theory indicates that the stored energy, at resonance, is given by,

$$\omega_o W = \frac{4Q_L^2}{Q_1} \cdot P_i \qquad (3.24)$$

The energy stored, W, in a cavity volume V' is given by :

$$W = \frac{E^2 V'}{8\pi} \qquad (3.25)$$

substituting from the relationship $S = \frac{E\mu_{12}}{\hbar}$ and $\overline{\mu}_{12}^2 = \frac{1}{3}|\mu|^2$

then :

$$W = \frac{3V'}{8\pi} \cdot \frac{\hbar^2 S^2}{|\mu|^2} \qquad (3.26)$$

Combining equations,

$$n_i \pi |\mu| \cdot \frac{1}{S} \cdot \sin^2\left[\frac{SL}{2v}\right] > \left[\frac{3V' FkT\Delta\nu}{\nu_o Q_o}\right]^{1/2} \qquad (3.27)$$

The left hand side is optimised when S is an optimum given by :

$$S_{opt} = 2{\cdot}33\,\frac{v}{L} \qquad (3.28)$$

The minimum detectable flux is then given by :

$$n_{i,min} = \frac{1{\cdot}52v}{|\mu|L} \cdot \left[\frac{V' FkT\Delta\nu}{\nu_o Q_o}\right]^{1/2} \qquad (3.29)$$

Now, equating the minimum detectable beam flux of the spectrometer, $n_{i,min}$, to the beam flux produced by a multipole focuser, equation (3.17), indicates the magnitude of the electric field in the focuser, since:

$$W_E \doteq \frac{\mu^2 E_s^2}{h\nu_o} \qquad (3.30)$$

where E_s is the electric field strength in the multipole focuser. Therefore, equating $n_{i,min}$ to equation (3.17),

$$f_i n_o \left[\frac{2L'}{\pi R}\right]^2 \left[\frac{W_E}{kT}\right]^2 = \frac{152 v}{\mu L} \cdot \left[\frac{V' F k T \Delta\nu}{\nu_o Q_o}\right]^{1/2} \qquad (3.31)$$

Substituting for W_E,

$$E_s = \left[\left[\frac{1.52 v}{f_i n_o \mu^5 L}\right] \left[\frac{\pi R h}{2L'}\right]^2 \left[\frac{V' F \Delta\nu}{Q_o}\right]^{1/2} (kT)^{5/2} \nu_o^{3/2}\right]^{1/4} \qquad (3.32)$$

An estimate for E_s may be obtained by substituting the following values in equation (3.32),

$h = 6.6 \times 10^{-34}$ J s
$\nu_o = 2.4 \times 10^{10}$ Hz
$v = 4 \times 10^{2}$ m s^{-1}
$R = 5 \times 10^{-2}$ m
$L' = 0.3$ m
$f_i = 3.6 \times 10^{-2}$
$L = 0.1$ m
$V' = 10^{-5}$ m^3
$F = 10^{2}$
$\Delta\nu = 800$ kHz
$Q_o = 10^{-4}$
$kT = 4 \times 10^{-21}$ J
$n_o = 10^{18}$ s^{-1}

Thus $E_s \sim 10$ V cm^{-1}. This results indicates the minimum electric

field strength in the focuser that will evoke a detectable signal from the spectrometer detection system. Having determined the basic criterion for the operation of a molecular beam maser by an electret focuser, suitable dielectric materials had to be selected that satisfied the remaining operating criteria.

3.5 Selection and preparation of suitable electret materials

Three basic criteria had to be satisfied if a maser was to be operated by an electret coated focuser :

(a) The electret material should have a sufficiently low vapour pressure at the operating temperature to allow the maser vacuum system to be evacuated to at least 10^{-5} torr.

(b) The electret had to bond to the metal substrate with sufficient strength to withstand interactions with electric fields $\sim$ 30 kV $cm.^{-1}$

(c) The electret had to be capable of maintaining electric fields at the surface $\sim$ 2 kV cm^{-1} in order to sustain maser signals of significant amplitudes.

Initially, the following materials were found experimentally to satisfy (a), (b), and (c):

Lead titanate Lead titanate electrets could be mixed in an epoxy resin compound. The compound chosen was BXL Hardener 19262 with BXL Epoxide Resin R18774/1. This compound combined together excellent mechanical and electrical insulation properties.

Carnauba wax This material has become a "classic" in the construction of electrets and was found to be suitable for vacuum work.

The general requirements for the preparation of electrets have been detailed elsewhere (Good and Stranathan, 1939). However, the general results will be summarised here. Electrets need not necessarily be formed by the cooling of a heated dielectric in a strong applied electric field (Thermoelectret : Eguchi, 1925). A number of experiments have been performed with electrets constructed by electrification of the dielectric while in the solid phase (Electroelectrets : Gross and Denard, 1945).

3.6 The focuser

The conventional molecular beam spectrometer and its associated detection system employed in the experimental investigation is described in Appendix I. The spectrometer was operated in conjunction with a multipole focuser constructed with eight nickel plated metal rods. The rods, 1.55 mm in diameter and 300 mm long, were equispaced on a 10 mm diameter pitch circle into PTFE insulators, as shown in figure 3.2. It was possible to radiatively cool the focuser electrodes to the triple point of ammonia (195 K) by a cylindrical dewar which contained liquid nitrogen. The dewar and state separator are illustrated together in figure 3.3.

To determine the charge storage properties of an electret

Figure 3.2

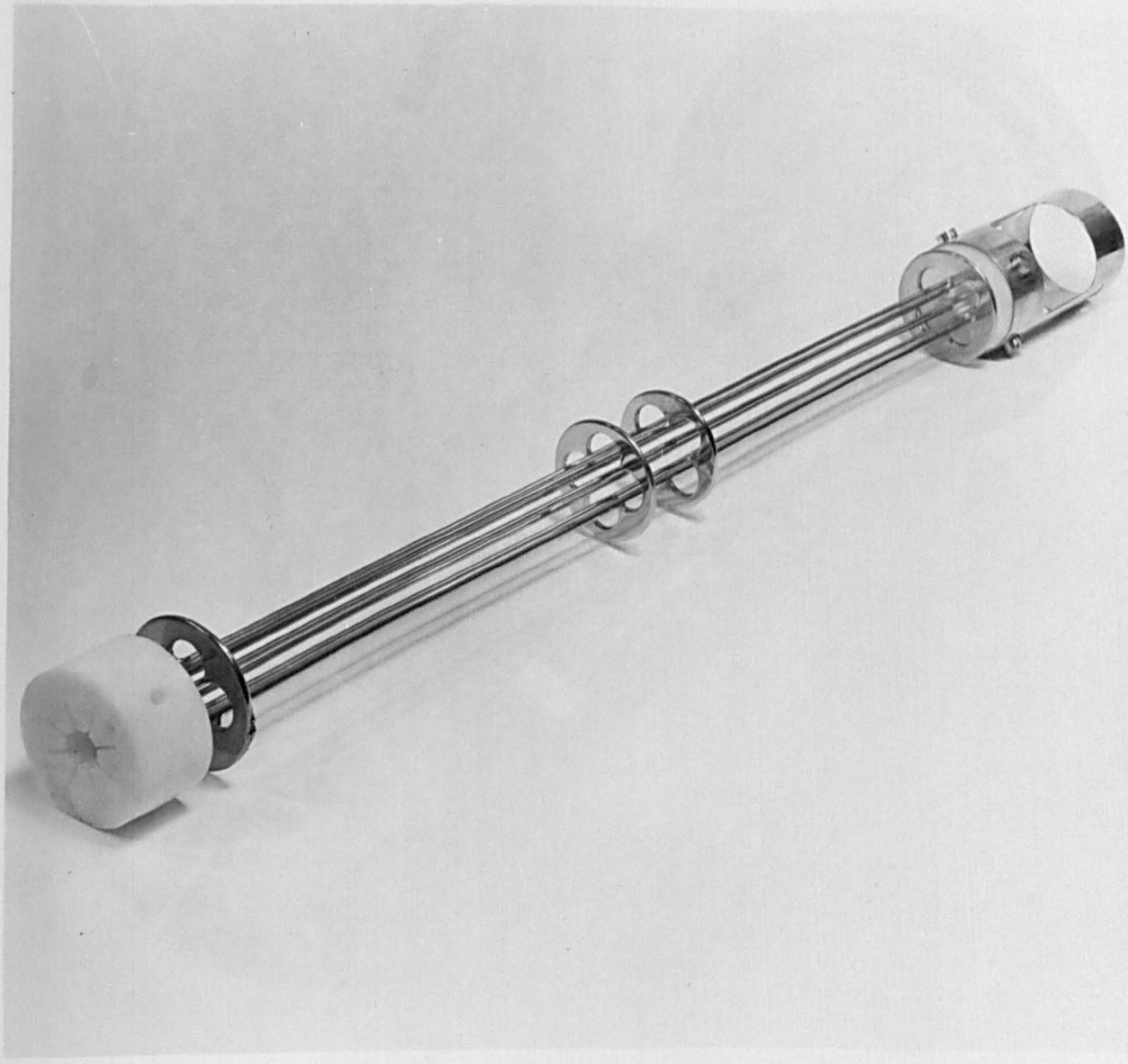

The multipole focuser.

Figure 3.3

The dewar and focuser assembly.

coating upon the focuser by means of the maser emission signal, it was necessary to isolate the capacitative charge storage properties of an uncoated focuser. It was also necessary to know that the relaxation of capacitative charge, in experiments where the focuser was not immediately short-circuited, should not appreciably interfere with the observations originating from the electret.

Thus the focuser was scrupulously cleaned and replaced in the maser which was subsequently evacuated. A maser emission signal was obtained and then the high voltage to the focuser was disconnected by using a specially constructed oil-immersed switch. The switch is illustrated in figure 3.4. The EHT cable to the focuser was normally held in the closed position by spring X. When the solenoid, S, was activated, the EHT was instantly disconnected.

Following the disconnection of the EHT supply, the decaying amplitude of the emission signal was measured at regular intervals and the resulting curve may be seen in figure 3.5. This figure is typical of several that were recorded to verify the effect. The results indicate that the charge had effectively decayed to insignificant proportions for maser purposes, within 4 ± 1 minutes. The major portion of error in this result probably arose from variations in atmospheric conditions, since the external leads to the focuser were exposed.

To mains supply.

Figure 3.4

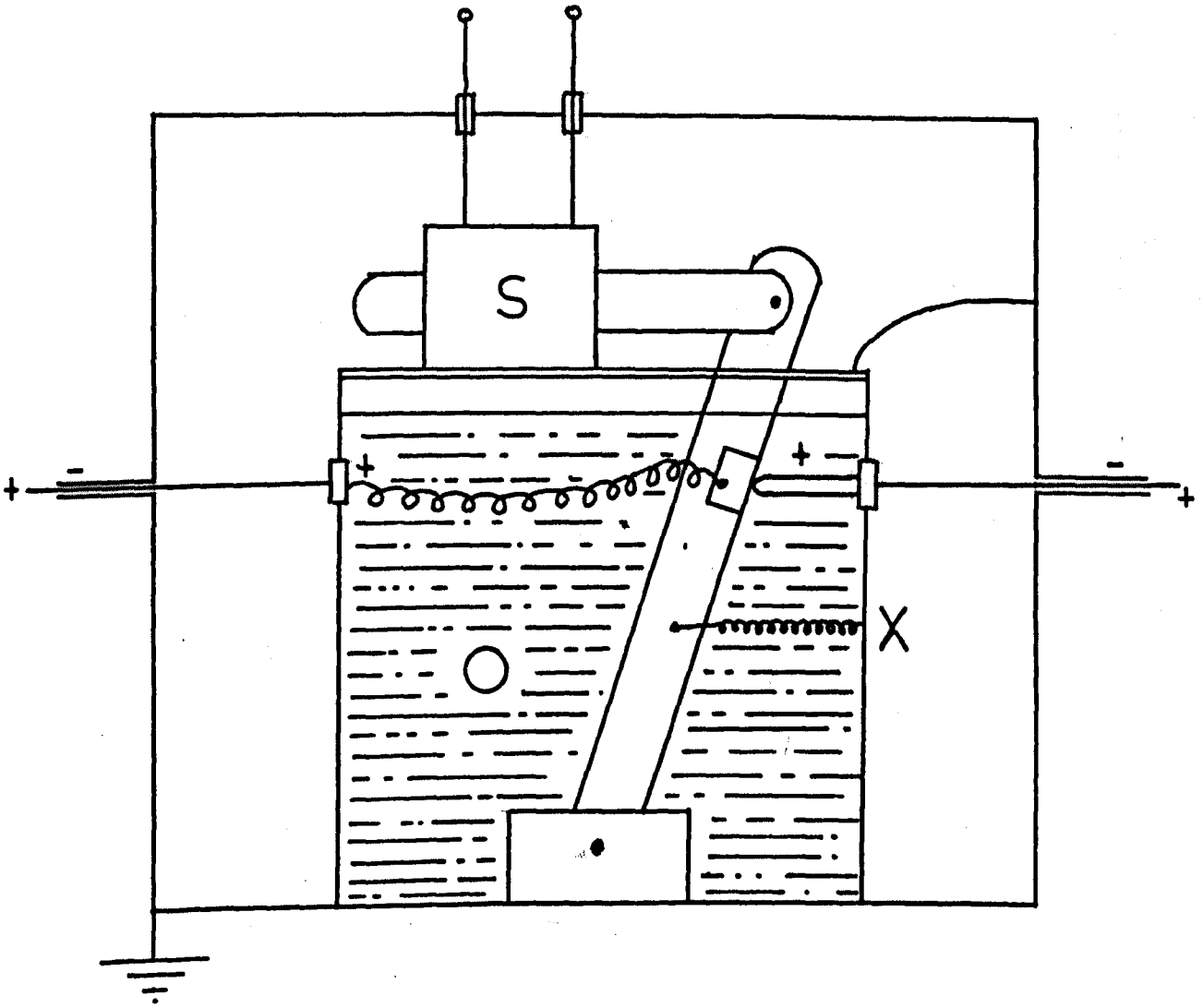

S = Solenoid (240 volts, 50 Hz)

O = Switch oil

X = Spring

The oil-immersed switch.

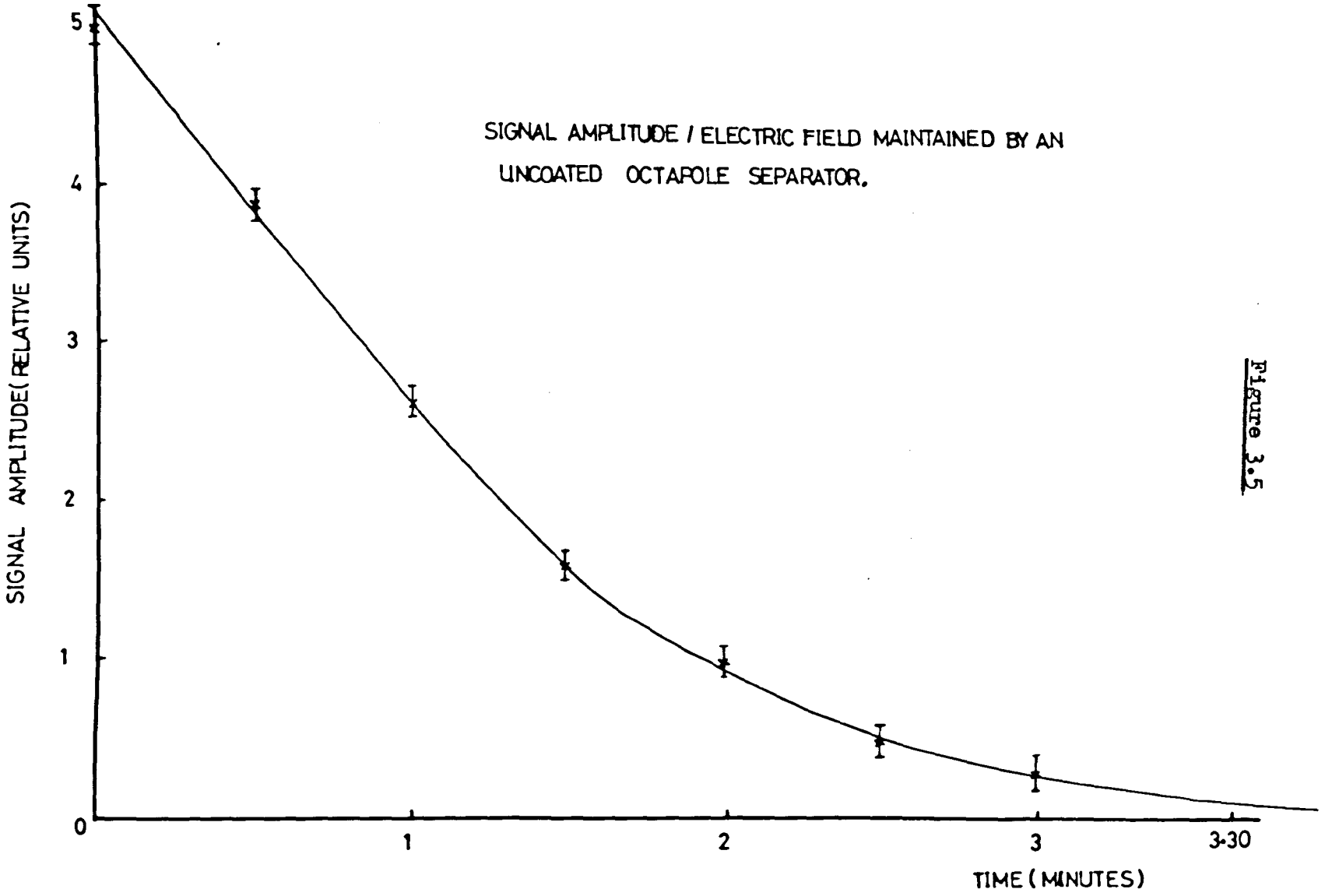
SIGNAL AMPLITUDE / ELECTRIC FIELD MAINTAINED BY AN UNCOATED OCTAPOLE SEPARATOR.
SIGNAL AMPLITUDE(RELATIVE UNITS)
5
4
3
2
1
0
1
2
3
3·30
TIME (MINUTES)

Figure 3.5

3.7 The lead titanate - epoxy resin electret

(i) Preparation

It was necessary to construct a duplicate focuser of the one described in section 3.6 in order to perform this experiment. This was because a coating of lead titanate - epoxy resin would have spoilt the nickel plated focuser for further experiments. The duplicate electrodes were made from copper plated metal rods. A mixture of 70% lead titanate and 30% epoxy resin (BXL Hardener Q19262 with BXL Epoxide Resin R18774/1) was coated on to each electrode in turn, while the focuser was dismantled. Each rod was then separately placed on the axis of a 10 mm internal diameter copper tube. A 4 kV cm^{-1} polarisation field was applied as the electret material was allowed to cure. The polarity of the polarising field of half the electrodes was different from the other half and when the focuser was reconstructed electrodes of opposite polarity were placed adjacent to one another. This fulfilled the requirement for multipole focusers that adjacent electrodes should carry opposite polarity electric charges.

(ii) Operation of the maser

When the background pressure in the vacuum system was $\sim 1 \times 10^{-5}$ torr the electret coated focuser which had been replaced in the maser was given an initial charging voltage of 11 kV. The voltage was applied to the focuser in the same sense as the electrodes had been originally polarised. The voltage

applied to the focuser was disconnected by using the oil-immersed switch. The amplitude of the stimulated emission signal was measured, in arbitrary units, at regular time intervals. This was done by allowing molecules to pass through the focuser only while readings were being taken. A nozzle pressure of 2.5 torr was employed.

(iii) Observation of electret behaviour in a lead titanate - epoxy resin mixture

Figure 3.6 indicates the time dependence of the stimulated emission signal after the electret focuser electrodes were short-circuited at time A. (Short-circuiting in this context is not to be confused with the term short-circuiting as used in the electret literature. There the surfaces of an electret carrying opposite polarity electric charges are short-circuited together). After approximately 55 minutes the signal amplitude began a rapid decay into the "noise". Within a further 10 minutes the signal dropped into the noise level of the spectrometer detection system.

(iv) Conclusion

Semipermanent electrification of a mixture of lead titanate and epoxy resin (BXL Hardener Q19262 with BXL Epoxide Resin R18774/1) was obtained. The external electric field of the electret effectively operated a multipole molecular beam focuser for 63 minutes.

The short electret lifetime of the mixture may partially be attributed to the relatively high conductivities of titanates,

Figure 3.6

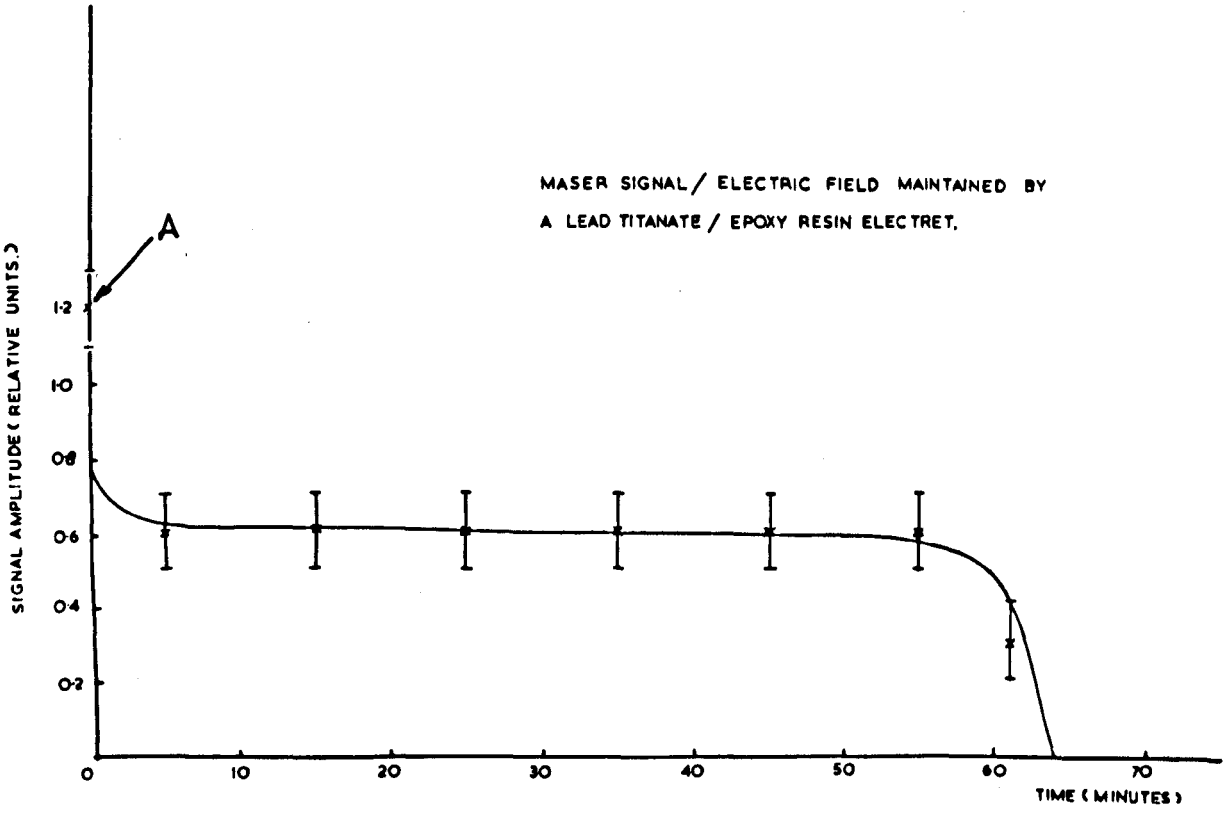
MASER SIGNAL / ELECTRIC FIELD MAINTAINED BY
A LEAD TITANATE / EPOXY RESIN ELECTRET.
A
SIGNAL AMPLITUDE (RELATIVE UNITS)
1·2
1·0
0·8
0·6
0·4
0·2
0
10
20
30
40
50
60
70
TIME (MINUTES)

typically $\sim 10^{-14}$ ohm $^{-1}$cm $^{-1}$, compared with other electret materials such as carnauba wax with a conductivity $\sim 10^{-18}$ ohm^{-1} cm^{-1} (Fridkin and Zheludev, 1960).

Practically, it was not convenient to uniformly coat the mixture to a thickness ~ 0.5 mm over each electrode. Although the lead titanate was finely sieved it is not possible to discount the presence of occlusions in the final solidified mixture which could have adversely affected its electret properties.

3.8 The carnauba wax electret I

The carnauba wax electret was constructed by dipping the octapole focuser (described in section 3.6), with an end insulator removed so that it was not coated in wax, into a glass container of liquid phase carnauba wax. The coated focuser was removed from the container and the surplus was shaken off. The wax was allowed to solidify upon the nickel plated metal electrodes and a layer of ~ 0.5 mm was obtained. Reconstruction of the focuser on to PTFE support insulators and insertion into the maser was accomplished within 15 minutes of the formation of the wax layer. It was necessary to replace the focuser in the maser as quickly as possible otherwise the wax layer became badly cracked in air. When the focuser had been replaced the maser was evacuated to a pressure of $\sim 5 \times 10^{-6}$ torr within 2 hours.

The carnauba wax was electrified in solid form when it was within the maser. The alternative method of polarising the

wax while solidifying from the liquid phase was unsatisfactory. This was because the wax layer cracked severely during the time taken to polarise the wax in air and to replace the complete focuser into the maser under vacuum conditions.

(ii) Operation of the maser

An oscillation signal was detected from the maser with a threshold voltage of 9.75 kV and a nozzle pressure of 2.6 torr. Previous attempts to achieve semipermanent electrification of carnauba wax had failed because of high voltage breakdown on the focuser, which caused carbonisation and so created charge leakage paths. For this reason the voltage applied to the focuser was slowly increased, without electrical breakdown, until 16 kV was obtained. The oil-immersed switch was used to disconnect the voltage applied to the focuser and the supply leads were removed but the input terminals to the focuser were not short-circuited.

(iii) Observation of electret behaviour in carnauba wax

An ammonia molecular beam was continuously passed through the electret focuser and the stimulated emission signal produced was monitored, the resulting curve as a function of time may be seen in figure 3.7. An initial rapid decay of signal amplitude was observed. This was probably due, in part, to a combination of a decay of electret surface charge and loss of capacitative charge upon the focuser electrodes. The ensuing decay of the signal amplitude continued at a reduced rate for approximately 60 minutes. The signal then decayed rapidly into the noise level of the

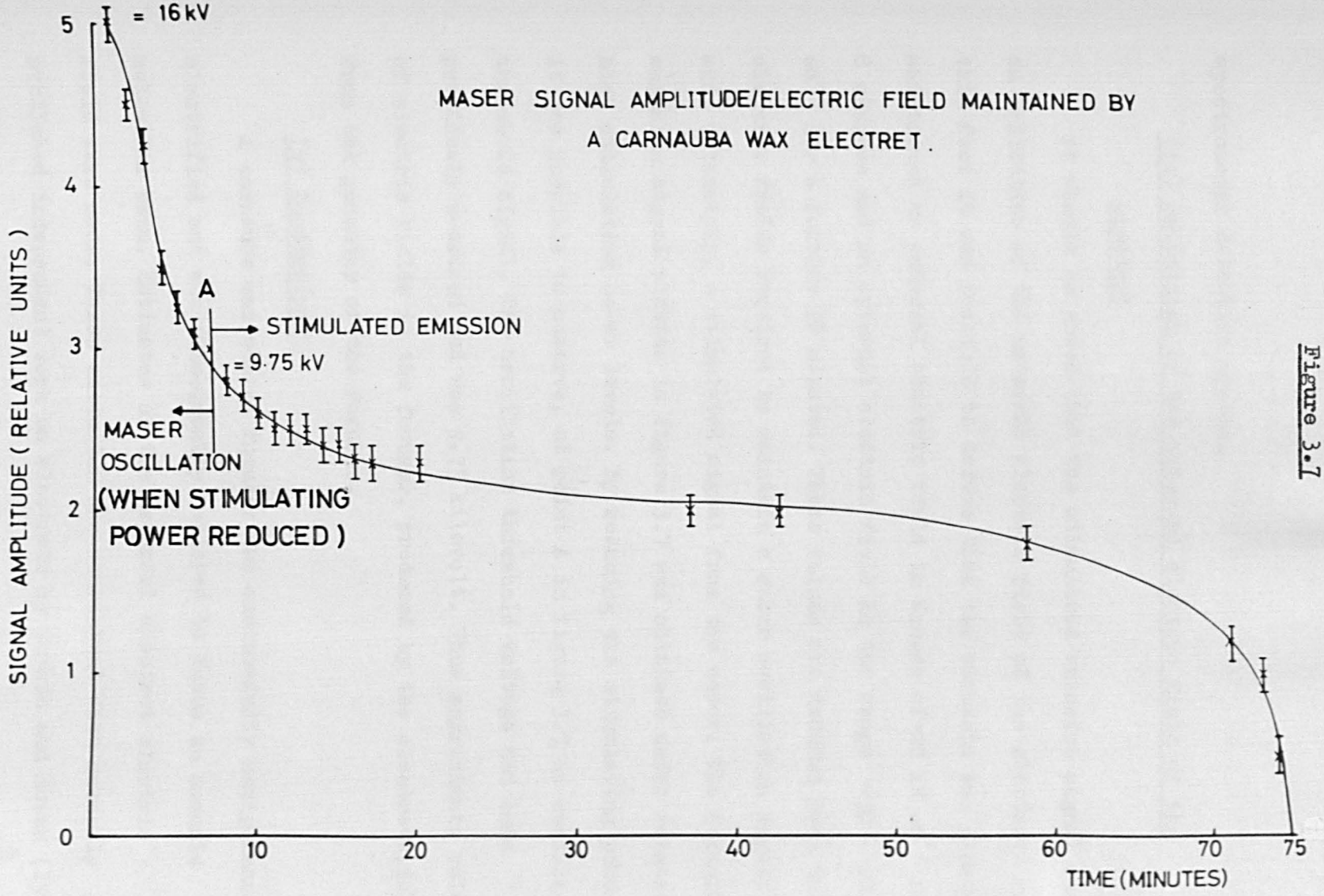
MASER SIGNAL AMPLITUDE/ELECTRIC FIELD MAINTAINED BY
A CARNAUBA WAX ELECTRET.
= 16 kV
A
STIMULATED EMISSION
= 9·75 kV
MASER
OSCILLATION
(WHEN STIMULATING
POWER REDUCED)
SIGNAL AMPLITUDE (RELATIVE UNITS)
TIME (MINUTES)
0
1
2
3
4
5
10
20
30
40
50
60
70
75

Figure 3.7

spectrometer detection system.

(iv) Estimation of the external electric field of the electret

It should be noted that the stimulated emission signal was an indication of the external electric field of the electret. From this fact it was possible to deduce that the carnauba wax electret maintained an external electric field in excess of ~20 kV cm^{-1} for 8 minutes and an external electric field in the range ~10 - 20 kV cm^{-1} for a further 60 minutes. These values are deduced from the electric fields required to maintain a maser oscillation signal and, ultimately, a stimulated signal from the maser. The stimulated emission signal plotted in figure 3.7 was obtained under relatively high stimulating power levels. By reducing the stimulating power it was possible to observe, at point A in figure 3.7, an oscillation threshold signal. The oscillation threshold voltage had been previously measured and was 9.75 kilovolt. Thus approximate values of electric fields in the focuser, produced by the electrets, follow from the geometry of the focuser.

(v) Conclusions

A carnauba wax coated focuser was successfully semipermanently electrified and was subsequently employed to focus an ammonia molecular beam. Estimates of the external electret electric field were made. These estimates are consistent with recently published independent work on electrets by Gubkin and Novak (1971).

These investigators studied the form and strength of the electric field produced in a quadrupole system of knife-edge polymer electrets.

They employed a conventional electrometer technique to probe the field and as a result of their findings suggested that an electret focuser might be employed in a beam maser, whereas here, electret focusers have been used directly in a beam maser.

The focuser, being radiatively cooled by the liquid nitrogen jacket, collected some diffused ammonia molecules from the beam. Possibly these molecules could have become strongly polarised and eventually reduced the focusing ability of the focuser. Gordon et al (1955) have reported electrostatic charge build up with polarised solid ammonia upon the focuser as a "nuisance". Also, Thaddeus and Krisher (1961), have reported that the stimulated emission signal, from their ammonia beam maser, decayed within an hour or two when operating with an external EHT supply. It was suggested that solid ammonia on the focuser was the cause.

3.9 The carnauba wax electret II

(i) Introduction

As mentioned in the previous section, Gordon et al (1955) and Thaddeus and Krisher (1961) have noted degrading of the efficiency of molecular beam focusers in their respective masers, ascribing it to electrostatic effects of solidified ammonia on the focuser electrodes. Shimoda (1958) has noted what he called "a

strange phenomenon". By inducing a slight discharge on the focuser, he found that the threshold focuser voltage for oscillation decreased. In fact he could obtain an oscillation signal with effectively zero voltage applied to the focuser. In figure 3.8 his plot of amplitude of oscillation with focuser voltage is shown.

Following the results obtained in section 3.8. further investigation of carnauba wax electrets was indicated but with periodic observation of the maser signal. This could be achieved by passing ammonia gas periodically through the maser and not continuously as before. In this way the total amount of ammonia gas allowed into the maser would be reduced. The effective operating time of the electret focuser would then be increased, if collection of solid ammonia upon the focusef electrodes was a factor in reducing the efficiency of the electret focuser.

(ii) Preparation

The focuser electrode configuration which was described in section 3.6 was thoroughly cleaned and recoated with carnauba wax, using the method described in section 3.8. A coating of wax $\sim$ 0.3 mm thick was obtained. The focuser was reassembled and replaced in the maser within 10 minutes. The vacuum system was evacuated and a background pressure $\sim 4 \times 10^{-6}$ torr was obtained within two hours.

The carnauba wax on the focuser electrodes was electrified when the assembled focuser was in position in the maser. The voltage applied to the focuser from the external EHT supply was slowly

Figure 3.8

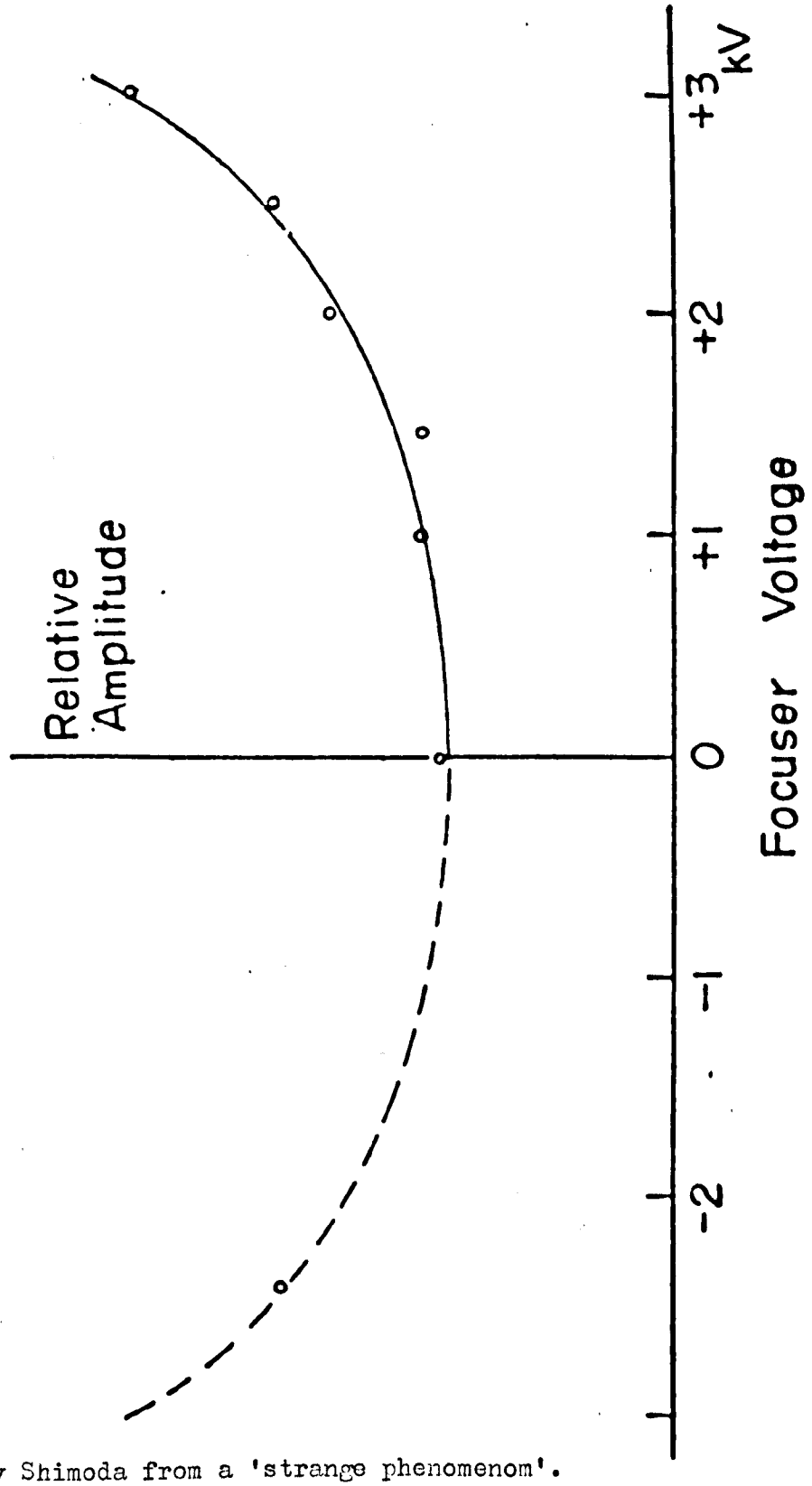

Results obtained by Shimoda from a 'strange phenomenom'.

increased up to 16 kV. At this point in time the EHT supply was disconnected by using the oil-immersed switch. When the EHT lead was removed from the maser, the capacitor charge was removed from the focuser by short-circuiting the input terminals.

(iii) Time variation of the external electret electric field

Immediately after short-circuiting the electrode system, the amplitude of the stimulated emission signal was displayed on the cathode ray oscilloscope when ammonia gas was passed through the focuser at a nozzle pressure of 2.6 torr. The amplitude of this signal was measured and readings were repeated when ammonia gas was periodically passed through the system. The resulting curve may be seen in figure 3.9. A spontaneous increase in the signal amplitude due to an increase in the external electret electric field was noted 640 minutes after the initial reading had been recorded. At the point marked as X in figure 3.9, the stimulating power was temporarily adjusted and an oscillation signal was observed. This indicated that an electric field in excess of ~ 20 kV cm^{-1} (the threshold field for oscillation) was present in the focuser. The stimulating power was adjusted to its previous value after this observation and the plot of signal amplitude with time was continued. After a total time of 700 minutes the signal reached a constant amplitude that did not diminish for a further 150 minutes, at which point the experiment was terminated. A possible mechanism for these results will be described in section 3.11.

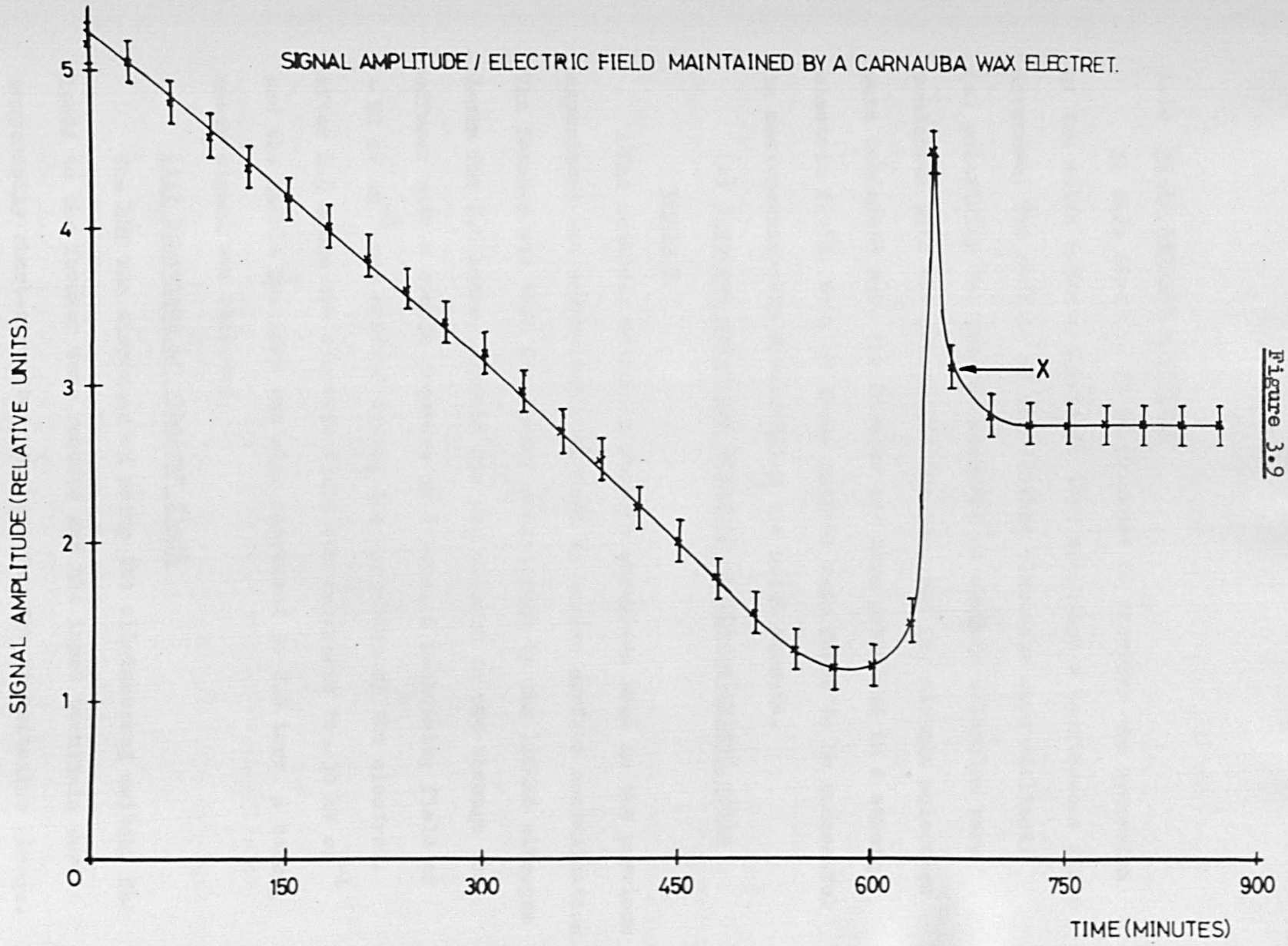
SIGNAL AMPLITUDE / ELECTRIC FIELD MAINTAINED BY A CARNAUBA WAX ELECTRET.
SIGNAL AMPLITUDE (RELATIVE UNITS)
0
1
2
3
4
5
150
300
450
600
750
900
TIME (MINUTES)
X

Figure 3.9

3.10 Solid ammonia electrets

In this section, it is proposed to describe the operation of two solid ammonia electrets that exhibited a spontaneous field increase. Two methods of fabricating electrets were utilised: (a) polarising the ammonia material as ammonia molecules were condensed onto the pre-cooled focuser, and (b) ammonia molecules were condensed onto the focuser and then polarised in a strong electric field. Both of these methods were found to be successful in semi-permanently electrifying the solid ammonia.

(i) Electret behaviour observed in pre-polarised solid ammonia

The octapole molecular focuser which was used in the previous experiment was scrupulously cleaned to remove surface contamination. The focuser was then pre-cooled radiatively by the liquid nitrogen dewar for 2.5 hours. Ammonia gas was allowed to pass through the effuser with a nozzle pressure of 2 torr. A polarising field of ~ 20 kV cm^{-1} was applied during the formation of the electret. After 2.5 hours the electric field was increased to ~ 30 kV cm^{-1} and the nozzle pressure was also increased to 2.6 torr. A strong maser signal was observed.

(ii) Behaviour of electret field

The EHT was disconnected using the oil-immersed switch. The leads to the focuser were removed and the input terminals were temporarily short-circuited, so removing the capacitative charge.

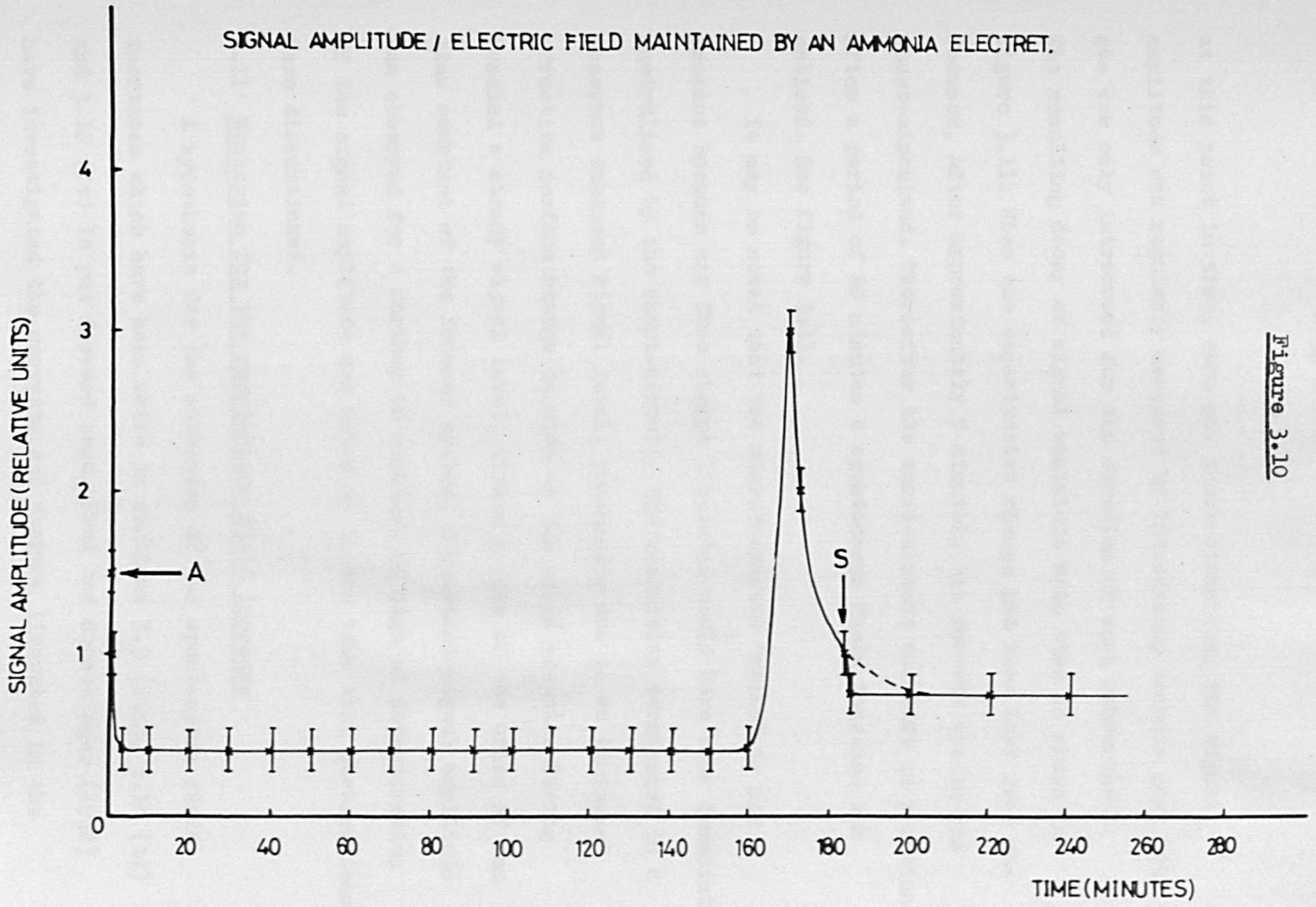
SIGNAL AMPLITUDE / ELECTRIC FIELD MAINTAINED BY AN AMMONIA ELECTRET.
SIGNAL AMPLITUDE (RELATIVE UNITS)
0
1
2
3
4
A
S
20
40
60
80
100
120
140
160
180
200
220
240
260
280
TIME (MINUTES)

Figure 3.10

at this point in time, were not short-circuited. The signal amplitude was regularly measured by introducing ammonia gas, but gas was only introduced for the duration of each measurement. The resulting decay of signal amplitude with time is shown in figure 3.11. When the capacitative charge had been lost from the focuser, after approximately 9 minutes, the focuser system was short-circuited. Thereafter the short-circuit was left in position. After a period of 60 minutes a spontaneous field increase was noticed. See figure 3.11.

It may be noted that the characteristic "spike" is not present because any free charge liberated would have been immediately neutralised by the short-circuit. The transition terminated in a somewhat enhanced signal level, presumably due to an increased effective surface charge density on the solid ammonia. Having reached a steady signal level, within a time of the order of the time constant of the focuser system, a constant signal amplitude was observed for a further 60 minutes. No sign of deterioration of the signal amplitude was noted up to the time that observations were discontinued.

3.11 Mechanism for the spontaneous field increase

A hypothesis for the mechanism of the spontaneous field increases which have been noted in sections 3.9 (iii), 3.10 (ii) and 3.10 (iv) is put forward here. Frei and Groetzinger (1936) have investigated the currents and charges liberated in the

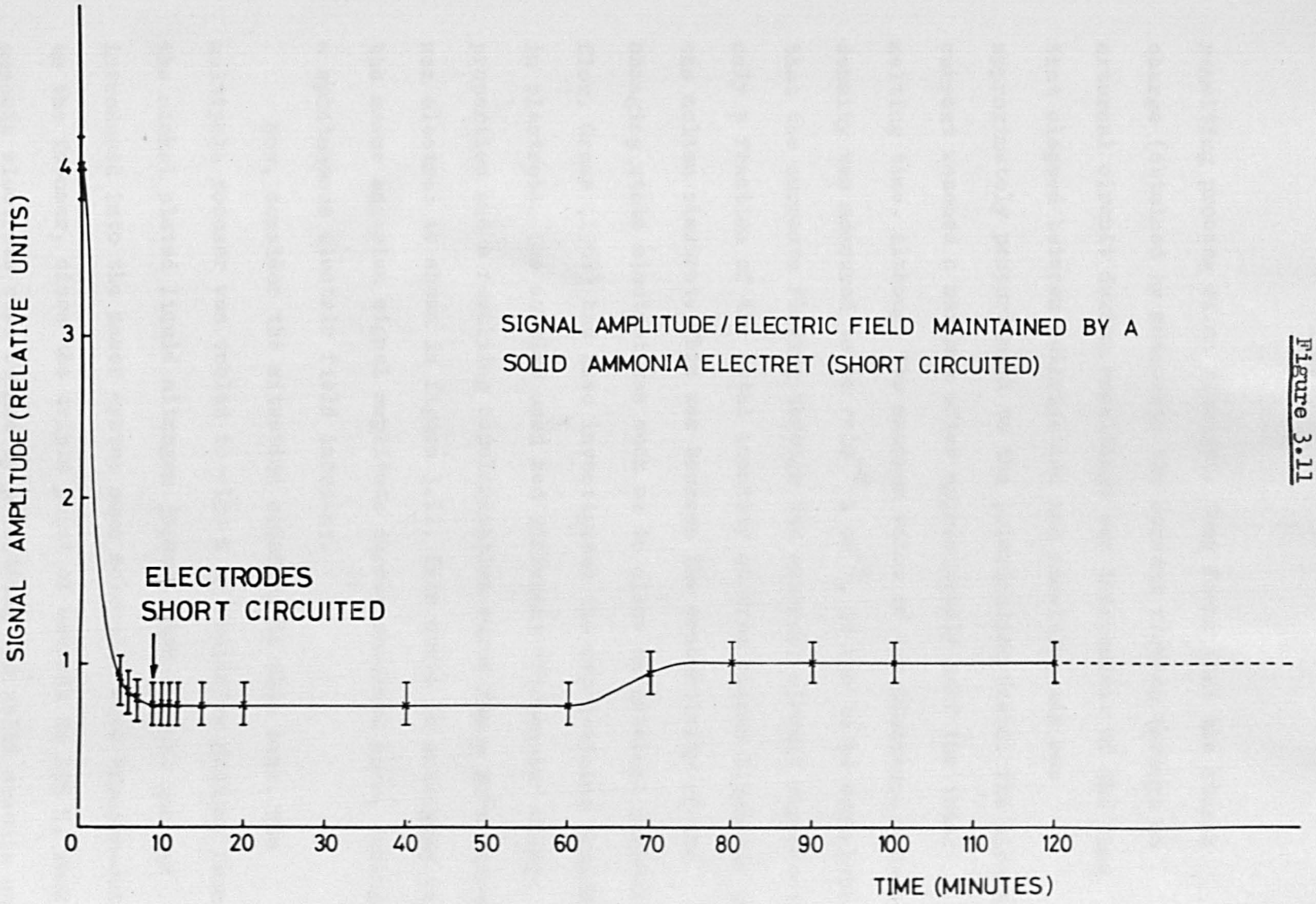
SIGNAL AMPLITUDE / ELECTRIC FIELD MAINTAINED BY A SOLID AMMONIA ELECTRET (SHORT CIRCUITED)
SIGNAL AMPLITUDE (RELATIVE UNITS)
4
3
2
1
ELECTRODES SHORT CIRCUITED
0
10
20
30
40
50
60
70
80
90
100
110
120
TIME (MINUTES)

Figure 3.11

remelting process of an electret. They found that the stored charge (obtained by measuring the current flowing through an external circuit during remelting) was independent of the time that elapsed between polarisation and remelting and was approximately proportional to the polarisation field. The disharge current reached a maximum after approximately half the total melting time. Although the maximum value of the discharge current density was measured to be $\sim 10^{-8}$ A cm^{-2}, it has to be remembered that the currents flowing through the external circuit represented only a fraction of the total quantity of free charge liberated in the molten electret. This was because the conductivity of the changing state electret was such as to allow an internal current flow. Gross (1968) has also investigated the depolarising phenomenom in electrets. The samples used had different "frozen-in" charge properties and a resulting depolarisation curve for a pure carnauba wax electret is shown in figure 3.12. This curve is analogous to the maser emission signal amplitude curves obtained here, during a spontaneous electric field increase.

Now, consider the situation obtained in this case. The multipole focuser was cooled to ~100 K by radiative cooling from the nickel plated liquid nitrogen jacket. When ammonia gas was introduced into the maser system some molecules were "frozen-out" on to the focuser, since the triple point of ammonia is 195 K. Thus ammonia electrets were formed by polarising the solid ammonia upon the

Figure 3.12

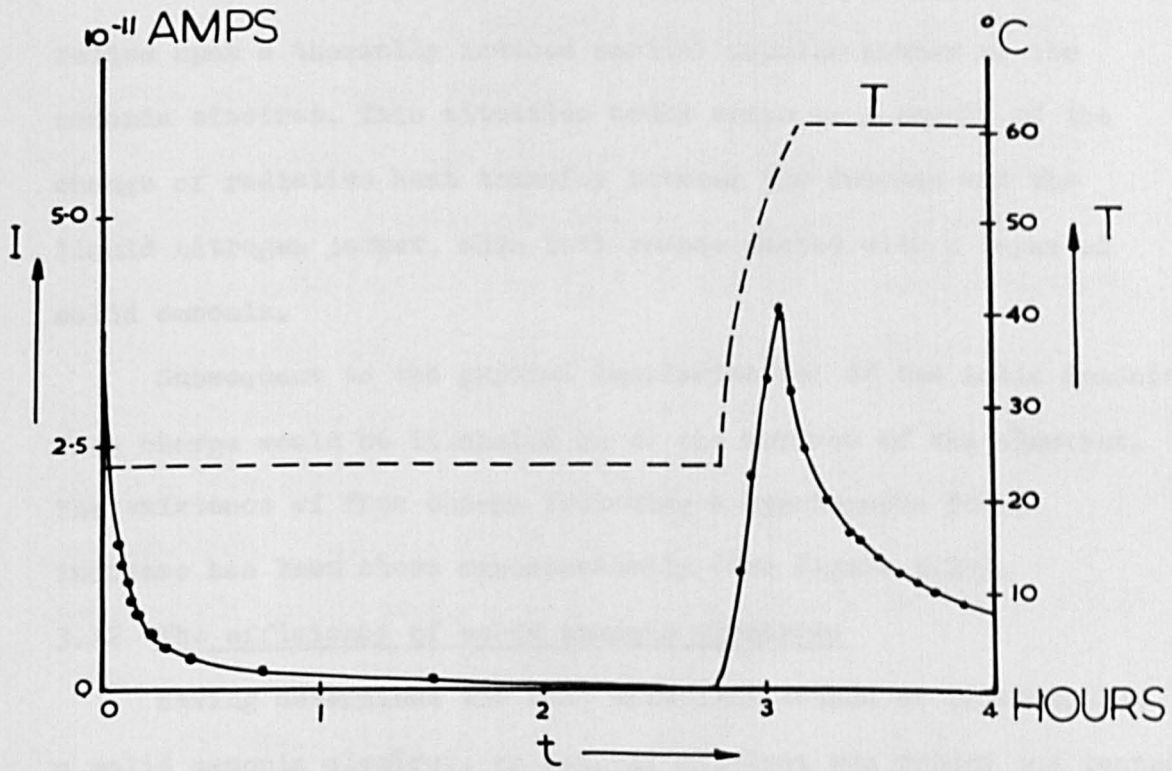

DEPOLARISATION CURVE.

(AFTER GROSS 1967)

focuser (or upon the surface of the carnauba wax electret focuser in 3.9 (iii)).It was observed that the liquid nitrogen jacket received a substantial coating of solid ammonia during the course of an experiment.

The mechanism proposed for the instantaneous field increase, relies upon a thermally induced partial depolarisation of the ammonia electret. This situation could arise as a result of the change of radiative heat transfer between the focuser and the liquid nitrogen jacket, when both became coated with a layer of solid ammonia.

Subsequent to the partial depolarisation of the solid ammonia, free charge would be liberated on to the surface of the electret. The existence of free charge following a spontaneous field increase has been shown experimentally. (See figure 3.10).

3.12 The efficiency of solid ammonia electrets

Having determined the most efficient method of constructing a solid ammonia electret, an ammonia electret was formed and tested.

(i) Construction of the solid ammonia test electret

The following processes were found to give the most satisfactory semi-permanent electrification of solid ammonia.

(a) The focuser was carefully cleaned and then replaced in the vacuum system. The maser system was evacuated and cooled with liquid nitrogen for ~ 3 hours.

(b) Ammonia gas was introduced into the system for ~ 2 hours at

a nozzle pressure of 2.6 torr and a background pressure of $\sim 5 \times 10^{-6}$ torr. It should be noted that the ionisation pressure gauge was not used while observation of the electret electric field was being made, in order to avoid any possibility of providing spurious free charges in the vacuum system which could affect the electret charge relaxation.

(c) The solid ammonia was polarised with a field of ~ 30 kV cm^{-1}, while the ammonia gas was being condensed onto the focuser.

(d) While monitoring the behaviour of the solid ammonia electret, the maser signal was detected and periodically observed using bursts of ammonia gas at a nozzle pressure of 2.6 torr. The ammonia gas was introduced only for the duration of signal amplitude measurement.

(e) The EHT was removed by using the oil-immersed switch and the focuser terminals were short-circuited.

(ii) Monitoring the electric field created by the solid ammonia electret

The maser emission signal amplitude was measured at regular intervals. The signal amplitude remained at a constant amplitude for 13 hours 30 mins. at which point a short-circuit was attached to the focuser input terminals. No alteration in signal amplitude was noted indicating that no free charge was present on these terminals. Observations were continued until the signal had been observed for a total of 18 hours 20 minutes when the system was closed down.

(iii) The solid ammonia electret

Eguchi (1925) has noted that electret surface charge reversal, if it takes place, usually occurs within the initial 24 hour period after the formation of the electret. The solid ammonia test electret which was monitored for more than 18 hours did not show any sign of surface charge reversal. Moreover, ammonia seems to be efficient as an electret, no decay of signal being noted during the monitoring period and there was no reason to suppose that if the system could be left cooled with liquid nitrogen and under vacuum it would not last for as long as Eguchi's carnauba wax type, that is at least ~ 4 years.

(iv) The formation of solid ammonia electrets

It was noted in experiments where ammonia gas was deposited on cleaned focuser electrodes to form an electret, that the decay of the initial charge varied with the period of ammonia deposition. This was observed when the focuser was not short-circuited. The effect was systematically investigated in a series of experiments with focusefs which had been pre-cooled by radiative heat transfer to the liquid nitrogen cooling jacket for at least 2 hours. The time required for the maser emission signal to decay to the detection system noise level, after disconnecting the EHT supply voltage to the focuser was recorded after measured gas deposition periods. Typical results may be seen plotted in figure 3.13.

A possible process that explains these results may be

Figure 3.13

CAPACITOR CHARGE NEUTRALISATION
BY SOLID NH_3
ASYMPTOTIC AT PRODUCTION OF NH_3 ELECTRET
TIME FOR DECAY OF SIGNAL TO NOISE LEVEL (MINUTES)
0
20
40
60
80
100
120
140
160
180
200
TIME (MINUTES)
TIME OF CONTINUOUS DEPOSITION OF NH_3 GAS
1
2
3
4
5
6
7
8
9

postulated as follows. Previous experiments with ammonia electret focusers, indicated that the solid ammonia retained its initial heterocharge, which is consistent with a dielectric material of comparatively high conductivity (Mikola, 1925). When an ammonia electret was formed on the metal substrate, the charge polarity upon the electrode/electret interface would be opposite to that upon the electret/vacuum interface. Further, due to the spatial distribution of molecules from the effuser, and the geometry of the focuser, a uniform solid ammonia coating would not be obtained and certain areas of electrodes would receive more molecules per unit area than others. In particular, electrode surfaces facing towards the molecular beam axis would be preferentially coated.

Electrode surfaces coated with solid ammonia would be capable of charge storage. The greatest charge leakage path, because ammonia is a good insulator, would be the external region between the electrode/electret and electret/vacuum interfaces. In this region ohmic leakage would take place.

Initially, the charge decay from a focuser uncoated with solid ammonia was recorded, by monitoring the decay of the maser stimulated emission signal. After a period of introducing ammonia gas into the maser, the EHT supply voltage was again disconnected and the decay of charge from the focuser was again monitored. In this case the charge decay time of the focuser was affected, probably by leakage of charge from partially formed solid ammonia electrets, neutralising

the capacitative charge of the focuser.

Further periods of ammonia deposition served to decrease the stimulated emission decay time after removal of the EHT voltage. This effect would be expected on the basis that increasing ammonia deposition would increase the surface area of solid ammonia and so, in turn, the charge leakage paths. In the limit, however, a uniform solid ammonia coating over the electrodes would be attained and the leakage paths would then be minimised. An electret with an almost asymptotic decay time would be formed and this was observed in practice.

3.13 General discussion

The operation of a molecular beam maser employing a focuser, with the electrostatic field provided by a system of electrets, has been shown to be feasible. The time dependence of the external electret electric field has been monitored by an electrically neutral molecular beam. Electrets monitored by short, occasional pulses or by continuous flow of the molecular beam, before the focuser had cooled sufficiently to freeze out molecules, produced comparable decay curves. This would indicate that normal electret decay processes affected the electret external electric field more than the focusing of the molecular beam.

Electret focusers have been formed from a number of materials : (a) carnauba wax, (b) a mixture of lead titanate and epoxy resin and (c) solid ammonia.

An independent proposal for the application of electret focusers has been made by Oraevskii (1964) in the conclusion to a review of molecular beam masers. Gubkin and Novak (1971) (published after the completion of the experimental work described in this chapter) investigated the configuration and strengths of the external electric field of a quadrupole system of knife-edge polymer electrets. These authors obtained their results by probing the field using an electrometer technique. They concluded that the lifetime of their system was about one year and that the configuration of the electric field was independent of time. Once again it was suggested that electret focusers should be employed in molecular beam masers.

Gubkin and Novak (1971) also suggested that greater electret stability could be obtained by using ceramic electrets rather than those made from polymers. Here, in the preparation of electret focusers for investigation, the sintering of titanates was attempted but was found to be unsuitable for the configurations which were required. Therefore, for this reason, lead titanate was bonded in an epoxy resin. The epoxy resin had suitable electrical properties, was room temperature cured and had resistance to thermal shock.(See Bakelite Technical Memorandum E165). However, in practice, the lead titanate - epoxy resin electret focuser was effective for only a short time compared with subsequent electret focusers which were investigated . This performance is attributed, in part, to the

relatively high conductivity of titanates ($\sim 10^{-14}$ ohm $^{-1}$ cm^{-1}) compared with other electret materials. The factor would enhance conduction loss (Fridkin and Zheludev, 1960). It is also possible, with this mixture, that occlusions developed during curing which would have further degraded its electret properties.

Carnauba wax electret focusers were subsequently employed to operate an ammonia beam maser. Practically, carnauba wax was a convenient material to form into an electret focuser. Its major disadvantage was that it cracked if left in air. Using the known oscillation threshold condition for the maser an estimate of the electric field produced by carnauba electrets in the focuser was possible. Electric fields ranging up to ~ 20 kV cm^{-1} were estimated. This result agrees with results indicated by Gubkin and Novak (1971) for a polymer quadrupole electret configuration.

An anomalous increase in the external electric field of a carnauba wax electret has been recorded in a prolonged experiment with an electret focuser of this type. This effect was attributed to the collection and the subsequent electrification of solid ammonia followed by a thermally induced partial depolarisation of the ammonia electret. Changes in the radiative cooling rate of the liquid nitrogen dewar followed when the dewar itself received a coating of diffused ammonia molecules from the beam. Isolation of the electret effect in solid ammonia (Lainé and Sweeting, 1971) was achieved by forming electrified solid ammonia upon a metal

relatively high conductivity of titanates ($\sim 10^{-14}$ ohm^{-1} cm^{-1}) compared with other electret materials. This factor would enhance conduction loss (Fridkin and Zheludev, 1960). It is also possible, with this mixture, that occlusions developed during curing which would have further degraded its electret properties.

Carnauba wax electret focusers were subsequently employed to operate an ammonia beam maser. Practically, carnauba wax was a convenient material to form into an electret focuser. Its major disadvantage was that it cracked if left in air. Using the known oscillation threshold condition for the maser, it was possible to estimate the electric field produced by the carnauba wax electrets in the focuser. Electric fields ranging up to ~ 20 kV cm^{-1} were estimated. This result agrees with results obtained by Gubkin and Novak (1971) for a polymer quadrupole electret configuration.

An anomalous increase in the external electric field of a carnauba wax electret has been observed in a prolonged experiment with an electret focuser of this type. This effect was attributed to the collection and subsequent electrification of solid ammonia followed by a thermally induced partial depolarisation of the ammonia electret. Changes in the radiative cooling rate of the liquid nitrogen dewar followed when the dewar itself received a coating of diffused ammonia molecules from the beam. Isolation of the electret effect in solid ammonia (Lainé and Sweeting, 1971) was achieved by forming electrified solid ammonia upon a metal

focuser. The spontaneous external electric field increase was again observed after the liquid nitrogen dewar became coated with diffused molecules. Ammonia electrets could be made following one of two methods. Firstly, the electret could be formed by polarising ammonia molecules in an electric field as they collected upon the metal electrodes which were continuously charged by an external EHT supply. Secondly, ammonia molecules could be collected upon the metal focuser electrodes and then polarised by instantly applying an electric field using an external EHT supply which was connected to the focuser electrodes. Once the temperature in the electret focuser system had reached an equilibrium value, then the ammonia electret focusing field remained constant for a considerable period of time, in one case for approximately 19 hours before the experiment was terminated.

The majority of materials used to make electrets have a complicated chemical structure. With this problem in view, work has recently been performed with ice electrets (Cross, 1968) in order to observe the electret effect in a relatively simple structured material. It is possible that the properties of thin film ice electrets might be investigated in the water maser (Bluyssen et al, 1967).

CHAPTER IV

COHERENT SPONTANEOUS EMISSION

4.1 Introduction

The importance of relaxation phenomena in microwave spectroscopy of gases, has been discussed in Chapter 1. The excitation of coherent spontaneous radiation from a medium has become a well used technique that is frequently used to investigate dephasing mechanisms. Dicke (1954) has analysed a system of radiators that, after excitation, spontaneously and coherently emits radiation in transitions between two non-degenerate energy levels. The effects of co-operative coherence were analysed. Dicke cited work by Hahn (1950) in the field of nuclear magnetic resonance, when spin echoes were obtained by exciting correlated states of atomic systems. The mechanism given by Hahn was a classical one, based upon the motion of a gyromagnet in a magnetic field. The nuclear induction formalism, as the classical motion is known, was originally proposed by Bloch (1946).

Dicke termed a gas which is radiating because of coherence, as "super-radiant". One method of making a gas super-radiant is to apply an exciting pulse of resonant radiation. Dicke showed that the intensity of the coherent radiation produced by an exciting pulse, is proportional to N^2, where N is the total number of molecules present. Treatments for spontaneous radiation processes, prior to that of Dicke, tacitly assumed that separate molecules radiated

independently, producing a radiation rate from excited molecules proportional to N, which is incorrect. The factor overlooked, was that the molecules interact with a common radiation field and hence cannot be treated as independent.

Spontaneous coherent radiation signals have been observed by Hahn (1950) and Gabillard (1951) in nuclear magnetic resonance and by Lainé (1966) and Jenkins and Wagner (1968) in electric dipole systems. Various techniques have been employed to obtain the requisite induced macroscopic polarisation in the active medium. Hahn (1950) and Jenkins and Wagner (1968) adopted pulsing with resonant driving fields, whereas, Gabillard (1951) and Lainé (1966) used the adiabatic fast passage technique. Adiabatic fast passage has two experimental advantages over the application of resonant pulses (a) it is not necessary to control the frequency of the excitation signal and (b) the exact duration and time dependence of the frequency sweep are not critical.

Gabillard (1951) observed "beating of beats" (See figure 4.1) in a magnetic dipole system. It occurred by intermodulation of two "wiggles" signals from two closely separated resonance lines. The effect may occur in nuclear magnetic resonance in a homogeneous magnetic field, with two samples whose resonant frequencies are slightly different because of chemical shifts (Bené et al, 1951) or different paramagnetic ion concentrations (Gabillard, 1951). The technique of "beating of beats" has been applied by Bené et

Figure 4.1

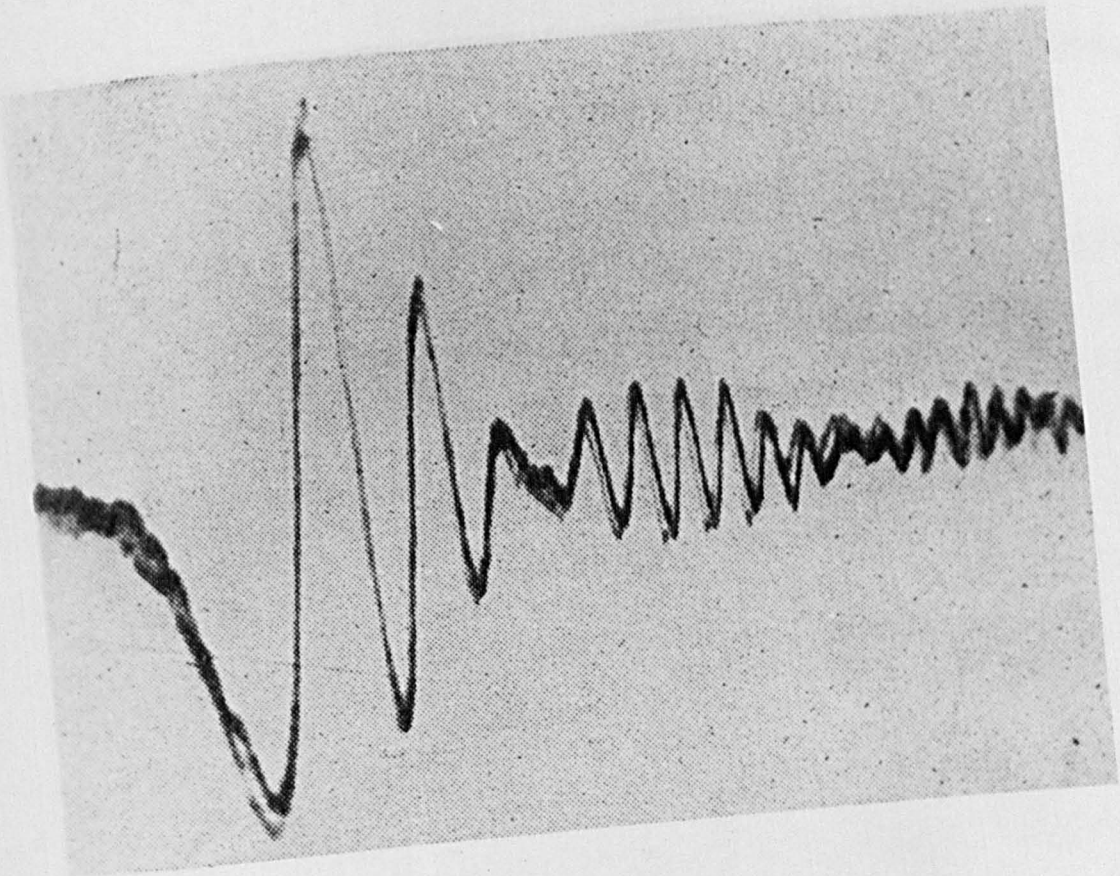

Nuclear magnetic resonance 'beating of beats'.

(after Gabillard,1952)

al (1953) to the measurement of small magnetic field gradients.

The adiabatic fast passage technique has been employed in this present work to excite coherent spontaneous emission from the naturally split main J = 1, K = 1 inversion transition of ammonia, to produce "beating of beats" in an electric dipole system as the electric analogue of the corresponding nuclear magnetic resonance phenomenon.

4.2 Relaxation effects

Relaxation mechanisms have been related to spectral line broadening in section 1.6. The T_1, T_2 notation for relaxation times, originates from the field of nuclear magnetic resonance. There they were used by Bloch (1946) to describe the time dependence of the induced macroscopic polarisation, M, of a system of nuclear spins, when subjected to a radiofrequency magnetic field perpendicular to a steady magnetic field. T_1 processes describe the decay of the component of magnetisation in the direction of the steady magnetic field. T_2 processes describe the decay of the transverse magnetisation components.

The results of a formalism developed by Feynman et al (1957) are indicated in section 4.3. Using this formalism, the analogous behaviour of non-interacting two level magnetic and electric dipole systems may be pictured intuitively. Echoes and other relaxation dependent effects will be discussed in section 4.5. The relaxation processes T_1 and T_2 will now be summarised.

(a) T_1 processes: If the total number of molecules in any particular energy state, i, of energy W_i is $N_i(W_i)$, then the total

internal energy is given by W, where,

$$W = \sum_i N_i(W_i) . W_i \qquad (4.1)$$

When the total energy of the molecular system differs from the equilibrium value W_{eq}, then spontaneous changes will occur. These will result in a net transfer of energy between the internal degrees of freedom of the molecular system and its environment, tending towards a state of thermal equilibrium. The processes that contribute to this exchange of energy are termed T_1 relaxation processes. The variation of the molecular energy, W, from its equilibrium value, W_{eq}, in most practical cases, decays exponentially with time,

$$\frac{d(W - W_{eq})}{dt} = -\frac{1}{T_1} . (W - W_{eq}) \qquad (4.2)$$

The reciprocal of the decay constant has the dimensions of time.

(b) T_2 processes: Since the equilibrium condition is one of a random distribution of molecular phases, any coherence between the various molecules in the system is equivalent to an ordered and hence non-equilibrium state. In this situation, the energy of the system need not necessarily vary from its equilibrium value, W_{eq}, to produce a non-equilibrium state. Relaxation processes destroying the coherence of the system are describable, phenomenologically, by a T_2 relaxation time. They can adequately be described by an exponential decay of the coherence of the system.

4.3 Two level systems

Feynman et al (1957) formulated a geometrical representation of the Schrödinger equation for both electric and magnetic two level systems. The motion of the magnetic dipole vector with a spin $\frac{1}{2}$ may be represented in a physical space. The axes of quantisation which determine the precession of the magnetic dipole are:

(a) the direction of the steady magnetisation of the system and (b) the radiofrequency magnetic field applied to the system. The net magnetisation of the system may be pictured as precessing about these two axes.

In the electric dipole system there is no axis representing a steady electric field because there is no preferred direction about which the electric dipole moments can precess. The corresponding motion of a vector, representing the macropolarisation of an electric dipole system, has to be represented in a mathematical space. In the case of an electric dipole system the axes represent:

(a) the macropolarisation of the electric dipole system,

(b) the characteristic transition frequency between the two energy levels of the system (in this case equal to the resonant frequency of the cavity containing the molecules),

and (c) the excess population between the two energy levels.

It is somewhat more convenient to visualise the motion of a precessing vector in a physical space rather than in a complex mathematical space. In the magnetic dipole system, the picture,

formulated by Feynman et al, has the same form as the three dimensional classical model of a gyromagnet in a steady magnetic field.

Therefore, the nuclear induction model has been used here to describe, analogously, the behaviour of electric dipole systems subjected to resonant radiation. The effect of relaxation mechanisms upon an electric dipole system is not immediately obvious in the geometrical picture but the effect is shown intuitively in the phenomenological treatment of the behaviour of a gyromagnet in a steady magnetic field (Bloch, 1946).

4.4 The phenomenological Bloch equation

4.4.1 Magnetic dipoles

The phenomenological Bloch equation,

$$\frac{d\bar{M}}{dt} = \gamma_m(\bar{M}\times\bar{H}) - \frac{(\bar{i}M_x+\bar{j}M_y)}{T_2} - \frac{\bar{k}(M_z-M_o)}{T_1} \qquad (4.3)$$

was formulated for a system of nuclear spins subjected to:

(a) a steady magnetic field H_o in the z direction,

and (b) a circularly polarised radiofrequency magnetic field H_1 which rotates in the xy plane at an angular frequency ω, in the same sense as the Larmor precession. It should be noted that the angular frequency ω is not necessarily equal to the resonance frequency ω_o.

In the equation (4.3) $\bar{i}, \bar{j}$ and $\bar{k}$ are unit vectors along the x, y and z axes, and,

$$\bar{H} = H_1(\bar{i}\,\mathrm{Cos}\,\omega t - \bar{j}\,\mathrm{Sin}\,\omega t) + \bar{k}H_o \qquad (4.4)$$

The constant γ_m is the gyromagnetic ratio and M_x, M_y and M_z are components of the net magnetisation of the nuclei, M. The magnetic dipoles perform a damped precessing motion, in which the rotating transverse components of M decay to zero with a characteristic time, T_2, whereas, M_z relaxes to its equilibrium value M_o with a characteristic decay time, T_1.

4.4.2. Electric dipoles

Abella et al (1964) employed the formalism of Feynman et al (1957) to picture the motion of a precessing dipole moment in an electric dipole system. The Hamiltonian for the electric dipole system was of the form,

$$\mathcal{H} = \bar{p}.\bar{\mathcal{E}} \qquad (4.5)$$

where $\bar{p}$ was the effective electric dipole moment and $\bar{\mathcal{E}}$ was the effective electric field. An analogous equation to the one which was derived by Bloch (equation 4.3) was obtained by deriving the time dependence of $\langle\bar{p}\rangle$ and subsequently adding phenomenological relaxation terms,

$$\frac{d\langle\bar{p}\rangle}{dt} = \gamma_e \langle\bar{p}\rangle \times \bar{\mathcal{E}} - \frac{(\bar{i}\langle p_x\rangle + \bar{j}\langle p_y\rangle)}{T_2} - \frac{\bar{k}(\langle p_z\rangle - \langle p_o\rangle)}{T_1} \qquad (4.6)$$

here γ_e is a constant which is analogous to the gyromagnetic ratio in nuclear magnetic resonance (see equation (4.3)). γ_e is a function of the average value of the electric dipole moment operator between

the two states of this assumed two level system, $\bar{i}$, $\bar{j}$ and $\bar{k}$ are unit vectors along the x,y and z axes. T_1 and T_2 represent the longitudinal and transverse relaxation times respectively. The quantity $\langle p_o \rangle$ is the thermal equilibrium value for the z-component of $\langle p \rangle$. The quantity T_1 is normally the radiative lifetime of the excited state.

4.5 Analogies

4.5.1 Echoes

Abella et al (1964) observed photon echoes analogous to the nuclear magnetic resonance echoes first observed by Hahn (1950). Hahn subjected a sample containing a large number of paramagnetic atomic nuclei, to two resonant pulses (a $\pi/2$ pulse followed a time τ later by a π pulse) of an oscillating magnetic field, while a large constant magnetic field was applied to the sample. The paramagnetic nuclei then generated an echo signal at a time τ after the second pulse. The mechanism for the echoes was explained in terms of a classical Bloch model.

When a large number of paramagnetic atomic nuclei of spin $\frac{1}{2}$ are placed in a large, constant magnetic field, the magnetic moments of the nuclei are polarised in the direction of the magnetic field. If a small, circularly polarised magnetic field, rotating in the plane perpendicular to the steady magnetic field, is applied at the precession frequency of the nuclei, then the nuclei will nutate around the resultant of the two magnetic

fields. The downward spiral motion followed by each nuclear magnetic dipole moment eventually brings them into the transverse plane. At this point in time, corresponding to a $\frac{\Pi}{2}$ pulse, the rotating magnetic field is removed.

The magnetic moments of all the nuclei are oriented at right angles to the constant magnetic field and are rotating together at the resonant frequency of the system. As a result, the coil housing the sample, has an electrical signal induced in it. The induced signal is reduced quickly to zero because of longitudinal relaxation, and magnetic field inhomogeneities dephase the magnetic moments in the transverse plane.

If a second resonant radiofrequency magnetic field pulse is applied for a period of time twice as long as the first (Π pulse) then the magnetic moments will ultimately precess to their former position, in the transverse plane in a time τ equal to the period between pulses. The important feature of the new magnetic dipole configuration, is that the relative phase angle of any two dipole moments, before and after the second pulse, is exactly reversed. After a time interval equal to the time it took the dipole moments to dephase in the first place, they again instantaneously precess together in the transverse plane. The result is that a temporary electrical signal is induced in the coil housing the sample. This is called the nuclear spin echo.

The preceding analysis for a nuclear spin echo was formulated

for a pulse sequence giving an optimum echo signal. Other pulse sequences will give weaker signals. The analysis of the echo phenomenon also holds for the case of electric dipole moments.

Abella et al (1964) observed a photon echo when chromium impurity ions in ruby were excited by circularly polarised light. The chromium impurity ions may be regarded as an ensemble of two-level systems, coupled by an interaction of the electric dipole moments of the ions with the rotating electric field vector of the circularly polarised light. The echoes produced by the chromium ions were pulses of light, formed by the oscillating dipole moment. The electric dipole moment of the atom arose from the induced polarisation of its electric charge distribution. An applied constant electric field was not required to act as an axis about which the dipoles could precess.

The narrow linewidths obtainable in molecular beam spectrometers make it possible in principle for electric dipole echoes to be observed in one of these devices (Oraevskii 1967). Jenkins et al (1968) have observed electric dipole echoes in bulk ammonia gas. They used the effect to investigate scattering cross-sections.

4.5.2. "Wiggles"

Bloembergen et al (1948) observed an effect which they termed "wiggles", in a nuclear magnetic resonance system. This effect is shown in figure 4.2. The effect occurred when an

Figure 4.2

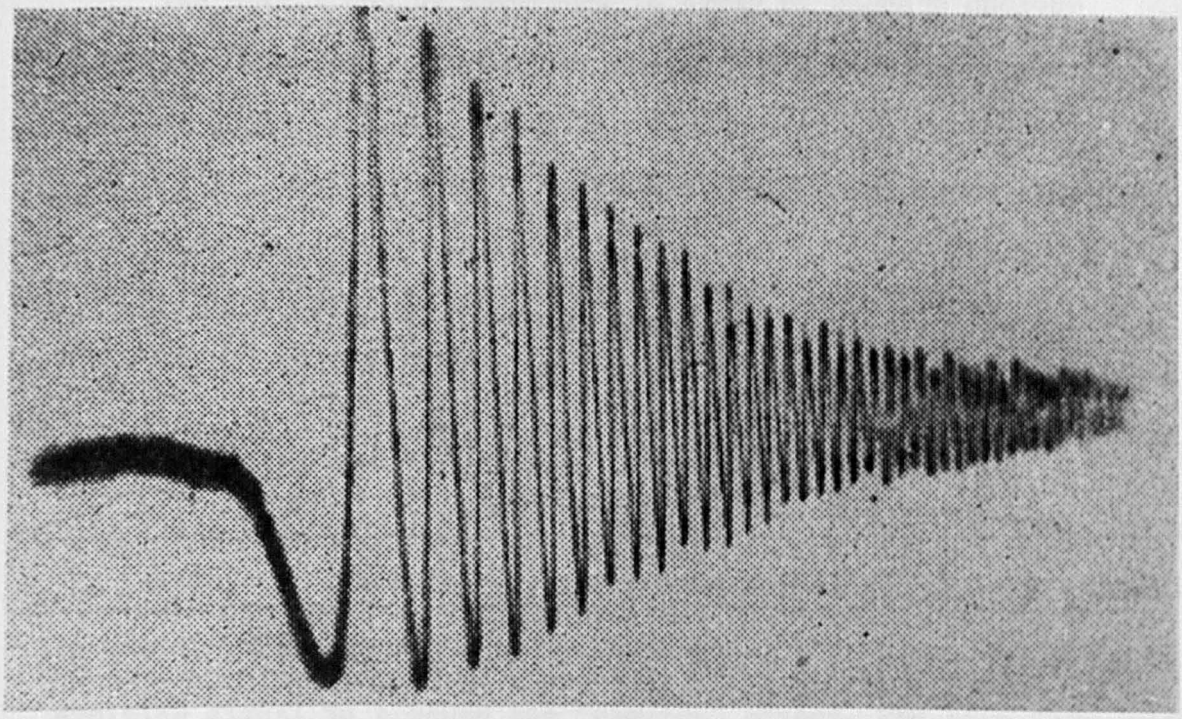

Nuclear magnetic resonance 'wiggles'.

(after Gabillard,1952)

exciting signal was swept through a resonance line, in a time short compared with T_1 and T_2 and $(\gamma_m \delta H_o)^{-1}$, where γ_m was the gyromagnetic ratio of the magnetic dipoles and δH_o was the inhomogeneity of the steady magnetic field, H_o, over the specimen.

The effect can be described in terms of Bloch's nuclear induction formalism. The nuclear magnetic dipole moments may be considered as precessing about the steady magnetic field, H_o. When the resonance condition between the electromagnetic field and H_o is satisfied,

$$2\pi\nu = \gamma_m H_o \qquad (4.7)$$

The nuclear dipole moments are brought into phase and the precessing net magnetisation, M, induces a signal in the coil housing the sample. The frequency of the induced signal increases with time (since $\omega = \gamma_m H_o$ and H_o increases with time) and beats with the exciting signal to produce the "wiggles" effect. The high frequency components of the "wiggles" are attenuated because of the amplifier band-pass limitations. The beats persist until the nuclear magnetic moments dephase.

In section 4.2 (ii) it was noted that the phase coherence of the nuclei would be destroyed in a time $\sim T_2$, and Bloch assumed that the decay to zero would be exponential. The decay envelope of the "wiggles" signal, produced by a Lorentzian lineshape, is a Fourier transform of the line and it may be described by a function

(Lainé et al, 1969),

$$A = A_o \exp\left[\frac{-t}{T_2}\right] \qquad (4.8)$$

where, A_o is the initial signal amplitude and A is the signal amplitude at a time t.

Lainé (1966) first observed the "wiggles" phenomenon in an electric dipole system. The effect followed the rapid passage of an exciting signal through the stimulated emission signal, from the J = 3, K = 3 inversion line of ammonia observed in a beam maser. The exciting signal was passed through the emission line in a time shorter than the mean transit time of molecules through the resonant cavity. Immediately after the passage of the exciting signal, the molecules in the cavity possessed an oscillating net polarisation at the molecular resonance frequency. Subsequently, as the molecules passed out of the cavity and T_2 decay processes took place, the coherent signal generated by the molecules decayed. The decaying ringing signal beat with the applied exciting signal and produced the "wiggles" phenomenon.

4.6 "Beating of beats"

In an electric dipole system, closely spaced spectral lines, suitable for the observation of the "beating of beats" effect, may be found in the hyperfine structure of molecular resonance spectra. The experimental observation of the beating of beats effect is described here, using the split main line of the J = 1, K = 1

inversion transition of ammonia. This particular spectral line was selected because the line is resolved into two main line components with a frequency difference ~25.5 kHz, a separation that allowed the wiggles of the last excited component to be superimposed upon the decaying wiggles signal of the first excited component.

The sensitivity of the molecular beam maser employed had to be optimised to obtain good signal to noise ratios for the J = 1, K = 1 inversion transition main spectral line. The main split line is weak in intensity in comparison with other spectral lines in the ammonia spectrum. The J = 1, K = 1, and J = 3, K = 3 inversion spectra have respective intensities of 1.6×10^{-4} cm^{-1} and 7.9×10^{-4} cm^{-1}. However, the resolved components of the main line of the J = 1, K = 1 transition have approximately equal amplitudes which, together with their close frequency separation, made the transition suitable for observing the "beating of beats" effect.

4.7 The spectrometer

An ammonia molecular beam spectrometer fitted with an open Fabry-Perot type resonant cavity was employed in the experimental work. This particular type of cavity had a tuning range which encompassed the J = 1, K = 1 inversion transition of ammonia. The internal structure of the spectrometer is shown in figure 4.3, and details of the spectrometer are described in Appendix I. However, the excitation and detection schemes will be described here.

Figure 4.3

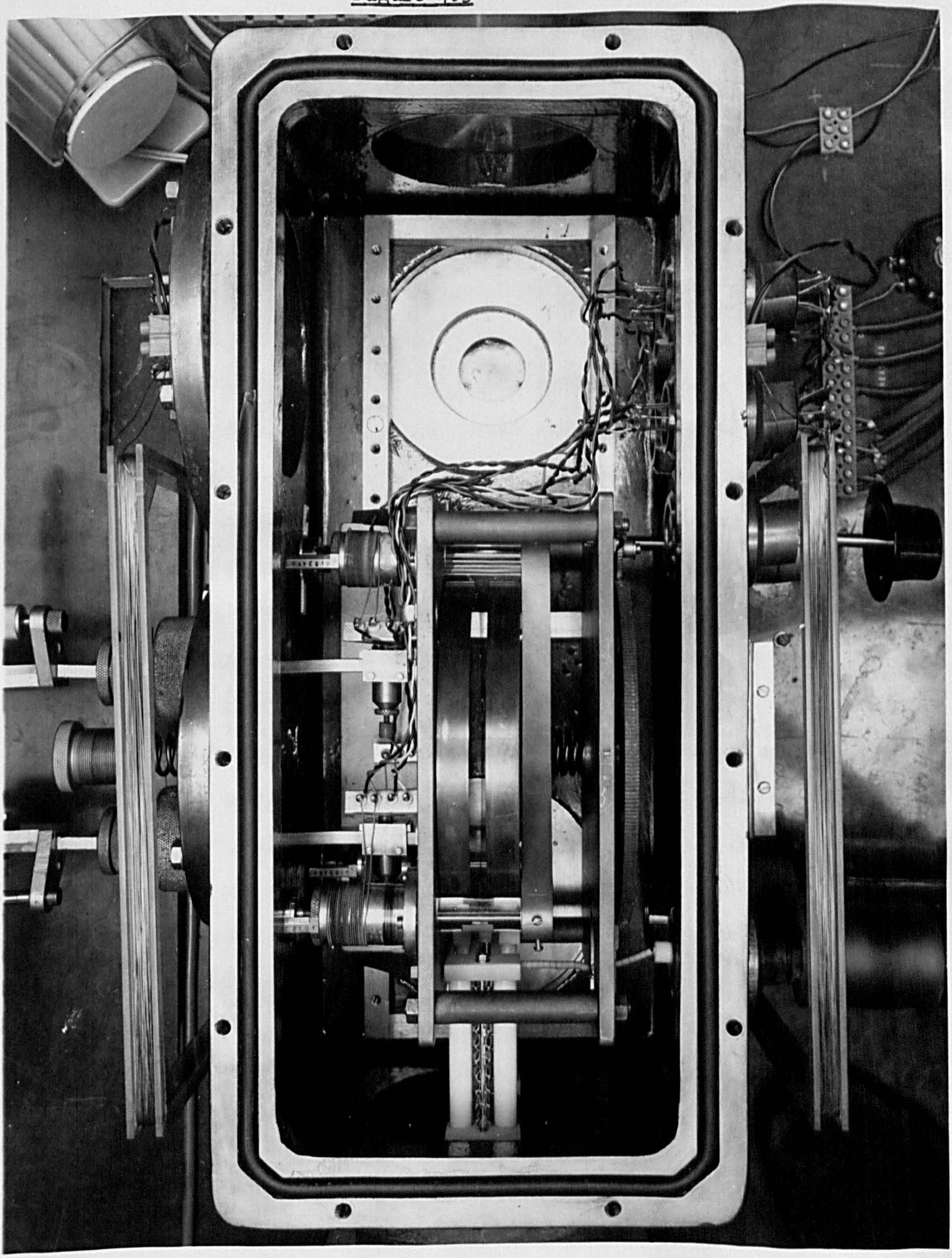

The internal structure of the spectrometer

4.7.1 Detection system

After the completion of the initial setting up procedure of the Fabry-Perot cavity using crystal video detection, the maser spectrometer was operated in transmission with a single klystron (Elliot - Lytton Type 12RK3) superheterodyne detection system. The exciting signal was one of the two sidebands produced by amplitude modulation of a portion of the local oscillator power. The superheterodyne detection system is shown schematically in figure 4.4.

Microwave power passed from the klystron towards circulator, C_2, via an attenuator A_2. Some microwave power was taken by a directional coupler and passed onto circulator C_1 via an attenuator A_1 and a microwave isolator. The microwave signal passed from circulator C_1 into a mixing diode (Sylvania IN26A) where it was mixed with a 30 MHz signal from a signal generator. The composite signal was returned to the circulator and then one sideband was matched into the Fabry-Perot cavity by using the matching unit M_2. The cavity was resonant at the frequency of the chosen sideband signal.

The microwave signal excited the cavity which was tuned to have only one maximum of electric field in the direction that the molecular beam was propagated. The cavity was operated in transmission and therefore a further iris was employed to extract a signal from the cavity. This signal was fed, via waveguide, through the matching unit M_1 to the circulator C_2. The microwave signal transmitted along the waveguide fitted with the attenuator A_2 passed circulator C_2 and

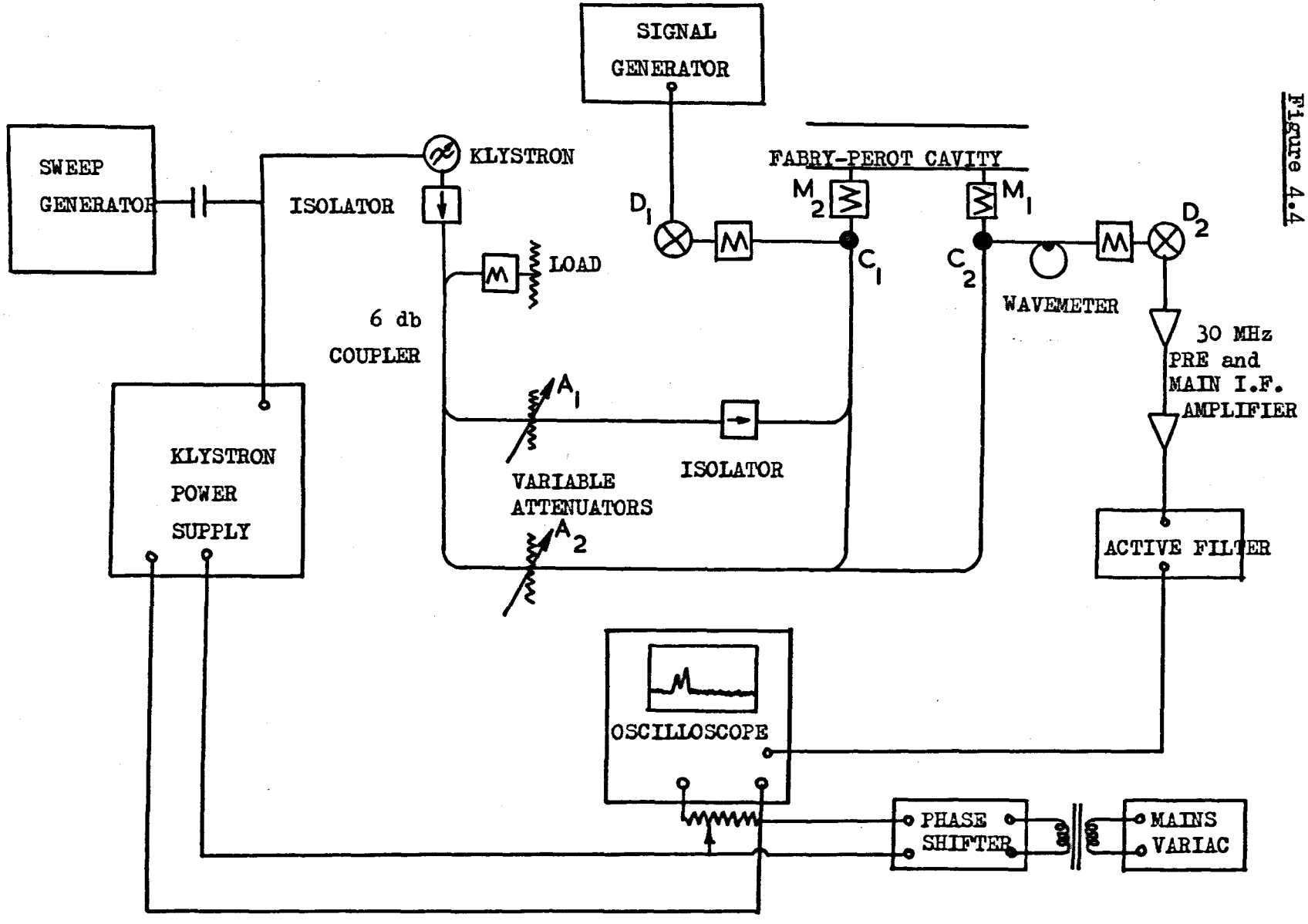

Figure 4.4

Schematic diagram of the apparatus used to observe "beating of beats".

then on to matching unit M_1 where it was mismatched and was thus reflected back to circulator C_2.

The diode D_2 then mixed the microwave signals that had,

(a) been received from the resonator, and

(b) been reflected from the resonator.

A Sylvania IN26A crystal was employed. The detected signal was amplified in a low noise (3 db) pre-amplifier initially and then in a 30 MHz main amplifier which had a diode connected across the output. The detected output signal from across the output diode was fed into a high gain amplifier which provided Y- deflection of the trace of a Telequipment D43 oscilloscope.

Two methods were available for electronically tuning the klystron. (a) A variable amplitude (0 to 120 volts) sawtooth voltage at a frequency of 50 Hz could be applied to the klystron reflector via a capacitor. In this case the oscilloscope timebase was synchronised to the sawtooth generator. (b) For high scanning rates, the 50 Hz generator described in (a) was unsuitable. The sweep voltage was replaced with one derived from the Telequipment D43 oscilloscope timebase unit. The control for this unit was calibrated and therefore the sweep rates could be evaluated. The oscilloscope sweep output was connected, via a potentiometer which controlled the voltage amplitude, to the klystron reflector. Any weak 50 Hz mains voltage "pick-up" signals were compensated by injecting small, mains derived voltages into the external klystron

reflector sweep line via a phase shifter.

4.8 The J = 1, K = 1 inversion spectrum of ammonia

The J = 1, K = 1 inversion spectrum of ammonia lies at 23.694 GHz. The reduced efficiency of the focuser in sorting molecules in this particular energy state, in comparison with molecules in the J = 3, K = 3 quantum state, resulted from a reduced energy interaction in the focuser electrostatic field. Thus a relatively low signal to noise ratio was obtained for spectral components of the J = 1, K = 1 inversion transition.

The naturally split main emission line of the J = 1, K = 1 transition may be seen in figure 4.5. This figure may also be compared with figure 4.6 where the theoretical lineshape, which was calculated by Gordon et al (1955), is illustrated.

4.9 Observation of the "beating of beats" effect

The setting-up procedure of the molecular beam spectrometer which has been described in section 4.7 was followed. It was possible to determine the frequency of the J = 1, K = 1 inversion transition of ammonia from standard tables which were prepared by Kisliuk and Townes (1952). The klystron was off-set in frequency by the I.F. frequency and the sideband signal was set to the J = 1 K = 1 transition frequency by a wavemeter. The Fabry-Perot cavity was then tuned to this frequency and stabilised by temperature controllers. At this stage the exciting signal was being scanned at a frequency of 50 Hz. After the introduction of an ammonia molecular beam into

Figure 4.5

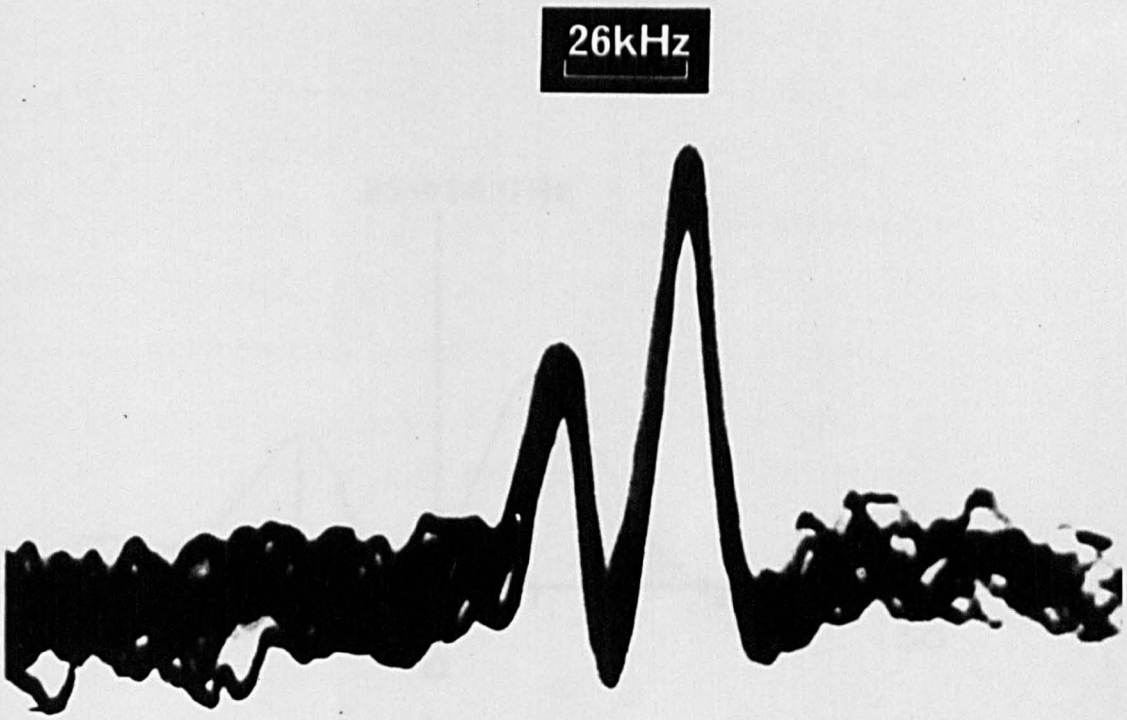

Oscilloscope photograph of the $^{14}NH_3$ J=1, K=1 inversion spectrum (split main line).

Figure 4.6

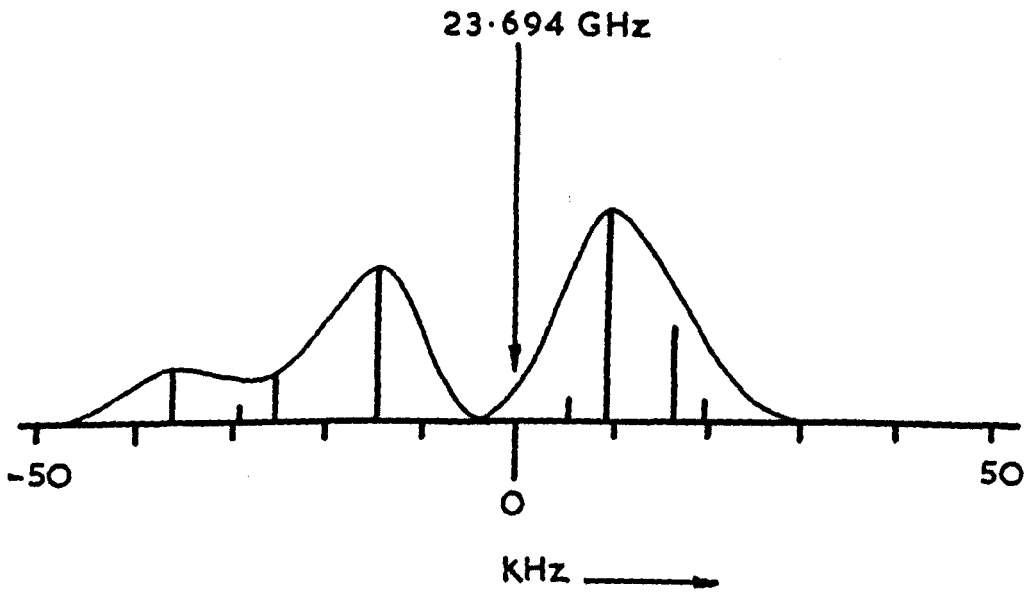

Theoretical spectrum of the J = 1, K = 1 inversion transition of ammonia.

(after Gordon, 1955)

the spectrometer, when the background pressure was $\sim 5 \times 10^{-6}$ torr, considerable adjustment of the detection system was required to increase its sensitivity before the weak J = 1, K = 1 main line inversion transition was observed.

To observe the "beating of beats" effect it was necessary to obtain a "wiggles" interference pattern produced by both of the resolved components of the J = 1, K = 1 main line. In practical terms this required the second of the components to be excited before the "wiggles" from the first had decayed to the noise level of the signal detection system. As noted in section 4.5.2, the amplitude of the "wiggles" signal, A, decays according to,

$$A = A_0 \exp\left[\frac{-t}{T_2}\right]$$

Thus rapid exciting signal scanning rates were required. These were achieved by employing a Telequipment D43 oscilloscope timebase in the way described in section 4.7.1.

Although the detection system had a large effective bandwidth ($\sim$ 800 kHz), the high frequency components of the "beating of beats" effect were strongly attenuated by the limited I.F. amplifier band-pass. To overcome this problem, the following procedure was adopted. It was possible to adjust the frequency of the klystron, which, together with the signal generator, produced a sideband signal that was swept to excite the J = 1, K = 1 main inversion transition frequency of ammonia. Thus the sideband frequency was adjusted so that a coincidence between the I.F. amplifier band-pass

and the J = 1, K = 1 inversion frequency, as shown in figure 4.7 was obtained. In this way, when the exciting signal was rapidly scanned, the high frequency interfering "wiggles" from the resolved components of the J = 1, K = 1 main line were amplified with an amplification that increased in frequency up to the centre of the I.F. amplifier band-pass. This procedure distorted the "beating of beats" decay envelope but the period of the beats, which was to be measured, was unaffected.

The resulting "beating of beats" interference pattern, observed using a scanning rate $\sim$ 500 MHz s^{-1}, with a repetition frequency of 10 kHz, is shown in figure 4.8.

4.10 Discussion

From measurements of the period of the decaying interference pattern shown in figure 4.8, it was possible to calculate the frequency separation of the resolved components of the J = 1, K = 1 main line inversion transition of ammonia. A value of $\sim$ 26 kHz $\pm$ 2 kHz was obtained. This result compares favourably with the value of 25.5 kHz recorded by Kukolich (1967) who employed a conventional beam maser spectroscopic technique.

The interference pattern from the closely spaced resolved components of the J = 1, K = 1 split main line precluded the accurate measurement of T_2 relaxation times. A similar problem was encountered by Lainé et al (1969) when "wiggles" from the main line of the J = 3, K = 3 inversion transition were observed in bulk

Figure 4.7

Scheme for optimising response of I.F. amplifier to high frequency components of 'beating of beats' signal.

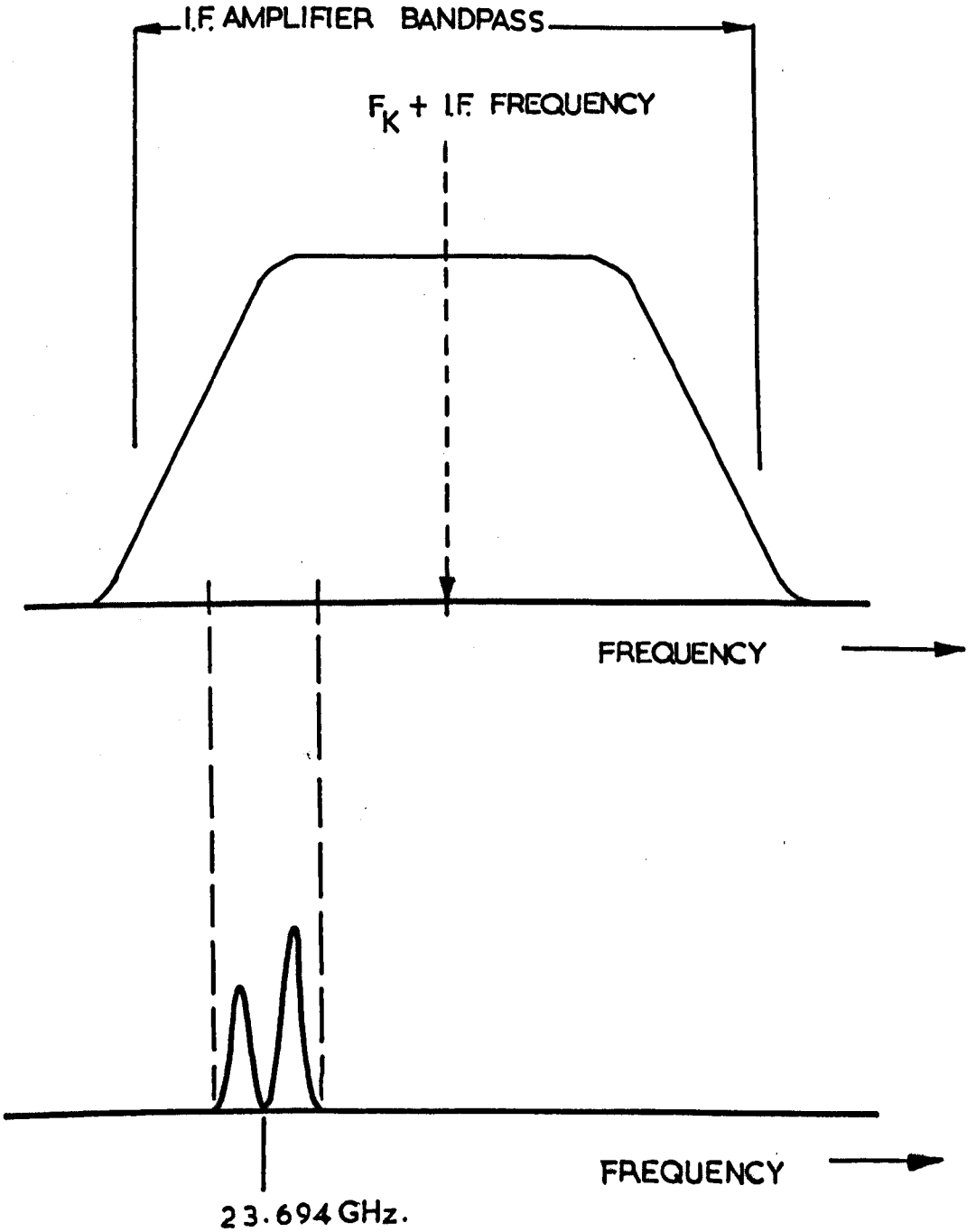

Figure 4.8

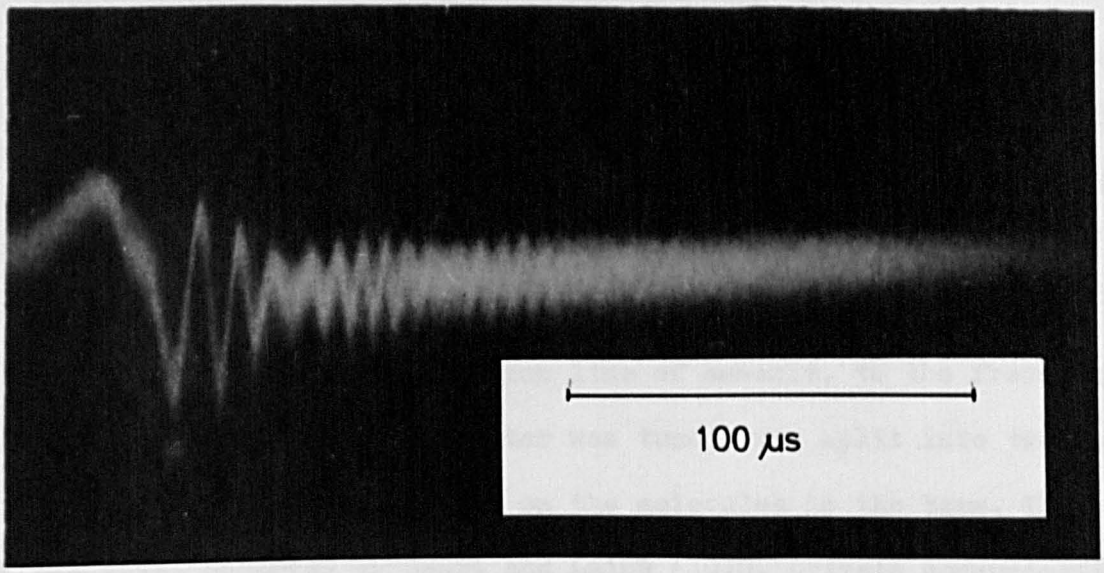

The 'beating of beats' effect following the rapid passage of an exciting signal through the naturally split main line of the J=1,K=1 inversion transition of ammonia.

ammonia gas. T_2 measurements were not possible because of partial interference of the decay envelope by "wiggles" produced by the quadrupole satellite lines.

Observation of the "beating of beats" effect in an electric dipole system is not restricted to naturally split spectral lines. It is possible to observe the effect when a normally single spectral line is artificially split. The splitting may be achieved by using the Zeeman effect. In this particular maser, the "beating of beats" effect was observed when a magnetic field was applied in a perpendicular direction to the plane of the Fabry-Perot plates. The main $J = 3$, $K = 3$ inversion line of ammonia, to the frequency of which the Fabry-Perot resonator was tuned, was split into two components because of the Zeeman effect on the molecules in the beam. The effect was first observed by Smart and Lainé (1970, private communication).

The "fast passage" technique, which was employed here to excite the molecules in the beam into a coherent state, was somewhat easier, from an experimental point of view, than pulsing the system with resonant microwave radiation. When using the pulse technique, the restraints on the frequency stability are critical. Radiation has to be injected into the molecular system within the linewidth of the required transition. Nevertheless it should be possible, in practice, to obtain the requisite $\pi/2$ and π pulse sequence (referred to in section 4.5.1) and so obtain echoes from a molecular beam, by pulsing the microwave source. The feasibility of observing this

phenomenon has been considered by Oraevskii (1967) and Bardo (1969), but no results for such an experiment have yet been reported.

CHAPTER V

CONCLUSIONS AND PROPOSALS FOR FUTURE WORK

5.1 Introduction

The material which is contained in this thesis may be conveniently divided into three sections: the focusing of molecular beams, electret focusers and coherent radiation produced by an idealised two energy level system. Therefore, the general conclusions and proposals for future work have been subdivided into the foregoing sections.

5.2 Electrostatic focusers for molecular beams

The coaxial focuser has been employed by Helmer et al (1960) to focus a molecular beam which was in a predominantly absorptive energy state. Here, a coaxial electrode configuration has been constructed and used to space focus, and sort with respect to quantum state, an ammonia molecular beam. In comparison with other focusers which were subsequently employed to focus absorptive molecular beams, the coaxial focuser produced a relatively weak enhanced absorption signal.(Enhancement factor ~ 2).

The limitations of the coaxial focuser may, in part, be attributed to both mechanical and electrical aspects of the design. Electrical breakdown frequently occurred at voltages $\sim$20 kV because of insulation problems and a localised increase in gas pressure in the vicinity of the nozzle. Modifications of the nozzle assembly solved the latter problem. Another major limitation of the design

was the lack of molecular trajectories without scattering. Firstly, the outer electrode, although it was made out of gauze, was probably not very transparent to diffused molecules. Thus a localised increase in gas pressure would be obtained in the focuser with a consequent scattering of the beam. Secondly, the coaxial focuser is not a "true" focuser, as noted in section 2.10.5. This is because periodic molecular trajectories along the focuser axis are prevented by the presence of the central electrode.

An improvement in the enhanced absorption signal was obtained when the single-wire focuser was employed. (Enhancement factor ~ 5). This design, which was used in conjunction with an on-axis beam source, allowed molecules a greater interaction with the strong sorting field near the central electrode than was the case with the coaxial focuser. The design also allowed free exit to diffused higher energy state molecules because of the absence of a gauze outer electrode. Furthermore, a stronger sorting field could also be obtained in the focuser because of improved insulation of the EHT leads permitting higher voltages to be applied to the system.

Experiments with the Maltese - cross electrode configuration did not produce enhanced absorption signals with molecules whose energy decreases in an applied electric field. In fact, the reverse situation was obtained. This result may be attributed to the intense quadrupole electric field which existed in the region of the focuser axis. It is possible that enhanced absorption signals could be

obtained if the inner region along the focuser axis was filled with PTFE to prevent molecules entering this region of the focuser. Four separate nozzles could then be employed to supply separate molecular beams to each segmental sorting region of the focuser. Alteration of the cross angles would increase the divergence of the focusing electric field.

The crossed-wire focuser (Lainé and Sweeting, 1971, Appendix II) was the most efficient of all the electrode configurations which were employed to focus molecules whose energy decreases in an applied electric field. With this type of focuser it was possible to obtain a maximum absorption signal enhancement factor conservatively estimated to be ~20 which may be compared with ~2 for a coaxial focuser. Even so, the crossed-wire focusers still have scope for improvement. The design, as it stands, is inherently simple and has good electrical properties. For example, large voltages (~30 kV) may be applied to the focuser without a sign of electrical breakdown occurring.

Possible variation of the ratio of the electrode diameter to electrode separation will lead to an optimum charge distribution in the focuser system. In this way the effectiveness of the sorting field will be improved. However, the electrode diameter may not be increased indefinitely because of the problem of molecular scattering by the electrodes. These factors appear in a theoretical treatment of the crossed-wire focuser which is due to Sweeting, Smith and Lainé (1972, unpublished, Appendix VI).

A limitation of molecular beam focusers is that the focal length of a molecule is a function of its velocity in the focuser. Therefore, because there is a molecular velocity distribution in the beam, there is an associated aberration which might be compared with chromatic aberration in an optical system. This problem has been encountered in electron optics and has been considered by Cosslett (1950). In optics the problem is overcome by combining converging and diverging lens elements. Here, it might be possible to combine molecular focusers in a similar manner to produce an analogous effect for molecules in particular quantum energy states. Thus, for example, a ring and crossed-wire focuser could be arranged in series with one another. The overall effect of this arrangement would be to increase the intensity of molecules at the system's focal point where a detector might be situated. In this way the sensitivity (and indirectly resolution) of a beam spectrometer would be increased.

Alternatively, the crossed-wire focuser may be usefully employed in enhanced absorption spectroscopy. This would possibly increase the sensitivity of molecular spectrometers, especially where molecules with a weak Stark interaction are being investigated. With beam maser techniques, the natural absorption for a thermal beam must first be cancelled before an appreciable stimulated emission signal can be observed. However, with enhanced absorption techniques using, say, a crossed-wire focuser, no cancellation of the natural

absorption is required.

Furthermore, maser action may be achieved in certain cases by using a crossed-wire focuser. This possibility, for example, applies to three of the $J = 2 \rightarrow 1$ hyperfine transitions of HCN where molecules are differentially deflected in an applied electric field according to their respective quantum states (De Lucia and Gordy, 1969). The energy levels and the Stark effect for HCN are illustrated in figure 5.1. Using a stacked quadrupole focuser, De Lucia and Gordy differentially deflected HCN molecules, which increase in energy in an applied electric field, into a resonant cavity and obtained emission signals. Transitions which produced emission signals are marked "E" in figure 5.1. However, molecules in quantum states with allowed transitions marked "A" in figure 5.1 produced considerably enhanced absorption signals. Thus, by using a crossed-wire focuser, the situation would be reversed since the differential deflection would reverse in sign. In this way the transitions marked "A" in figure 5.1 would produce emission signals.

5.3 Electret focusers

The investigations employing electrets have been concerned primarily with selecting suitable electret materials to operate molecular beam focusers. However, the possibility has remained in view of employing a neutral molecular beam as a probe to monitor the time dependence of external electret electric fields.

The lead titanate - epoxy resin electret produced marginally

Figure 5.1

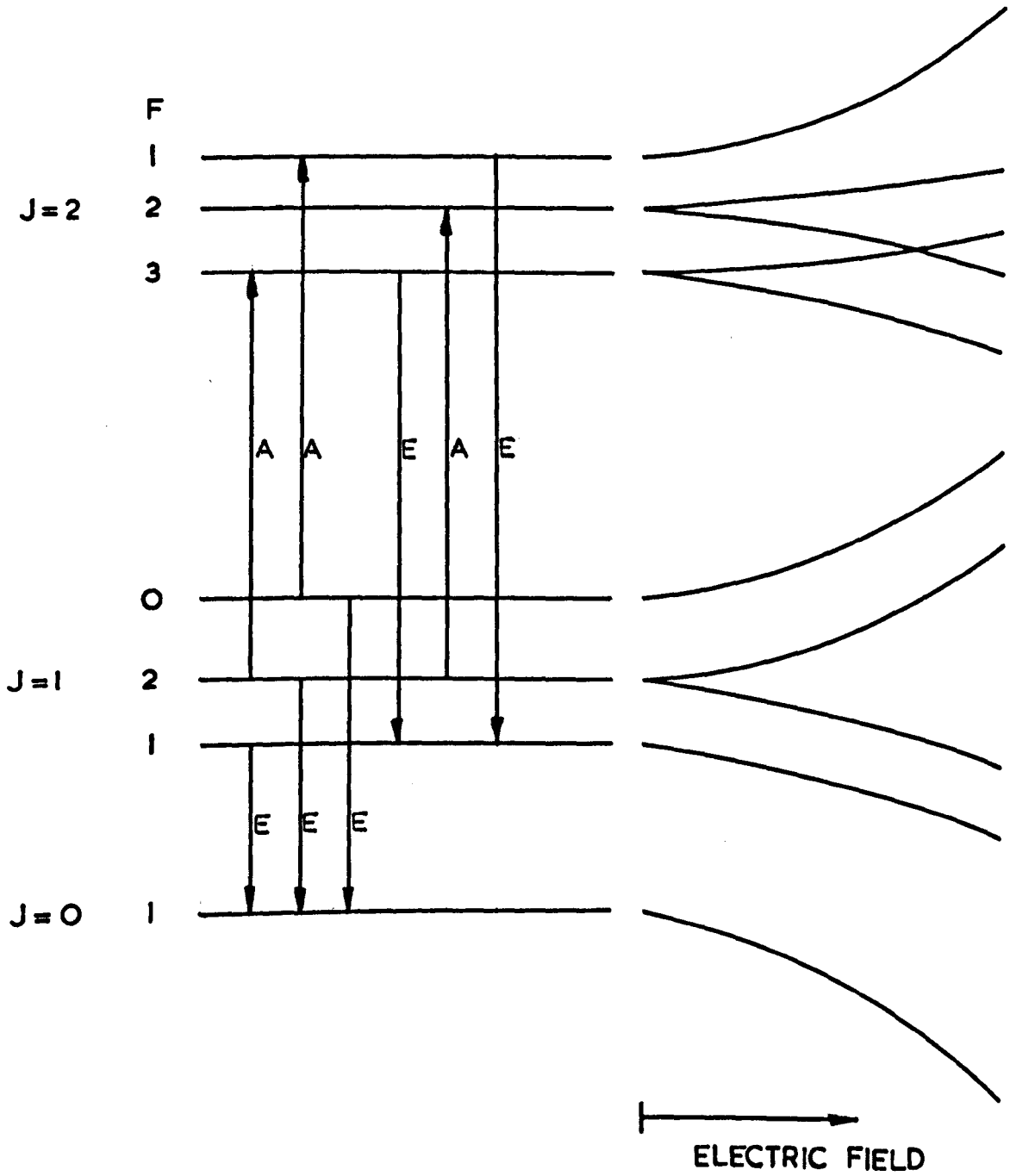

Energy levels and Stark effect for HCN.

(after De Lucia and Gordy, 1969)

emissive ammonia molecular beams. The major difficulties with this electret were the forming and electrification processes and the relatively high conductivity ($\sim 10^{-14}$ ohm^{-1} cm^{-1}) of the mixture compared with other electret materials. Improved molecular beam focusing was obtained when carnauba wax was employed as the electret material. The wax was easier to coat onto the base electrodes and set rapidly. Electrification of the carnauba wax was achieved with the coated focuser in situ in the maser. However, imperfections in coating the focuser raised the probability of localised electrical breakdown of the wax layer if large voltages were applied ($\sim$ 25 kV).

A development of this aspect of electret focusers would be to coat the electrodes of the focuser with polymer materials such as PTFE. This material has good vacuum properties and is an electret material which has already been investigated. A model of a quadrupole focuser has been made from knife-edge shaped PTFE electrets by Gubkin and Novak (1971). The field strength and configuration when plotted with a conventional electrometer probe suggested the application of one of these devices in a beam maser. At the time of the proposal by Gubkin and Novak, a publication was in preparation, describing the operation of a beam maser with electret focusers (Lainé and Sweeting, 1971, Appendix III), which has subsequently been published.

The electret effect in solidified ammonia has been isolated

(Lainé and Sweeting, 1971, Appendix IV) and its behaviour has been investigated. The experiments were performed by cooling a metal base electrode focuser radiatively to ~100 K by means of a liquid nitrogen dewar which surrounded the focuser. Subsequently ammonia electrets were formed in two ways. Firstly, an ammonia layer was formed upon the focuser electrodes and then polarised by applying a voltage between the focuser electrodes using an external EHT unit. Secondly, a steady voltage was supplied to the focuser electrodes from an external EHT unit so that ammonia molecules were polarised in an electric field as they were frozen-out on to the metal base electrodes. In both cases the external EHT supply was disconnected by using the oil-immersed switch. Partial depolarisation phenomena have been observed from solid ammonia electrets and the effect has been attributed to a change in the radiative cooling rate of the liquid nitrogen dewar.

Although cryogenic pumping of maser systems has experimental disadvantages when monitoring the behaviour of some electret focusers, it is necessary when forming solid ammonia electrets. Results described in this thesis indicate that efficient solid ammonia electrets (lasting at least 18 hours) may be made. It is possible that ice and solid formaldehyde electrets may be formed respectively in water (Bluyssen et al, 1967) and formaldehyde (Krupnov and Skvortsov, 1966) masers by freezing out layers of active molecules from the beam upon the focuser electrodes.

The stability of ceramic electrets might be usefully employed

in beam masers, an environment which enhances the stability of electrets in general because of its vacuum and low humidity conditions. Apart from focusing applications of electrets in beam masers, the performance of electrets might be investigated by neutral molecular beams. This objective has been partially achieved with electret focusers but may be extended by employing a two cavity maser system. Here, an electret might be placed between two resonant cavities which are in series in a beam maser. Thus, by keeping the voltage applied to a conventional focuser constant, using an external EHT supply, the ringing signal produced in the second cavity by the decaying oscillating polarisation carried by the molecular beam, could be monitored. Changes in the external electret electric field would affect the T_2 relaxation time (spectral line broadening) of molecules in the beam and in turn would modify the decay of the oscillating polarisation.

Stable electric fields of the order of several tens of kV cm^{-1} may be obtained in electret focusers. These fields are comparable with those found in conventional molecular beam focusers and would satisfy oscillation requirements.

5.4 Coherent radiation from two level systems

Electric resonance "beating of beats" has been observed in a molecular beam maser (Lainé and Sweeting, 1971, Appendix V). The effect was observed following the rapid passage of an exciting signal through the two resolved components of the main J = 1, K = 1

inversion transition at a frequency of 23.694 GHz.

According to Oraevskii (1967), who considered the formation of radiative echoes, spectral line broadening mechanisms may be defined as follows:

(a) relaxation mechanisms cause "homogeneous" broadening of spectral lines,

(b) the difference between the resonance frequencies of individual radiators contribute to a so-called "inhomogeneous" broadening.

The difference between the two types of broadening mechanism may be established in terms of reversible or irreversible processes. Effects causing "homogeneous" broadening are irreversible and therefore any coherence of the system lost by them is irreversible. However, loss of coherence by "inhomogeneous" broadening effects is reversible. This fact is employed in the phenomenon of echoes.

The echoes effect should be readily observed in a molecular beam maser where it is possible to obtain narrow spectral linewidths. Here, such factors as the frequency stability of the exciting signal and the coupling of power from the exciting signal to the maser cavity have to be considered. In the former case, the frequency of the exciting signal has to remain within the spectral linewidth of the maser transition which is being used to generate echoes, in order to obtain an optimum response from the molecular system. In the latter case, sufficient power must be coupled into the

maser cavity to satisfy the $\frac{\pi}{2}$ and π pulse sequence. These requirements have been considered for the case of radiative echoes in solids by Abella et al (1966).

In the molecular beam case echoes will not be formed if the time of flight of the molecules through the cavity (the analogue of T_1) is not larger than the inverse of the Doppler width of the spectral line employed. According to Oraevskii (1967), the Doppler width of a spectral line $\Delta\nu_D$ in a cylindrical cavity operating in the E_{01m} mode is,

$$\Delta\nu_D \doteqdot \left[\frac{v}{L}\right] m \qquad (5.1)$$

where L is the length of the resonator, v is the mean velocity of the molecules and m is the number of half waves along the resonator in the direction of beam propagation. Using the same approximation the time of flight of molecules through the resonator is given by $t = L/v$. Therefore, the condition on m is,

$$m \gg 1 \qquad (5.2)$$

To ensure that the maser cavity is suitably excited by the molecular beam, it is necessary that m be odd.

APPENDIX I

MOLECULAR BEAM SPECTROMETERS

Details of spectrometers vary from one to another and in the experimental work, described in this thesis, two different designs have been employed. Each had particular features suited to the experiments in which it was used. Experiments with molecular beam focusing and electret focusers were performed on a spectrometer equipped with a cylindrical cavity, whereas a spectrometer fitted with a Fabry-Perot cavity was employed to investigate spontaneous coherence phenomena. In the former case the cavity had a suitable longitudinal electric field mode pattern while, in the latter case, the cavity also had the requisite frequency tuning range.

AI.1 The cylindrical cavity spectrometer

(i) The vacuum system and ammonia supply

To achieve the operation of a molecular beam maser a background pressure less than $\sim 10^{-5}$ torr was required in order to allow the molecules in the beam to have a long mean free path. Background pressures better than 10^{-5} torr were obtained in practice (when an effuser was supplying $\sim 10^{18}$ molecules/second into the system) by employing a 100 mm silicone oil diffusion pump (with a limiting pressure of 10^{-7} torr) augmented with liquid nitrogen pumping. Superfluous ammonia molecules were condensed onto the surfaces of a dewar which was filled with liquid nitrogen. The dewar shown in figure 3.3 (chapter III) was surrounded by a glass flow tube 350 mm

long and 100 mm in diameter. Other lengths of glass flow tubes were available to suit different focuser lengths. The cavity was mounted on the axis of a metal vacuum tube which was approximately 100 mm in diameter and incorporated a diffusion pump baffle at one end. The cylinder was placed on a common axis to the glass flow tube and they were vacuum sealed together with an 'O' ring. The metal tube had on the side one vacuum flange which matched the cavity flange shown in figure AI.1. A section of K-band waveguide was mounted and vacuum sealed in the cavity flange as shown, together with four PTFE insulated ('O' ring sealed) electrical leadthroughs. These leadthroughs carried connections for the cavity heater and sensor coils (see section (v)). When the flange was bolted in position, with an 'O' ring between it and the flange on the metal vacuum tube, the cavity was automatically positioned on the spectrometer axis by carefully measured metal spigots placed between the rims of the flanges.

The end of the metal vacuum tube incorporating the diffusion pump baffle was fitted to the input port of the diffusion pump and sealed with a vacuum 'O' ring. The open end of the glass flow tube was fitted with a flat 'O' ring sealed metal end plate. The end plate carried the molecular effuser, liquid nitrogen input and output to the dewar, and support brackets for the focuser.

The ammonia source was a pressure cylinder containing anhydrous liquid ammonia. The cylinder was connected to a pressure reducing valve which allowed ammonia gas to pass through further pipework

Figure AI.1

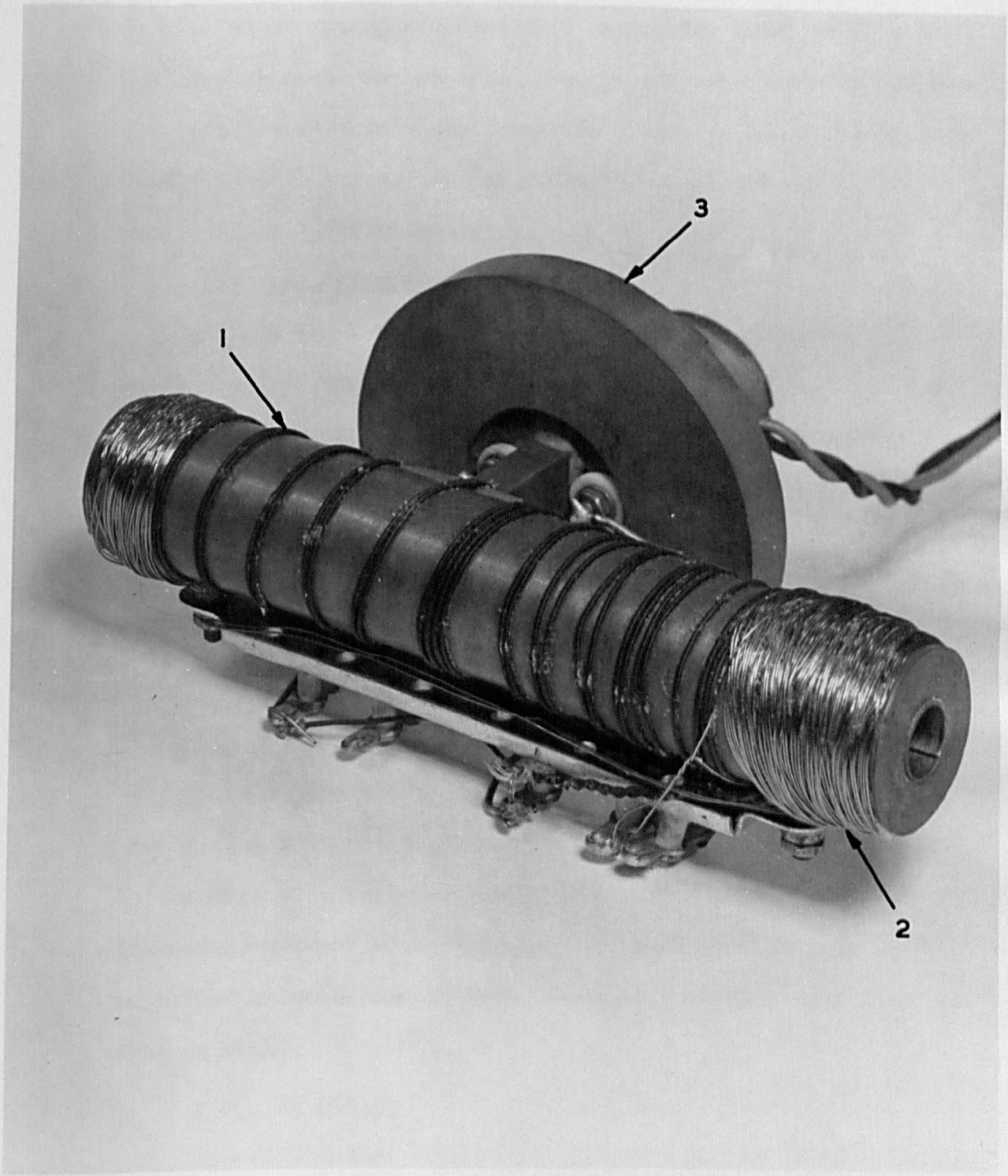

A cylindrical cavity.

Attachments: (1)Heater coil(2)Sensor coil(3)Vacuum flange.

into a liquid nitrogen cooled cold trap, where impurities in the gas were removed. The purified ammonia gas was stored in a reservoir. Gas from the reservoir was passed in a pipe to the effuser via a needle control valve. The gas pressure behind the effuser was monitored by a Pirani gauge.

(ii) The effuser

In all experiments discussed in this thesis where a cylindrical cavity was employed, a piece of klystron grid stock was used as the effuser, except in conjunction with the Maltese-cross focuser (See section 2.10.4). This type of effuser has good directivity and its characteristics have been investigated by Helmer et al (1960). The klystron grid stock used was about 5 mm in length, 3.5 mm in diameter and consisted of a honeycomb of fine parallel tubes 0.25 mm in diameter.

(iii) The focuser

A molecular beam focuser was placed on a common axis with the effuser and cavity. Details of focusers are given in Chapter II together with a discussion of their experimental characteristics. However, a focuser which was used to prepare a flat beam of molecules suitable for an open cavity will be described later in this appendix.

(iv) The cavity

The cylindrical type cavity was used in the first molecular beam maser by Gordon et al (1955).

Two types of modes may exist in a cavity of this type. These are (a) Transverse Electric and (b) Transverse Magnetic. In case (b) the electric field is parallel to the axis of the resonator and is therefore useful in a maser, as a long electric interaction time is required with the molecular beam. The resonant condition for E modes is given by (Montgomery, 1947),

$$\lambda_o = 4\left[\left[\frac{p}{z_o}\right]^2 + \left[\frac{2U_{m,n}}{\pi a}\right]^2\right]^{-1/2}$$

where,

λ_o = resonant wavelength

p = an integer equivalent to the number of half period variations of the wave along the resonator axis

$2z_o$ = length of resonator

a = radius of resonator

$U_{m,n}$ = n th root of the m th order Bessel function $J_m(U) = 0$

Using the notation $E_{m,n,p}$, m is the number of whole period variations of either magnetic or electric field along a path concentric with the resonator axis, n is one more than the number of whole period variations along a radius of the resonator and p is given above.

If m = 0 and n = 1 and p = 0 i.e. in the case of E_{010} mode, 2a = 0.9614 cm for a resonant frequency of 23.87 GHz.

The cavity manufactured for use in the electret investigations was made slightly undersize. This was to allow stabilisation at the required operation frequency by controlled heating. However the end effects of the resonators had to be compensated by increasing

the diameter of the mandrel by 0.005 mm. The waveguide was maintained beyond cut-off by inserting metal end caps into the resonator. The caps allowed the molecular beam to pass through the cavity but had the effect of increasing the Quality Factor, Q, of the resonator.

[Definition: $Q = \frac{\lambda_o}{\delta\pi} \cdot \frac{U_{m,n}}{(2+R)}$, where δ is the skin depth of the cavity wall material and $R = a/z_o$]

The cavity was obtained by depositing copper electrolytically onto a stainless steel mandrel (Type S80), using an acidic copper sulphate solution. The anode was oxygen free, high conductivity copper. The solution was composed of 200 grammes of copper sulphate, 56 grammes of pure sulphuric acid (R.D. 1.84) and water (distilled) to 1000 ml.

The mandrel was rotated slowly using a synchronous motor. To reduce the possibility of uneven deposition of copper on to the mandrel, the current flowing through the electrolytic tank was reversed one third of a one minute cycle. When the electroform had reached a diameter of approximately 25 mm deposition was stopped.

The electroform was put on a lathe and machined to an outside diameter of 20 mm. Microwave coupling to the cavity was by means of an iris and was somewhat under the critical coupling condition. Previous experience within the Maser Group indicated an iris of 2.54 mm diameter and wall thickness 0.25 mm was necessary. The waveguide mount and wall thickness was machined with the

mandrel within the electroform to prevent deformation of the cavity.

The mandrel was then removed from the cavity by heating the two together in an oil bath. Differential expansion took place and the mandrel was easily removed. To prevent distortion of the cavity, while the coupling hole was being drilled, balsa wood was temporarily placed inside the cavity. The cylindrical cavity, complete with vacuum flange and input waveguide is shown in figure AI.1.

(v) Cavity stabilisation

It was typical for the cavity to be operated between 20 and 30°C above room temperature in order to maintain positive temperature stabilisation. This was achieved in practice by employing an Airmec N.299 Temperature Controller, connected to a heater coil (glass covered Eureka wire) and a sensor coil (insulated copper wire). The positions of these coils on the cavity are shown in figure AI.1.

(vi) The detection system

The cylindrical cavity formed part of a conventional microwave superheterodyne spectrometer detection system. The system was based on a design described by Herrmann and Bonanomi (1956). During setting-up procedures, the system had the facility to display the klystron mode and the cavity resonance in crystal video. The basic elements of the bridge may be seen in figure AI.2, when it was set up for superheterodyne detection. The two modes of operation: (a) crystal video and (b) superheterodyne, will now be summarised. In the summaries reference will be made to figure AI.2.

Figure AI.2

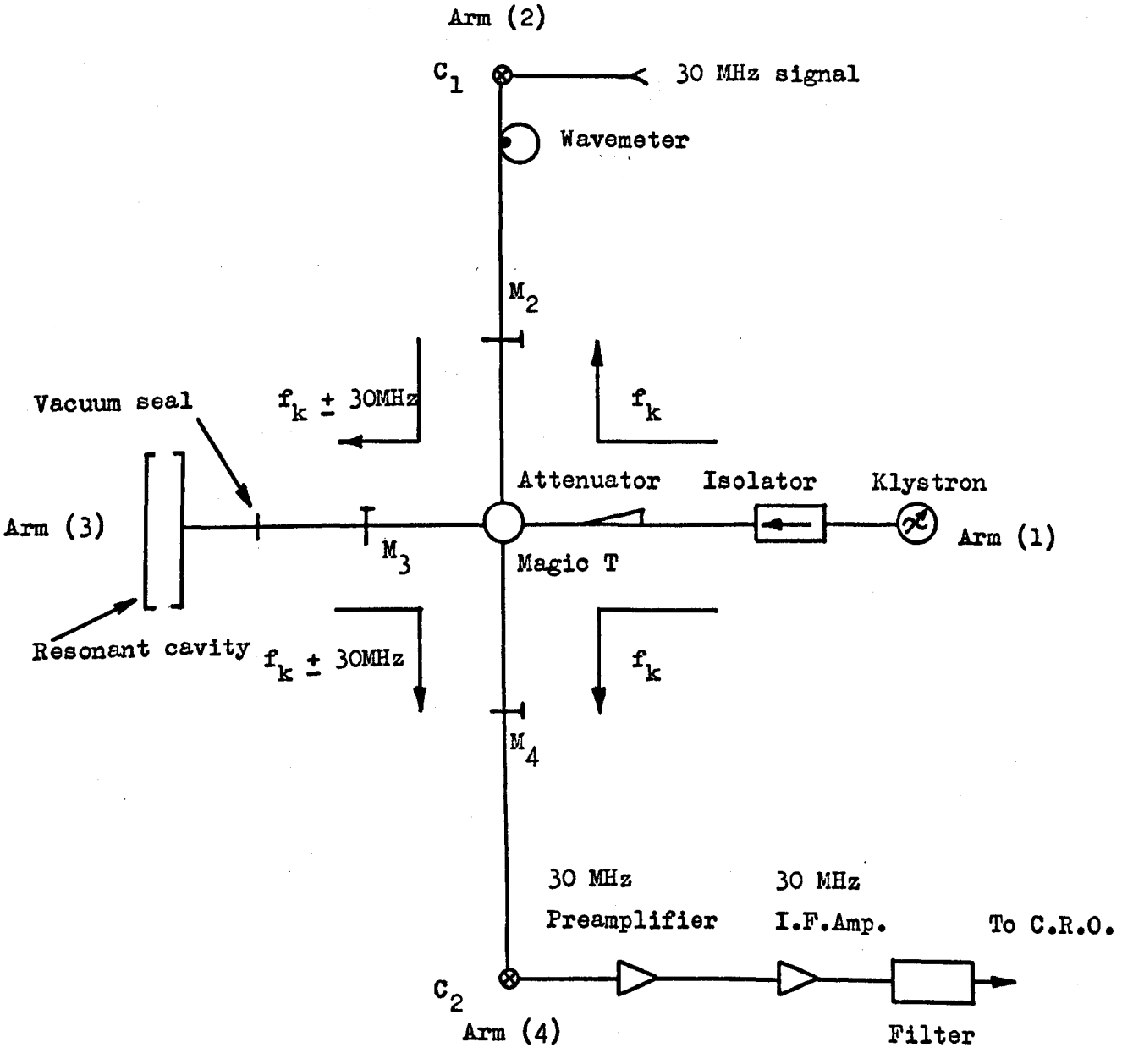

Schematic diagram of the superheterodyne detection system.

(a) Crystal video detection

Microwave power passed from the klystron through an isolator and attenuator to a magic T. There the power was divided between Arm (2) and Arm (4). Power was reflected back down Arm (2) and passed into Arm (3) entering the resonant cavity via a matching unit (M_3). Some power was reflected from the cavity and passed down Arm (4) to the detector crystal (C_2). If the gas within the resonant cavity had a resonant transition at frequency f_k, the associated signal was transmitted, by reflection, to the magic T and along Arm (4). By suitable matching, the resonance information was converted by a IN26A detector crystal (C_2) into a signal that was passed directly to the audio frequency vertical amplifier of a Telequipment type TD41 oscilloscope. The klystron was swept over its electronic frequency tuning range by a sweep voltage which was generated by a unit that also synchronised the oscilloscope timebase. Scan rates of 50 Hz were generally used. Thus the klystron mode was displayed together with a dip corresponding to the cavity absorption.

(b) Superheterodyne detection

Having determined that the spectrometer cavity was tuned to the requisite resonant transition, by using the crystal video technique, a superheterodyne method was used to increase the sensitivity. A signal generator was used to inject a 30 MHz signal into the mixing crystal (C_1). Ingram (1957) has summarised the factors involved in selecting a suitable Intermediate Frequency (I.F.).

The excess noise produced by the detecting system may be plotted against the frequency of modulation used in detection. (See figure AI.3). On the left hand side is a straight line graph which decreases from a large value at low frequencies to a low value at high frequencies. This represents the excess flicker noise due to the detecting crystal itself and indicates why a simple crystal video detector is very noisy. Apparently, increasing the modulation frequency would progressively reduce the noise of the detection system. However, this is not the case, since above about 50 MHz the noise of the I.F. amplifier becomes appreciable. This effect is represented by the remaining straight line rising towards the right in figure AI.3. The composite curve from the two noise sources mentioned, represents the total excess noise contributed by the detecting system. A broad minimum is obtained at about 30 MHz. Thus optimum sensitivity is obtained in the microwave detection system by employing an I.F. frequency of about 30 MHz.

Therefore, a 30 MHz I.F. amplifier with a low noise (3db) pre-amplifier was connected to the detector crystal C_2. The output of the I.F. amplifier was detected by a diode and the de-modulated signal was passed through a device to filter out frequencies in excess of 10 kHz. The signal was then passed into the vertical audio amplifier of a Telequipment Type TD41 oscilloscope.

The operation of this detection system depends upon the frequencies in the different arms of the microwave bridge shown

Figure AI.3

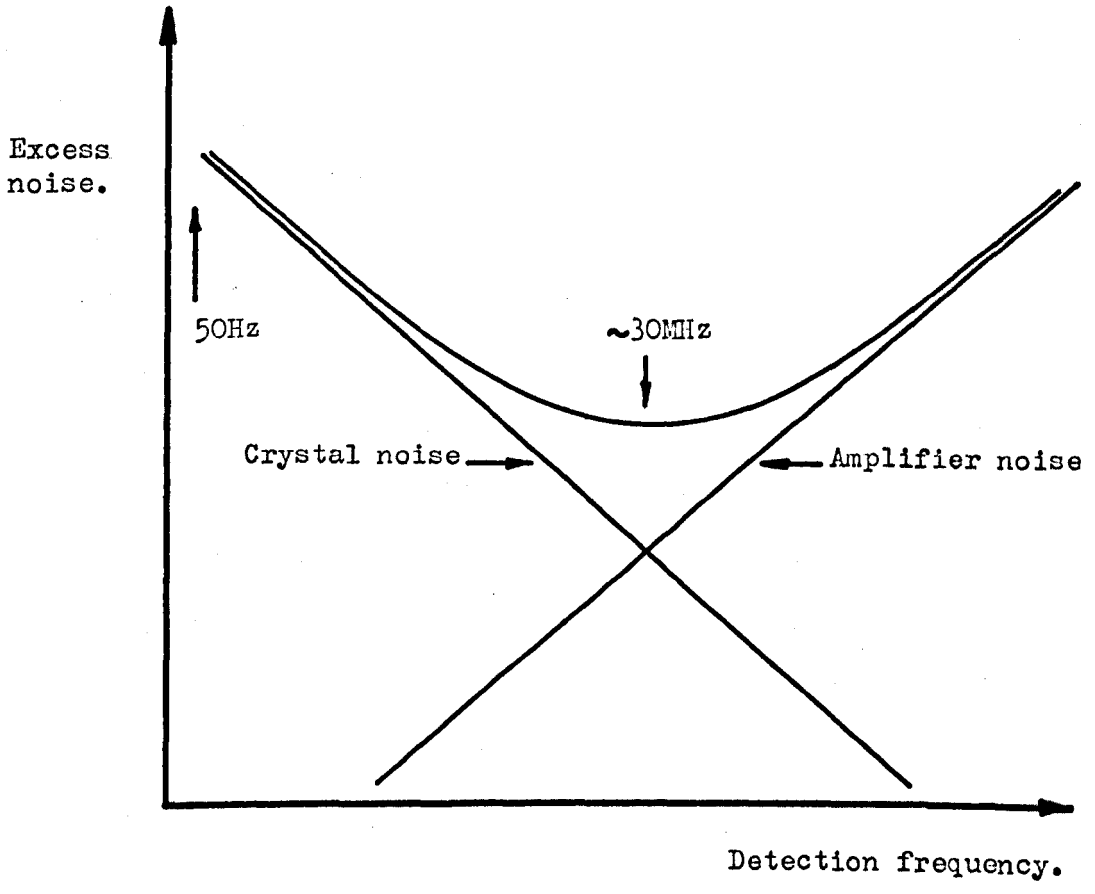

Excess system noise as a function of detection frequency.

in figure AI.2. The klystron frequency was off-set by a frequency equal to 30 MHz from the resonant transition frequency of the J = 3, K = 3 transition of ammonia. At the magic T, the signal of frequency f_k was split between Arm (2) and Arm (4). Adjusting the matching unit (M_2) allowed a suitable mixing of the signal of frequency f_k and the injected 30 MHz signal to take place in crystal (C_1). The compound signal, $f_k \pm 30$ MHz, then passed to the magic T and along Arm (3). One component, for example $f_k + 30$ MHz, was able to interact with the gas in the resonant cavity and the associated signal was reflected back to the magic T. This signal was mixed with the signal from the klystron, at a frequency f_k, in the crystal (C_2). The resulting beat signal passed into the I.F. amplification system. The spectroscopic signal was then displayed on the oscilloscope.

AI.2 The Fabry-Perot cavity spectrometer

(i) The vacuum system and ammonia supply

The main vacuum chamber used with the Fabry-Perot cavity has been illustrated in Chapter IV (figure 4.3). It consisted of an aluminium bronze casting, approximately 430 mm x 190 mm x 180 mm, that was sealed on the outside surface with Araldite and on the inside surface with silicone varnish. The top of the chamber was fitted with a rolled brass lid which carried two liquid nitrogen cold traps. A further flange, shown in figure 4.3, carried two K-band waveguides to the Fabry-Perot cavity. Also shown is the end elevation of the machined panel which carried mechanical and electrical

leadthroughs. The mechanical leadthrough was connected to gearing that was used to adjust the separation of the Fabry-Perot plates from outside the vacuum system. All the flanges and inputs, including the Araldite insulated EHT input, were sealed with vacuum 'O' rings.

The nozzle chamber, attached to the main vacuum chamber by a flange, was made of rolled brass tubes 100 mm and 75 mm in diameter. The nozzle chamber was fitted with two flanges. One carried a liquid nitrogen trap and ammonia gas input to the effuser, while the other flange carried a mechanical vacuum leadthrough that allowed external adjustment of the nozzle position.

The forechamber was pumped with a 50 mm diffusion pump while the main chamber was pumped by two 50 mm diffusion pumps. The diffusion pumps were charged with silicone oil with a limiting vapour pressure of 10^{-7} torr. The diffusion pumps were backed by a single rotary pump.

A similar ammonia gas supply and purification system to the one already described in section AI.1.(i) was employed.

A differential pumping scheme was employed with this spectrometer in contrast to the spectrometer described previously. This was necessary because increased pumping efficiency was required when a multichannel effuser was used. Of the molecules that passed through an effuser only a small solid angle is captured by a focuser. The remaining molecules, if a differentially pumped system is not used, tend to spoil the overall vacuum and thereby reduce the mean free

path of molecules in the beam. When a differentially pumped system is employed, molecules that are not selected by a diaphragm for entry into the focuser are pumped away in the forechamber. Differentially pumped systems have been successfully employed previously by Grigor'yants and Zhabotinskii (1961) and Bardo and Lainé (1971).

(ii) The effuser

A flat molecular beam, in thermal equilibrium with its environment, was formed by passing purified ammonia gas through a multichannel effuser which consisted of a linear array of 33 holes, 1 mm in diameter and 10 mm in length. The effuser is illustrated in figure AI.4 in its proper position with respect to the resonant cavity. The gas pressure behind the effuser was controlled by a needle valve and monitored by a Pirani type pressure gauge. A diaphragm with a slit machined in it was interposed between the effuser and focuser in order to collimate the flat molecular beam. The diaphragm is shown in its proper position in figure AI.4.

(iii) The focuser

The ladder-type focuser employed with the Fabry-Perot cavity is illustrated, between the cavity and diaphragm, in figure AI.4. The characteristics of ladder-type focusers have been investigated by Becker (1963b). Here, the focuser was of the non-parallel double ladder type. The length was 55 mm and the spacing between ladders varied linearly with distance along the focuser (in the direction

of beam propagation) from 1.6 mm at the entrance to 4.8 mm at the exit.

The molecular beam of ammonia, after passage through the focuser, consisted predominantly of upper inversion level molecules. The focused beam was directed through the Fabry-Perot cavity.

(iv) The cavity

The Fabry-Perot cavity which was used to observe "beating of beats" (referred to in chapter IV and Lainé and Sweeting, 1971) was constructed by another member of the Keele Maser Group, G.D.S.Smart. Resonators of this type have been thoroughly investigated previously, for example by Krupnov and Skvortsov (1964) and Checcacci and Scheggi (1965). However, a brief description of the device will be given here. The cavity is illustrated in figure AI.4.

The plates consisted of 150 mm diameter copper discs 12 mm in thickness. The copper discs, which were flat to 1.5×10^{-3} mm (Lainé and Smart, 1971), were supported in a brass framework with one disc being screwed to the front plate of the frame. The remaining disc was pressed against three micrometer driven glass rods by a spring loaded pressure plate. The three micrometers were temperature controlled (see section AI.2.(v)) and thus the cavity was frequency stabilised. The microwave coupling to the cavity, which was operated in transmission, was achieved by two waveguides. The two waveguides were coupled with their electric field vectors parallel to the beam axis and were equispaced from the resonator centre by 37 mm on a

Figure AI.4

The Fabry-Perot cavity and 'ladder' type focuser.

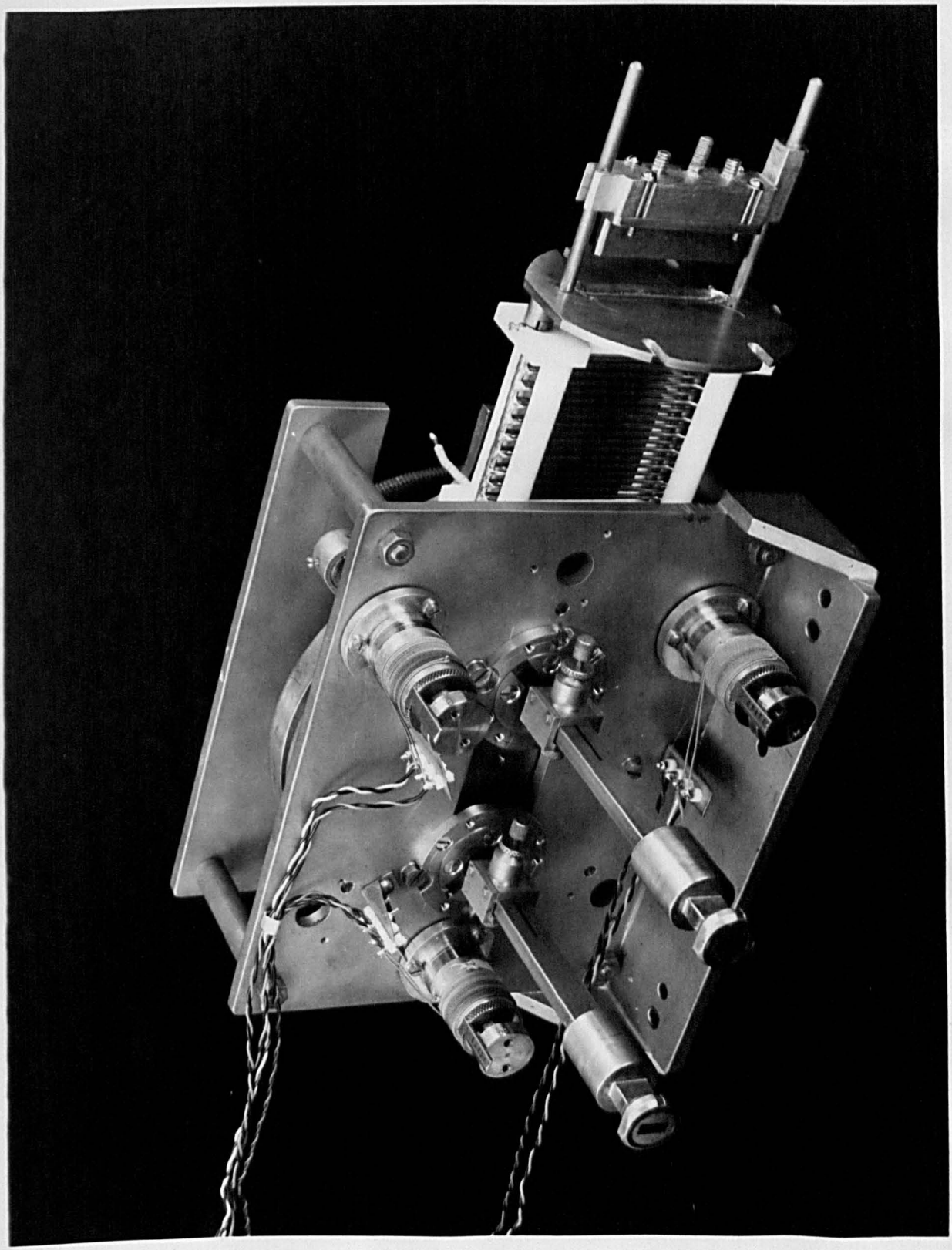

diameter of the fixed disc. The coupling holes were 2.5 mm in diameter and had a wall thickness of 0.5 mm.

The separation of the Fabry-Perot plates was $\lambda/2$ ($\sim$ 6.25 mm for the J = 1, K = 1 main inversion transition of ammonia). The mode was selected which had a single maximum of electric field in the direction of beam propagation. The cavity was initially tuned while it was outside the main vacuum chamber. Metal spacers were used to obtain an approximate $\lambda/2$ plate separation. The three micrometers were then carefully adjusted until the first order mode appeared (for a description of the spectrometer detection system during setting-up, and operation see section 4.7.1, Chapter IV) and further adjustment of the micrometers and microwave matching units optimised the mode. To ensure that the correct mode had been selected the electric field in the cavity was probed following a method employed by Checcacci and Scheggi (1965). In this case, a small lead sphere (approximately 1 mm in diameter), was transported by means of a fine nylon thread, between the Fabry-Perot plates, in the direction of beam propagation. Maxima and minima of electric field were observed as amplitude variations of the cavity mode curve, due to changes in the microwave power transmitted by the cavity. If the resonator had been excited with more than one maximum of electric field along the direction of the molecular trajectory then the emission line would have had two peaks symmetrically placed about the transition frequency. The frequency displacement, in the latter case, can be associated with

Doppler frequency shift. The cavity was then tuned approximately 6 MHz above the required operating frequency (measured by using the cavity wavemeter) to allow for frequency shift when the resonator was under vacuum conditions. The cavity was then mounted in the vacuum system as illustrated in figure 4.3, Chapter IV. Once under vacuum, the resonant frequency of the cavity could be further adjusted by varying the pressure applied to the pressure plate by the mechanical vacuum drive shaft attached to gear wheels. The adjustment of the pressure plate made no observable effect on the Q of the cavity. The Q of the resonator was measured by Smart to be ~2500. This measurement was performed by injecting a signal into the mode curve by using a frequency multiplier chain.

(v) Temperature stabilisation

Temperature control of the cavity micrometers and thus temperature stabilisation of the cavity was achieved by constructing the micrometer barrels of stainless steel and the sleeves of aluminium. The aluminium sleeves were wound with glass covered heater coils and copper sensor wires. A three channel variation of the Airmec N.299 Temperature Controller (due to Smart) was employed and this allowed a controlled, continuous current to pass through the heater coils instead of the switched current from the normal Airmec N299 unit. A temperature stability of $0.1^{o}C$ could be achieved.

(vi) The detection system

The spectrometer detection system employed with the Fabry-Perot cavity has been described in Chapter IV, section 4.7.1.

APPENDIX VI

CROSSED-WIRE FOCUSER THEORY

The focusing action of the crossed-wire focuser will be considered here using a mathematical method which is based upon the continuity of asymptotes to particular trajectories of molecules throughout the focuser. Each electrode of the focuser is considered as a single element. For given co-ordinates and direction cosines of a given molecule with a particular velocity in the input median plane the corresponding parameters for the molecule are formulated for it in the output median plane to the wire being considered. The median plane is defined here as that plane which is equidistant between adjacent electrode wires and is perpendicular to the focuser axis. Having obtained the parameters of a molecule for one wire it is indicated how the same parameters may be obtained for the adjacent wire by a transformation of axes. The formulae relating molecular trajectory parameters are shown to reduce to an iterative form. It is concluded that this iterative form may be computed and, since it is quite general, be applied to a number of different types of molecules which may be space focused in a crossed-wire focuser.

AVI.1 The analysis

For the purpose of this theory it is implicitly assumed that the interaction of the electric fields due to the wires is negligible in the median plane. Thus the molecule passes through electric field regions which have radial symmetry. The theory is

quite general but, where applicable, molecular constants are noted in terms of the ammonia molecule.

A cartesian co-ordinate system of axes is defined such that the x and y axes are mutually perpendicular to each other and to the focuser axis. It is also noted that x and y define the planes of focusing elements, as illustrated in figure AVI.1.

The problem is generalised by considering a molecule entering the input median plane to the first wire at a skew angle. This generalisation allows iteration of the problem later. The first wire lies in the y plane. Let the initial asymptote to the input trajectory have the following parameters,

$$x = (v \operatorname{Cos} \alpha_n)t + a_n \qquad (1)$$

$$y = (v \operatorname{Cos} \beta_n)t + b_n \qquad (2)$$

$$z = (v \operatorname{Cos} \gamma_n)t + c_n \qquad (3)$$

where α_n, β_n, γ_n are direction cosines and,

$$\operatorname{Cos}^2\alpha_n + \operatorname{Cos}^2\beta_n + \operatorname{Cos}^2\gamma_n = 1 \qquad (4)$$

v is the velocity of the molecule and,

$$v \operatorname{Cos} \gamma_n > 0 \qquad (5)$$

so that the molecule has a positive forward velocity component through the focuser.

In the section in which the molecule is moving,

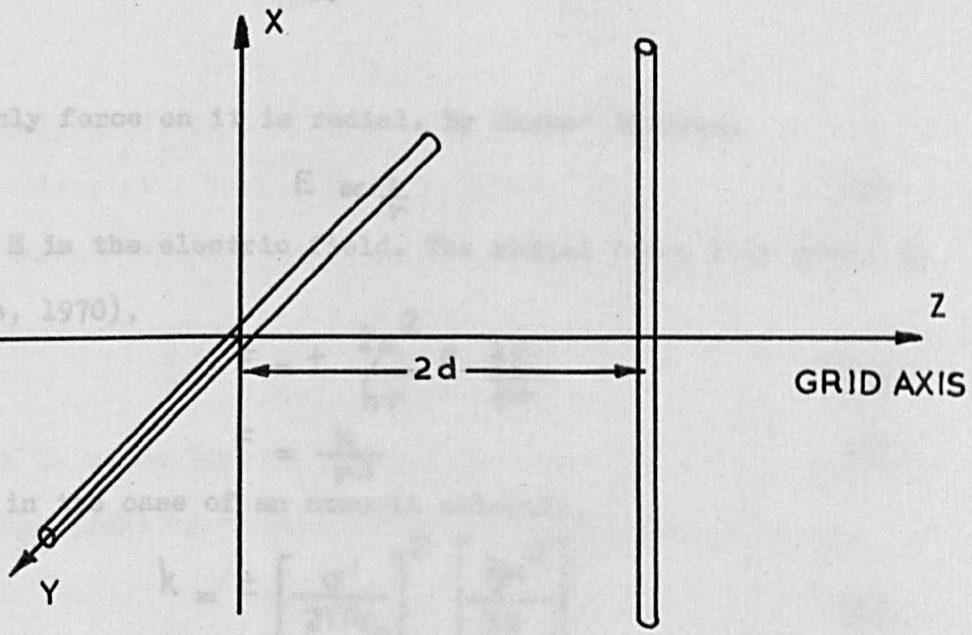

Figure AVI.1

Schematic diagram of adjacent electrodes in a crossed-wire focuser.

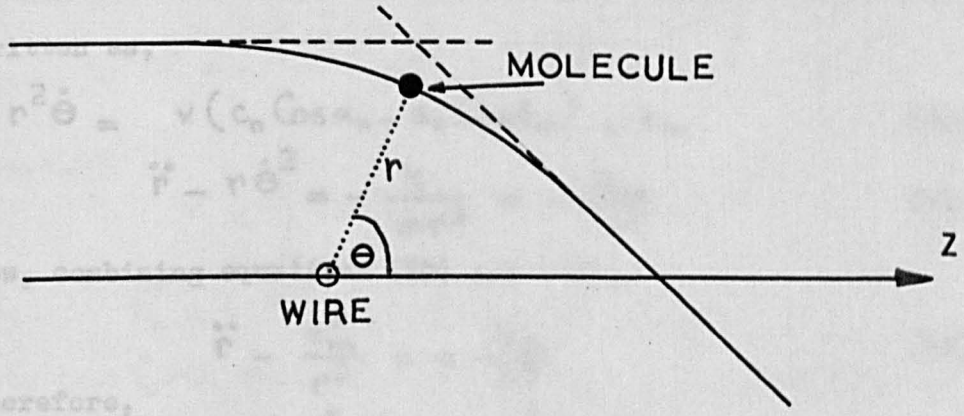

Figure AVI.2

The motion of a molecule around an electrode.

the only force on it is radial. By Gauss' theorem,

$$E \propto \frac{1}{r} \tag{6}$$

where E is the electric field. The radial force F is given by (Laine, 1970),

$$F = \pm \frac{2\mu^2}{h\nu} E \frac{\partial E}{\partial r} \tag{7}$$

Thus,
$$F = \frac{k}{r^3} \tag{8}$$

Here, in the case of an ammonia molecule,

$$k = \pm \left[\frac{\sigma'}{2\pi\epsilon_o}\right]^2 \left[\frac{2\mu^2}{h\nu}\right] \tag{9}$$

where σ' is the charge per unit length upon the wire electrode and ϵ_o is the permittivity of vacuum.

So referring to figure AVI.2, and by using polar co-ordinates, the equations of motion of an ammonia molecule of mass m may be written as,

$$r^2\dot{\theta} = v(c_n \cos\alpha_n - a_n \cos\gamma_n) = e_m \tag{10}$$

$$\ddot{r} - r\dot{\theta}^2 = -\frac{k}{mr^3} = -\frac{k_m}{r^3} \tag{11}$$

Now, combining equations (10) and (11),

$$\ddot{r} - \frac{e_m^2}{r^3} = -\frac{k_m}{r^3} \tag{12}$$

therefore,

$$\ddot{r} = \left[\frac{e_m^2 - k_m}{r^3}\right] \tag{13}$$

Molecular paths where $e_m^2 \ll k_m$ are discarded since these molecules

are not focused and only those for which $e_m^2 > k_m$ are now considered.

Multiplying each side of equation (13) by $\dot{r}$ and integrating with respect to time,

$$\frac{1}{2}\dot{r}^2 = -\frac{(e_m^2 - k_m)}{2r^2} + A \tag{14}$$

where A is a constant of integration. Solving for the constant of integration: as $r \longrightarrow \infty$, $\dot{r} \longrightarrow -v'$, therefore,

$$A = \frac{1}{2} v'^2 \tag{15}$$

where v' is the resolved velocity component of the molecule perpendicular to the electrode being considered. Substituting for A in equation (14),

$$\dot{r}^2 = -\frac{(e_m^2 - k_m)}{r^2} + (v\,\mathrm{Cos}\,\alpha_n)^2 + (v\,\mathrm{Cos}\,\gamma_n)^2 \tag{16}$$

where,

$$v' = \left[(v\,\mathrm{Cos}\,\alpha_n)^2 + (v\,\mathrm{Cos}\,\gamma_n)^2\right]^{1/2} \tag{17}$$

Let $$f_n^2 = (v\,\mathrm{Cos}\,\alpha_n)^2 + (v\,\mathrm{Cos}\,\gamma_n)^2 \tag{18}$$

note that $f_n > 0$. Then, separating terms in equation (15) and integrating with respect to time,

$$\int \frac{r}{\left[f_n^2 r^2 - (e_m^2 - k_m)\right]^{1/2}} dr = t + g_n \tag{19}$$

$$\therefore \quad \frac{1}{f_n^2} \cdot \left[f_n^2 r^2 - (e_m^2 - k_m)\right]^{1/2} = t + g_n \tag{20}$$

$$\therefore \quad f_n^2 r^2 - (e_m^2 - k_m) = f_n^4 (t + g_n)^2 \tag{21}$$

From equation (10), $$\dot{\theta} = \frac{e_m}{r^2} \tag{22}$$

Therefore, $$\dot{\theta} = \frac{e_m f_n^2}{(e_m^2 - k_m) + f_n^4 (t + g_n)^2} \tag{23}$$

Integrating equation (23) with respect to time using a standard integral form,

$$\theta = \frac{e_m}{(e_m^2 - k_m)^{1/2}} \tan^{-1}\left[\frac{f_n^2 (t + g_n)}{(e_m^2 - k_m)^{1/2}}\right] + h_n \tag{24}$$

where g_n and h_n are two integration constants.

Determination of the integration constants g_n and h_n

By expanding equation (21), (25)

$$f_n r = \left[f_n^4 t^2 + 2 f_n^4 t g_n + g_n^2 f_n^4 + (e_m^2 - k_m)\right]^{1/2}$$

$$\doteq f_n^2 t \left(1 + \frac{2 g_n}{t}\right)^{1/2} \tag{26}$$

$$\doteq f_n^2 t \left(1 + \frac{g_n}{t}\right) \tag{27}$$

$$\doteq f_n^2 t + f_n^2 g_n \tag{28}$$

Now, by noting that on the approach asymptote,

$$r = (x^2 + z^2)^{1/2} \tag{29}$$

$$= \left\{\left[(v \cos \alpha_n) t + a_n\right]^2 + \left[(v \cos \gamma_n) t + c_n\right]^2\right\}^{1/2} \tag{30}$$

$$\doteqdot \left[(v^2\cos^2\alpha_n + v^2\cos^2\gamma_n)t^2 + 2(a_n v\cos\alpha_n + c_n v\cos\gamma_n)t\right]^{1/2} \tag{31}$$

Writing $(v^2\cos^2\alpha_n + v^2\cos^2\gamma_n) = f_n^2$ and expanding equation (31) in Binomial form,

$$r \doteqdot f_n t\left[1 + \frac{(a_n\cos\alpha_n + c_n\cos\gamma_n)}{f_n^2}\cdot\frac{v}{t}\right] \tag{32}$$

equations (28) and (32) may be compared. Thus,

$$g_n = \frac{v(a_n\cos\alpha_n + c_n\cos\gamma_n)}{f_n^2} \tag{33}$$

Now, for Θ as $t \longrightarrow \infty$, from equation (24),

$$\Theta \doteqdot -\frac{e_m}{(e_m^2 - k_m)^{1/2}}\cdot\frac{\pi}{2} + h_n \tag{34}$$

It may be noted that, on the approach asymptote,

$$\tan\Theta = \frac{x}{z} \tag{35}$$

$$= \frac{(v\cos\alpha_n)t + a_n}{(v\cos\gamma_n)t + c_n} \tag{36}$$

$$\doteqdot \frac{\cos\alpha_n}{\cos\gamma_n} \quad \text{as } t \longrightarrow -\infty \tag{37}$$

Substituting equation (37) into (34),

$$\tan\left\{h_n - \left[\frac{\pi e_m}{2(e_m^2 - k_m)^{1/2}}\right]\right\} = \frac{\cos\alpha_n}{\cos\gamma_n} \tag{38}$$

$$\therefore\ h_n = \tan^{-1}\left[\frac{\cos\alpha_n}{\cos\gamma_n}\right] + \left[\frac{\pi e_m}{2(e_m^2 - k_m)^{1/2}}\right] \qquad (39)$$

The exit asymptote

The exit asymptote leads to the output median plane of the wire electrode which is being considered. Having solved the equation of this asymptote then the direction cosines and cartesian co-ordinates of the molecule may be found at the output median plane. The inclination of the exit asymptote to the molecular trajectory (with respect to the focuser axis, z) as it leaves the influence of the electric field due to the charged wire electrode, has to be calculated.

From equation (28),

$$r \doteq f_n t + f_n g_n \qquad (40)$$

For convenience of manipulation, let t = 1/u, so that,

$$\theta = \frac{e_m}{(e_m^2 - k_m)^{1/2}} \tan^{-1}\left[\frac{f_n^2(1/u + g_n)}{(e_m^2 - k_m)^{1/2}}\right] + h_n \qquad (41)$$

Now, expanding θ as a power series in powers of u, the first two terms are sufficient to determine θ. If $\theta = f(u)$, (42)

then,

$$\theta = f(0) + uf'(0) \qquad (43)$$

$$f(0) = \frac{e_m}{(e_m^2 - k_m)^{1/2}} \cdot \frac{\pi}{2} + h_n \qquad (44)$$

$$f'(u) = \frac{e_m}{(e_m^2 - k_m)^{1/2}} \cdot \frac{1}{1 + \left[\frac{f_n^2(1/u + g_n)^2}{(e_m^2 - k_m)^{1/2}}\right]^2} \cdot \left[\frac{-f_n^2}{(e_m^2 - k_m)^{1/2}}\right] \cdot \frac{1}{u^2} \qquad (45)$$

$$f'(0) = -\frac{e_m}{f_n^2} \tag{46}$$

Thus,

$$\theta \doteq \left[h_n + \frac{e_m}{(e_m^2 - k_m)^{1/2}} \cdot \frac{\Pi}{2}\right] - \frac{e_m}{t f_n^2} \tag{47}$$

$$\doteq q_n - \frac{e_m}{t f_n^2} \tag{48}$$

where, $$q_n = h_n + \frac{e_m}{(e_m^2 - k_m)^{1/2}} \cdot \frac{\Pi}{2} \tag{49}$$

Therefore,

$$\text{Cos}\,\theta \doteq \text{Cos}\left(q_n - \frac{e_m}{t f_n^2}\right) \tag{50}$$

$$\doteq \text{Cos}\, q_n + \left[\frac{e_m}{t f_n^2}\right] \text{Sin}\, q_n \tag{51}$$

$$\text{Sin}\,\theta \doteq \text{Sin}\left(q_n - \frac{e_m}{t f_n^2}\right) \tag{52}$$

$$\doteq \text{Sin}\, q_n - \left[\frac{e_m}{t f_n^2}\right] \text{Cos}\, q_n \tag{53}$$

Thus the parametric equations for the exit asymptote may be written as,

$$x = r\,\text{Sin}\,\theta \tag{54}$$

$$= \left[f_n g_n \text{Sin} q_n - \frac{e_m}{f_n} \cdot \text{Cos}\, q_n\right] + (f_n \text{Sin}\, q_n)t \tag{55}$$

$$y = (v \text{Cos}\,\gamma_n)t + c_n \tag{56}$$

$$z = r \cos \theta \tag{57}$$

$$= \left[f_n g_n \cos q_n + \frac{e_m}{f_n} . \sin q_n \right] + (f_n \cos q_n) t \tag{58}$$

It may be noted here that a condition for the molecule to continue through the focuser and not return in the direction from which it came is satisfied if,

$$\cos q_n > 0 \tag{59}$$

that, from equation (49),

$$\left| h_n + \frac{e_m}{(e_m^2 - k_m)^{1/2}} . \frac{\Pi}{2} \right| < \frac{\Pi}{2} \tag{60}$$

The molecule now proceeds into the influence of the adjacent wire which is perpendicular to the wire already treated. A similar treatment to the one just given may be performed if the following transformation of axes is made,

$$\left.\begin{aligned} x &\longrightarrow y' \\ y &\longrightarrow -x' \\ z &\longrightarrow z' + 2d \end{aligned}\right\} \tag{61}$$

where 2d is the distance between adjacent wires, along the focuser axis.

From equations (54) to (58) and (61) the approach asymptote to the

second wire may be written with parametric equations,

$$x' = -(v \cos \gamma_n)t + c_n \tag{62}$$

$$y' = \left[f_n g_n \sin q_n - \frac{e_m}{f_n} \cdot \cos q_n\right] + (f_n \sin q_n)t \tag{63}$$

$$z' = \left[f_n g_n \cos q_n + \frac{e_m}{f_n} \cdot \sin q_n - 2d\right] + (f_n \cos q_n)t \tag{64}$$

Comparing these equations with equations (1), (2) and (3),

$$\begin{aligned} a_{n+1} &= c_n \\ b_{n+1} &= f_n g_n \sin q_n - \frac{e_m}{f_n} \cdot \cos q_n \\ c_{n+1} &= f_n g_n \cos q_n + \frac{e_m}{f_n} \sin q_n - 2d \\ \cos \alpha_{n+1} &= -\cos \gamma_n \\ \cos \beta_{n+1} &= \frac{f_n}{v} \cdot \sin q_n \\ \cos \gamma_{n+1} &= \frac{f_n}{v} \cdot \cos q_n \end{aligned} \tag{65}$$

The exit asymptote to the second wire can be found by using the same procedure as with the first wire but with,

a_{n+1} , b_{n+1} , c_{n+1} , $\cos \alpha_{n+1}$, $\cos \beta_{n+1}$, $\cos \gamma_{n+1}$

as the direction cosines and cartesian co-ordinates in the input median plane. This process establishes an iteration.

REFERENCES

ABELLA,I.D., KURNIT,N.A., HARTMANN,S.R. Phys. Rev. 141, (1964) 391.

AUERBACH,D., BROMBERG,E.E.A., WHARTON,L. J. Chem. Phys. 45, (1966) 2160.

BARDO,W.S. Ph.D. Thesis. University of Keele, (1969).

BARDO,W.S., LAINÉ,D.C. J. Phys. E: Scientific Instrum. 4, (1971) 595.

BASOV,N.G., ORAEVSKII,A.N. Sov. Phys. -JETP. 37, (10) (1960) 761.

BASOV,N.G., PROKHOROV,A.M. Zh. Eksper. Teor. Fiz. 27, (1954) 431.

BECKER,G. Z. angew. Phys. 15, (1963a) 281.

BECKER,G. Z. angew. Phys. 15, (1963b) 13.

BENÉ,G.J., DENIS,P.M., EXTERMANN,R.C. Physica 17, (1951) 308.

BENÉ,G.J., DENIS,P.M., EXTERMANN,R.C. Helv. Phys. Acta. 26, (1953) 267.

BLOCH,F. Phys. Rev. 70, (1946) 460.

BLOEMBERGEN,N., PURCELL,E.M., POUND,R.V. Phys. Rev. 73, (1948) 679.

BLUYSSEN,H., DYMANUS,A., VERHOEVEN,J. Phys. Letters 24A, (1967) 482.

CHECCACCI,P.F., SCHEGGI,A.M. App. Optics 4, (1965) 1529.

CHRISTOFOLIS,N.C. (1950) U.S.Patent, 2, 736, 799, (issued Feb 28, 1956).

CLOUSER,P.L., GORDY,W. Phys. Rev. 134, (1964) A 863.

COSSLETT,V.E. In: "Introduction to electron optics", Clarendon Press, Oxford 2nd Edition (1950) p 138.

COURANT,E.D., LIVINGSTON,M.S., SNYDER,H.S. Phys. Rev. 88, (1952) 1190.

CROSS,J.D. In: "Electrets and related electrostatic charge storage phenomena", editors L.M.Baxt and M.M.Perlman (The Electrochemical Soc. Inc., New York, 1968) p 45.

DE LUCIA, F., GORDY,W. Phys.Rev 187, (1969) 58.

DICKE,R.H. Phys.Rev 93, (1954) 99.

EGUCHI,M. Phil.Mag.49, (1925) 178.

FEYNMAN,R.P., VERNON Jnr., F.L., HELLWARTH,R.W. J.App.Phys. 28, (1957) 49.

FREI,H., GROETZINGER,G. Phys.Zeits. 37, (1936) 720

FRIDKIN,V.M., ZHELUDEV,I.S. "Photoelectrets and the electrophotographic process". Publishing House of Academy of Sciences.Moscow. (1960).

GABILLARD,R. C.R.Acad. Sci. Paris 232, (1951) 1551.

GABILLARD,R. Phys.Rev.85, (1952) 694.

GEMANT,A. Phil. Mag. 20, (1935) 929.

GESHWIND, S. GUNTHER-MOHR, G.R., SILVEY,G. Phys. Rev.85, (1952) 474

GOOD,W.M., STRANATHAN,J.D. Phys.Rev. 56, (1939) 810.

GORDON,J.P., ZEIGER,H.J., TOWNES,C.H. Phys.Rev. 95, (1954) 282.

GORDON,J.P., Phys. Rev. 99, (1955) 1253.

GORDON,J.P., ZEIGER,H.J., TOWNES,C.H. Phys. Rev. 99, (1955) 1264.

GRIGOR'YANTS,V.V., ZHABOTINSKII,M.E. Radio Eng.and Electron.Phys. 6, (1961) 260.

GROSS,B. Phys.Rev. 66, Nos.1 and 2 (1944) 26.

GROSS,B. J.Chem.Phys. 17, (1949) 866

GROSS,B. in: "Electrets and related electrostatic charge storage phenomena". editors L.M.Baxt and M.M.Perlman (The Electrochemical Soc. Inc., New York, 1968) p.9

GROSS,B. , DENARD,L.F. Phys.Rev.67, (1945) 253.

GUBKIN,A.N. Sov.Phys. - Tech.Phys. 2, (1957) 1813.

GUBKIN,A.N., MATSONASHVILI,B.N. Sov.Phys. - Solid State 4, (1962) 878.

GUBKIN,A.N., NOVAK,M.M. Zh.Tekh.Fiz. 41, (1971) 1697

GUTMAN,F. Rev.Mod. Phys. 20, (1948) 457 .

HAHN,E.L. Phys.Rev. 80, (1950) 580.

HEAVISIDE,O. Electrical Papers 1, (1885) 488.

HELMER,J.C., JACOBUS,F.B., STURROCK,P.A. J.App.Phys. 31,(1960) 458

HERRMANN,J., BONANOMI,J. Helv.Phys.Acta. 29, (1956) 448.

HIGA,W.H. External publication No:381. Maser Engineering. Jet propulsion laboratory. U.S.A. (1957).

HILL,R.M., KAPLAN,D.E., HERRMANN,G.F., ICHIKI,S.K. Phys.Rev.Letters 18, (1967) 105.

HUGHES, H.K. Phys.Rev. 72, (1947) 614.

HUGHES, R.H., WILSON Jnr., E.B. Phys.Rev. 71, (1947) 562.

HUISZOON,C., DYMANUS,A. Phys.Letters 21, (1966) 164.

HUISZOON,C. Rev.Sci.Instrum. 42, (1971) 477.

INGRAM,D.J.E. "Spectroscopy at radio and microwave frequencies". Butterworths. London (1955).

JENKINS, J.L. WAGNER,P.E. App.Phys. Letters 13, (1968) 308.

JOHNSON,H.R., STRANDBERG,M.W.P., Phys.Rev. 85, (1952) 503.

KAKATI,D. Ph.D. Thesis.University of Keele. 1968.

KAKATI, D., LAINÉ, D.C. Phys.Letters 24A,(1967) 676.

KAKATI,D., LAINÉ, D.C. Phys.Letters 28A, (1969) 786.

KAKATI,D., LAINÉ,D.C. J. Phys.E: Scientific Instrum. 4,(1971) 269.

KING,W.C., GORDY,W. Phys.Rev. 90, (1953) 319.

KISLIUK,P., TOWNES,C.H. Molecular microwave spectra tables National Bureau of Standards Circular No: 518.Washington U.S.A. (1952) p.84.

KUKOLICH,S.G. Phys.Rev. 156, (1967) 83.

KRUPNOV,A.F. Radiofizika 2, (1959) 658.

KRUPNOV,A.F., SKVORTSOV,V.A. Zh.Eksper.Teor.Fiz. 47,(1964) 1605.

KRUPNOV,A.F., SKVORTSOV,V.A. Radio Eng. and Electron.Phys. 10, (1965) 320.

KRUPNOV,A.F., SKVORTSOV,V.A. Soviet Radiophysics 9, (1966) 488.

LAINÉ,D.C. Phys.Letters 23, (1966) 557.

LAINÉ,D.C. Repts on Prog.in Phys. 33, (1970) 1001.

LAINÉ,D.C., KAKATI,D., UPPAL,G.S., SMART,G.D.S., BARDO,W.S. Phys.Letters 29A, (1969) 376.

LAINÉ,D.C., SMART,G.D.S. J.Phys. D: App.Phys. 4, (1971) L 23.

LAINÉ, D.C., SMART,G.D.S. University of Keele. private communication (1971).

LAINÉ,D.C., SWEETING,R.C. Phys.Letters 36A, (1971) 391.

LAINÉ,D.C., SWEETING,R.C. Phys.Letters 36A, (1971) 469.

LAINÉ,D.C., SWEETING,R.C. J.Phys.D: Appl.Phys.4, (1971) L 39.

LAINÉ,D.C., SWEETING,R.C. Phys.Letters 34A (1971) 144.

LAINÉ,D.C., SWEETING,R.C. Entropie 42, Nov-Dec (1971) 165 (to be published)

MEDNIKOV,O.L., PARYGIN, V.H.Radio Eng.and Electron Phys. 8,(1963) 685.

MIKOLA,S. Zeits.f.Physik 32, (1925) 476.

MONTGOMERY,C.G. Radiation Laboratory Series,Vol.II (1947) McGraw-Hill, New York.

NAUMOV,A.I. Sov.Phys - Tech.Phys,8, (1963) 88

NETHERCOT,A.H. Symposium on submillimetre waves at the University of Illinois. (1951).

NEWELL Jnr., G., DICKE,R.H. Phys.Rev. 83, (1951) 1064.

NORTON,L.E. IRE Trans.on microwave theory and techniques MTT-5 (1957) 262.

ORAEVSKII,A.N. in: Molecular Generators (Moscow:Nauka) 1964.

ORAEVSKII,A.N. Sov.Phys. - Uspekhi 10, (1967) 45.

PERLMAN,M.M. in: "Electrets and related electrostatic charge storage phenomena". editors L.M.Baxt and M.M.Perlman (The Electrochemical Soc.Inc., New York, 1968) p.3.

PETER,M., STRANDBERG,M.W.P. J.Chem.Phys. 26, (1957) 1657.

PETER,M., VENKATES,H.G.R., STRANDBERG,M.W.P. J.App.Phys.31,(1960) 693.

ROMER,R.H., DICKE,R.H. Phys.Rev 99, (1955) 532.

RUSK,J.R., GORDY,W. Phys.Rev. 127, (1962) 817.

ROOS,J. J.App.Phys. 40, (1969) 3135.

SCHEGLOV, V.A. Radiofizika 4, (1961) 648.

SHIMODA,K., WANG,T.C., TOWNES,C.H. Phys.Rev. 102, (1956) 1308.

SHIMODA,K. J.Phys.Soc.Japan 12, (1957) 1006.

SHIMODA,K. J.Phys.Soc.Japan 13, (1958) 939.

SHIMODA,K. Rendiconti S.I.F. XVII Corso (1960) p.1.

SHIMODA,K. J.Phys.Soc. Japan 16, (1961) 777

STRANDBERG,M.W.P., DREICER,H. Phys.Rev. 94, (1954) 1393.

STRAKHOVSKII,G.M., TATARENKOV,V.M. Izv.Vyssh.Uch.Zav.Radiofiz. 7, (1964) 992.

THADDEUS,P., KRISHER,L.C. Rev.Sci.Instrum. 32, (1961) 1083.

TOWNES,C.H. (1954) in: "Microwave spectroscopy". By C.H.Townes and A.L.Schawlow. McGraw-Hill. New York. (1955)

TOWNES,C.H., GESHWIND,S. J.Appl.Phys. 19, (1948) 795

VONBUN,F.O. J.App.Phys. 29,No:4 (1958) 632.

YAMANKA,C. J.Phys.Soc. Japan. 9, (1954) 425.

ZUEV,V.S., CHEREMISKIN,I.V. Radio Eng.and Electron.Phys 7, (1962) 869